

---

Electronic Thesis and Dissertation Repository

---

8-16-2019 10:30 AM


## Assessing the structure-function relationships of the apolipoprotein(a) kringle IV sub-type 10 domain

Matthew J. Borrelli  
*The University of Western Ontario*

Supervisor  
Koschinsky, Marlys L.  
*Robarts Research Institute*

Graduate Program in Physiology and Pharmacology  
A thesis submitted in partial fulfillment of the requirements for the degree in Master of Science  
© Matthew J. Borrelli 2019

Follow this and additional works at: <https://ir.lib.uwo.ca/etd>

 Part of the [Biochemistry Commons](#), [Cardiovascular Diseases Commons](#), [Cellular and Molecular Physiology Commons](#), [Circulatory and Respiratory Physiology Commons](#), [Genetic Phenomena Commons](#), and the [Molecular Biology Commons](#)

---

### Recommended Citation

Borrelli, Matthew J., "Assessing the structure-function relationships of the apolipoprotein(a) kringle IV sub-type 10 domain" (2019). *Electronic Thesis and Dissertation Repository*. 6461.  
<https://ir.lib.uwo.ca/etd/6461>

This Dissertation/Thesis is brought to you for free and open access by Scholarship@Western. It has been accepted for inclusion in Electronic Thesis and Dissertation Repository by an authorized administrator of Scholarship@Western. For more information, please contact [wlsadmin@uwo.ca](mailto:wlsadmin@uwo.ca).

## Abstract

Elevated plasma lipoprotein(a) (Lp(a)) is the most prevalent heritable risk factor in the development of cardiovascular disease. The apolipoprotein(a) (apo(a)) component of Lp(a) is strongly implicated in the pathogenicity of Lp(a). It is hypothesized that the inflammatory potential of Lp(a)/apo(a) is mediated by the lysine binding ability of the apo(a) kringle IV<sub>10</sub> (KIV<sub>10</sub>) domain, along with its covalently bound oxidized phospholipid (oxPL). Using targeted mutagenesis, two novel null alleles for the *LPA* gene that generate non-secretable apo(a) species have been identified, resulting from amino acid substitutions in the KIV<sub>10</sub> domain. A potential mechanism by which KIV<sub>10</sub> oxPL modification is enriched was identified. Finally, RNA-Seq was utilized to demonstrate gene regulation in macrophage-like cells in response to the lysine binding function and covalent oxPL of the KIV<sub>10</sub> domain. It was determined that the lysine binding ability and covalent oxPL of apo(a) KIV<sub>10</sub> are both implicated in vascular cell inflammation and atherosclerosis.

## Keywords

Cardiovascular disease, atherosclerosis, Lipoprotein(a), apolipoprotein(a), inflammation, oxidized phospholipid, lysine-binding protein, kringle, null allele

## Lay Summary

In humans, fats and cholesterol are transported in the blood stream as components of particles called lipoproteins. A high level of one lipoprotein variety, lipoprotein(a) (Lp(a)), has been determined to be the single most prevalent heritable risk factor for developing cardiovascular diseases by contributing to the build-up of plaques within the arteries, or “atherosclerosis”. Lp(a) is very similar to the more commonly known low-density lipoprotein (LDL), which is typically considered the “bad” cholesterol (in comparison to high density lipoprotein (HDL), which is typically considered the “good” cholesterol). Lp(a) contains a protein component called apolipoprotein(a) (apo(a)), which distinguishes Lp(a) from LDL, and is thought to be responsible for the increased pathogenicity of Lp(a) in comparison to LDL. Apo(a) contains many sub-sections, or “domains”, that contribute in different ways to its characteristics. One domain, kringle IV sub-type 10 (KIV10), is thought to be particularly important for the harmful effects of Lp(a) in the blood stream. Here, we investigated the implications of the functions of the KIV10 domain, and the potential roles this domain may have in the development of atherosclerosis. The KIV10 domain is able to bind lysine, which allows apo(a) or Lp(a) to associate closely with cell surface proteins and other ligands. Additionally, the KIV10 domain is modified covalently with an oxidized phospholipid (oxPL). The lysine binding ability of KIV10 has been determined to have atherosclerosis-related effects in certain vascular cell types, as have oxPLs. Together, this suggests that the KIV10 domain may represent an important factor in mediating the harmful effects of Lp(a) in the blood stream. We have determined that either of two independent amino acid substitutions in KIV10 can prevent the secretion of apo(a) entirely, and that a different substitution can change the amount of oxPL added to this domain. Beyond that, we have determined that the lysine binding ability and covalent oxPL of the KIV10 domain are implicated in many gene-regulatory processes that can potentially facilitate the development of atherosclerosis in humans.

## Co-Authorship Statement

All data presented in this thesis was collected by Matthew Borrelli. Dr. Marlys Koschinsky and Dr. Michael Boffa contributed to the generation of appropriate experimental designs, editing of this thesis, and general supervision.

This thesis incorporates the outcomes of joint research in collaboration with:

- Dr. E Stroes (University of Amsterdam), who identified human patients with elevated Lp(a) and unexpectedly low oxPL, and sent our group blood samples from these patients.
- Dr. M Junop (University of Western Ontario), with R Szabla, who performed molecular modeling for the Met64 and Thr64 variants of the apo(a) KIV<sub>10</sub> domain.
- David Carter (London Regional Genomics Center), who facilitated the RNA-Seq analysis, and developed the RNA-Seq methods detailed in Section 2.10.

The use of figures in this thesis from previously published works has been approved by the respective copyright holders.

## Acknowledgments

I would first like to sincerely thank my supervisor, Dr. Marlys Koschinsky, for welcoming me to her research program during my undergraduate studies, and for giving me the opportunity to pursue graduate studies under her supervision. I am grateful for the support, the knowledge, and the numerous opportunities you have generously shared with me. Your influence has been instrumental in my development as a trainee. I would also like to thank Dr. Michael Boffa for all of your guidance and ever-constructive feedback, and for the laughs I have had the pleasure of sharing with you.

Next, I would like to thank my advisory committee members, Dr. Nica Borradaile and Dr. John Di Guglielmo. Your feedback was always incredibly helpful in the problem solving and adaptation this work required. Thank you both for your out-of-meeting support as well; I am grateful for everything you have done to help me succeed – you have gone above and beyond.

I would like to extend my thanks to the members of the Koschinsky-Boffa lab group. Dr. Amer Youssef, thank you for sharing your vast knowledge with me, and for the calm and focused presence you bring to the lab. You inspire me to work hard inside of the lab and out, to better myself as a researcher and as a person. Julia St. John, thank you for your support over these years and for enabling so much of the work our group does. Justin Clark, thank you for your support, your friendship, and like you said, for the laughs. Tasnim Reza, thank you for your unwavering kindness and selflessness.

To Dr. Corey Scipione, thank you for the efforts you made to train me, and for the patience you showed. This project presented many challenges, but the resourcefulness and problem solving I learned from you helped every step of the way. To Dr. Zainab Bazzi, thank you for your continued friendship even from the other side of the country, and for always lending an ear to listen.

And finally, those who mean the most to me: to my closest friends and family, thank you for your constant support and encouragement. Mom, I'd like to thank you for nothing short of everything you and Dad have ever done for me. You always put me first. Dad, though you can't be here with us today, I know you are proud of me. You always were. Thank you.

# Table of Contents

Abstract.....	ii
Lay Summary.....	iii
Co-Authorship Statement.....	iv
Acknowledgments.....	v
Table of Contents.....	vi
List of Tables.....	ix
List of Figures.....	x
List of Abbreviations.....	xii
Chapter 1.....	1
1 Introduction.....	1
1.1 Lipoprotein(a).....	1
1.1.1 Structure.....	1
1.1.2 Apolipoprotein(a).....	6
1.1.3 Lp(a) metabolism.....	9
1.1.4 Determinants of plasma Lp(a) concentration.....	14
1.1.5 Cardiovascular disease and atherosclerosis.....	15
1.1.6 Pathophysiology of Lp(a).....	18
1.1.7 Lp(a) as a risk factor for CVD.....	23
1.1.8 Lipoprotein(a)-lowering therapies.....	24
1.2 Aims, rationale, & hypotheses.....	28
1.2.1 Aim 1: generation of 17K apo(a) containing the KIV <sub>10</sub> His33→Ala substitution.....	28
1.2.2 Aim 2: characterize the KIV <sub>10</sub> mutations Met64→Thr and Arg10→Gln.....	29
2 Materials and Methods.....	30
2.1 Cell culture.....	30
2.2 Generation of apo(a) expression plasmids.....	30
2.2.1 17K H33A.....	33
2.2.2 14K mutants.....	33
2.2.3 6K mutants.....	33
2.2.4 10-P mutants.....	33
2.2.5 KIV <sub>10</sub> KV mutants.....	34
2.3 Generation of stably-expressing cell lines.....	34

2.3.1	17K H33A.....	34
2.3.2	KIV <sub>10</sub> KV R10Q and KIV <sub>10</sub> KV M64T .....	34
2.4	Preparation of conditioned medium and cell lysates from stable- and transiently-transfected cells.....	35
2.4.1	Stably-expressing cell lines.....	35
2.4.2	Transiently transfected cells .....	35
2.5	Purification of recombinant apo(a) .....	36
2.5.1	Purification of recombinant 17K apo(a) species.....	36
2.5.2	Purification of recombinant KIV <sub>10</sub> KV apo(a) species .....	36
2.6	Purification of plasma-derived Lp(a) .....	37
2.7	Determination of lysine binding status of recombinant apo(a) using a lysine binding assay.....	38
2.8	Determination of covalent oxPL modification of apo(a) by E06 immunoblotting	38
2.9	Detection of apo(a) by immunofluorescence microscopy .....	39
2.9.1	Sample preparation .....	39
2.9.2	Imaging of apo(a)-expressing cells.....	39
2.10	Illumina MiSeq Next Generation Sequencing: characterizing the apo(a) transcriptome in human macrophage-like cells.....	40
2.11	Statistical methods for data analysis .....	41
3	Results.....	42
3.1	The amino acid residues KIV <sub>10</sub> His33 and KIV <sub>10</sub> Arg10 are required for processing and secretion of apo(a).....	42
3.1.1	17K H33A is translated, but not secreted by HEK293 cells.....	42
3.1.2	Truncated apo(a) species with additional KIV <sub>10</sub> His33 substitutions are translated, but not secreted by HEK293 cells .....	46
3.1.3	17K H33A is retained in the endoplasmic reticulum in HEK293 cells ....	50
3.1.4	6K R10Q is translated, but not secreted by HEK293 and HepG2 cells....	53
3.1.5	14K R10Q and 14K R10A recombinant apo(a) variants are translated, but not secreted by HEK293 and HepG2 cells .....	55
3.2	Met/Thr at KIV <sub>10</sub> position 64 modulates the degree of covalent oxPL modification, but not sLBS function.....	57
3.3	The structure and functions of apo(a) KIV <sub>10</sub> are implicated in the induction of pro-atherogenic phenotypes in macrophage-like cells.....	62
3.3.1	The KIV <sub>10</sub> covalent oxPL has functions in enabling immune function....	66
3.3.2	The lysine-binding function of apo(a) facilitates the induction of inflammatory responses .....	68

3.3.3	Differential regulation of genes with atherogenic implications.....	71
4	Discussion .....	74
4.1	A molecular basis for novel transcript-positive apo(a) null alleles.....	75
4.2	Substitutions of apo(a) KIV <sub>10</sub> Arg10: a double-edged sword?.....	76
4.3	Implications of the requirement of KIV <sub>10</sub> His33 for apo(a) secretion .....	78
4.4	KIV <sub>10</sub> Thr64 and the implications of enriched covalent oxPL modification .....	79
4.5	Apo(a) LBS-facilitated gene regulation effects have atherogenic implications ...	82
4.5.1	LBS-facilitated effects in inflammation and chemotaxis: roles for <i>CCL4L1, CCL15, CCL19, CXCL14, IL1A, IL6, IL12B, IL23A, TNFAIP2,</i> <i>TNFAIP2, and TNFSF15</i> .....	83
4.5.2	LBS-facilitated effects in cell-cell adhesion and extravasation: roles for <i>CD302, JAML, and SELE</i> .....	84
4.5.3	LBS-facilitated effects in extracellular matrix remodeling: roles for <i>HAS2</i> <i>and MMP13</i> .....	85
4.6	Study limitations and future directions .....	86
4.7	Summary and conclusions .....	87
	References.....	89
	Curriculum Vitae .....	104



## List of Tables

Table 1.1. Therapies that have been shown to reduce plasma Lp(a) concentrations. ....	27
Table 2.1. Primer pairs used for KIV <sub>10</sub> sequencing and mutagenesis reactions. ....	32
Table 3.1. Selected genes differentially expressed in THP-1 macrophages in response to the presence of the KIV <sub>10</sub> covalent oxPL addition to apo(a). ....	67
Table 3.2. Top 15 enriched GO terms in THP-1 macrophages treated with 17K apo(a) compared to those treated with 17K apo(a) + 200 mM $\epsilon$ -ACA. ....	69
Table 3.3. Top 15 enriched KEGG pathways in THP-1 macrophages treated with 17K apo(a) compared to those treated with 17K apo(a) + 200 mM $\epsilon$ -ACA. ....	70

# List of Figures

Figure 1.1. Schematic representation of the Lp(a) particle.....	3
Figure 1.2. Electron micrographs of LDL and Lp(a).....	4
Figure 1.3. Schematic representation of apo(a). .....	5
Figure 1.4. Crystal structure of KIV <sub>10</sub> . .....	8
Figure 1.5. Proposed two-step model for Lp(a) formation. ....	13
Figure 1.6. Effects of Lp(a)/apo(a) on vascular cell phenotypes. ....	22
Figure 2.1. Schematic representations of recombinant apo(a) species. ....	31
Figure 3.1. HEK293 17K H33A cells exhibit abundant apo(a) content. ....	44
Figure 3.2. 17K H33A is not secreted, and is found at a reduced molecular weight in cell lysates.....	45
Figure 3.3. 10-P apo(a) variants with substitutions to KIV <sub>10</sub> His33 are not secreted. ....	47
Figure 3.4. 6K H33N apo(a) is not secreted by HEK293 or HepG2 cells. ....	49
Figure 3.5. 17K H33A apo(a) exhibits increased co-localization with calnexin compared with wildtype 17K.....	52
Figure 3.6. 6K R10Q apo(a) is not secreted by HEK293 or HepG2 cells. ....	54
Figure 3.7. R10Q and R10A variants of 14K apo(a) are not secreted by HEK293 or HepG2 cells. ....	56
Figure 3.8. The KIV <sub>10</sub> KV M64T apo(a) variant binds Lysine Sepharose® in a comparable manner to the Met64 variant. ....	58
Figure 3.9. Representative immunoblots comparing E06 reactivity of apo(a) KIV <sub>10</sub> KV M64T to KIV <sub>10</sub> KV D56A and Met64 KIV <sub>10</sub> KV. ....	60

Figure 3.10. Relative oxPL signal abundance determined by E06 immunoblot densitometry of apo(a) KIV <sub>10</sub> KV Met64 and M64T variants.....	61
Figure 3.11. Experimental design of functional assay used to generate RNA for RNA-Seq analysis.....	64
Figure 3.12. t-SNE plot of biological replicates for RNA sequencing samples. ....	65
Figure 3.13. Subset of genes which are differentially regulated by apo(a) dependent on the KIV <sub>10</sub> sLBS and covalent oxPL, rationalized by a potential role in the pathology of inflammation and atherosclerosis. ....	73
Figure 4.1. Molecular modeling overlay of Met64 (blue) and Thr64 (orange) variants of apo(a) KIV <sub>10</sub> , with $\epsilon$ -ACA as the bound ligand.....	81

## List of Abbreviations

17K, 14K, 6K, 10-P, KIV<sub>10</sub>KV – defined graphically in Figure 2.1

aPES – asymmetric polyethersulfone

Apo(a) – apolipoprotein(a)

ApoB-100 – apolipoproteinB-100

ASO – antisense oligonucleotide

BCA – bicinchoninic acid

CAD – coronary artery disease

CE – cholesteryl ester

CM – conditioned medium

COX-2 – cyclooxygenase 2 (prostaglandin-endoperoxidase synthase 2)

CVD – cardiovascular disease

DMEM/F12 – Dulbecco's modified eagle medium nutrient mixture F-12

ECM – extracellular matrix

EEA1 – early endosome antigen 1

ELISA – enzyme-linked immunosorbent assay

ER – endoplasmic reticulum

ERAD – endoplasmic reticulum-assisted degradation

FBS – fetal bovine serum

FC – free cholesterol

FGF-19 – fibroblast growth factor 19

GM-CSF – granulocyte-macrophage colony-stimulating factor

GO – Gene Ontology

HBS – HEPES-buffered saline

HEK293 – human embryonic kidney 293 cells

HepG2 – hepatocellular carcinoma G2 cells

HoFH – homozygous familial hypercholesterolemia

HS2 – hyaluronan synthase 2

HUVEC – human umbilical vein endothelial cell

ICAM-1 – intercellular cell adhesion molecule 1

IFN- $\gamma$  - interferon- $\gamma$

JAML – junctional adhesion molecule-like\

KEGG – Kyoto Encyclopedia of Genes and Genomes

KIV – kringle IV  
KV – kringle V  
LA – lipoprotein apheresis  
LAMP-1 – lysosomal-associated membrane protein 1  
LASX – Leica Application Suite X  
LDL – low density lipoprotein  
LDLR – low density lipoprotein receptor  
Lp(a) – lipoprotein(a)  
LRGC – London Regional Genomics Centre  
M-CSF – macrophage colony-stimulating factor  
MCP-1 – monocyte chemoattractant protein 1  
MEM – minimum essential medium  
MMP – matrix metalloproteinase  
MMP13 – matrix metalloproteinase 13  
NAFLD – non-alcoholic fatty liver disease  
NASH – non-alcoholic steatohepatitis  
oxLDL – oxidized LDL  
oxPL – oxidized phospholipid  
PARC – pulmonary activation-regulated chemokine  
PBS – phosphate-buffered saline  
PCSK9 – proprotein convertase subtilisin/kexin type 9  
PDGF – platelet-derived growth factor  
PGE<sub>2</sub> – prostaglandin E<sub>2</sub>  
PIC – protease inhibitor cocktail  
PL – phospholipid  
PLA<sub>2</sub> – phospholipase A<sub>2</sub>  
PLG-R<sub>KT</sub> – plasminogen-receptor KT  
PMA – phorbol-12-myristate-13-acetate  
PMSF – phenylmethylsulfonyl fluoride  
PVDF – polyvinylidene difluoride  
RhoA – Ras homolog gene family, member A  
RNAi – RNA interference  
ROS – reactive oxygen species

RPMI-1640 – Roswell Park Memorial Institute  
SDS-PAGE – sodium dodecyl sulfate polyacrylamide gel electrophoresis  
sLBS – strong lysine binding site  
SMC – smooth muscle cell  
SNP – single nucleotide polymorphism  
SREBP – sterol regulatory element-binding protein  
t-SNE – t-distributed stochastic neighbour embedding  
TBS – Tris-buffered saline  
TFPI – tissue factor pathway inhibitor  
TG – triglyceride  
TGF- $\beta$  - transforming growth factor  $\beta$   
TGN46 – *trans*-Golgi network integral membrane protein 2  
THP-1 “macrophages” – THP-1 monocytes incubated with 100 mM PMA for 72 hours;  
macrophage-like cells  
THP-1 monocytes – THP-1 human monocytic leukemia cells  
TLR – toll-like receptor  
TNF $\alpha$  – tumor necrosis factor  $\alpha$   
tPA – tissue plasminogen activator  
UPR – unfolded protein response  
VCAM-1 – vascular cell adhesion molecule 1  
VLDL – very low density lipoprotein  
VLDLR – very low density lipoprotein receptor  
wLBS – weak lysine binding site  
 $\epsilon$ -ACA –  $\epsilon$ -aminocaproic acid

## Chapter 1

### 1 Introduction

#### 1.1 Lipoprotein(a)

##### 1.1.1 Structure

Lipoprotein(a) (Lp(a)) is a unique class of lipoprotein found only in humans, apes, and Old World Monkeys. Originally discovered in 1963 by Kåre Berg, Lp(a) is comprised of two fundamental components: a lipoprotein moiety virtually indistinguishable from low density lipoprotein (LDL), and a single molecule of apolipoprotein(a) (apo(a))<sup>1</sup> (**Figure 1.1**). The LDL-like lipoprotein component contains a cholesteryl ester- and triglyceride-rich core, a free cholesterol/phospholipid monolayer outer shell, and a single copy of apolipoproteinB-100 (apoB-100); in the case of Lp(a), apo(a) is bound covalently to apoB-100 via a single disulfide bond<sup>2</sup>. Under normal conditions, apo(a) maintains a lysine binding-dependent “closed” conformation in association with the apoB-100 component of Lp(a), which can be inhibited by the addition of the lysine analog  $\epsilon$ -aminocaproic acid ( $\epsilon$ -ACA) to produce a “ball-and-chain”-type “open” conformation. This conformation can be visualized using electron microscopy to demonstrate both the single site of covalent linkage between apo(a) and apoB-100, as well as the “beads on a string” appearance of the kringle domains of apo(a)<sup>3</sup> (**Figure 1.2**).

The presence of apo(a) imparts unique properties and characteristics to Lp(a) that differ from those of LDL, largely owing to the presence and functions of multiple kringle domains in apo(a) that are highly homologous to plasminogen kringle 4 (KIV)<sup>4</sup> (**Figure 1.3**). Beginning at the amino terminus, the KIV domains in apo(a) are classified into ten sub-types (KIV<sub>1</sub> through KIV<sub>10</sub>), each differing from the others based on the amino acid sequence and, in turn, dictating their characteristics and functions in the mature protein<sup>4</sup>. Each KIV subtype is present in apo(a) in a single copy with the exception of KIV<sub>2</sub>, which appears in a variable number of identical copies (from 3 to >35 in humans); the number of KIV<sub>2</sub> domains is encoded at the genomic level by the *LPA* gene, giving rise to extensive heterogeneity in apo(a) isoform size in the human population<sup>2</sup>. Carboxyl-terminal to the KIV sequences, apo(a) contains single copies of kringle V- (KV) and protease-like domains, each highly homologous to the corresponding kringle 5 and protease domains of plasminogen. Unlike plasmin, the protease-

like domain of apo(a) is enzymatically inactive<sup>5,6</sup>. The close homology between apo(a) and plasminogen contributes to the disruption of the balance between thrombosis and fibrinolysis, since apo(a) inhibits plasminogen activation in a number of contexts, resulting in prolonged blood clot breakdown<sup>5</sup>.

Some specific functionalities relevant to the assembly and molecular pathology of Lp(a) are attributable to the lysine binding capabilities of certain KIV domains in apo(a). Low-affinity, or “weak” lysine binding sites (wLBS) are present in each of the KIV<sub>7</sub> and KIV<sub>8</sub> domains of apo(a). The functionality of these wLBS are required for initial non-covalent interactions with exposed lysine residues in the amino-terminal globular domain of apoB-100, thereby facilitating the first stage of assembly of the Lp(a) holoparticle<sup>6-9</sup>. This lysine binding-dependent non-covalent association is followed by the formation of a single covalent disulfide bond between Cys<sup>4057</sup> of apo(a)<sup>10</sup>, found in the KIV<sub>9</sub> domain, and a still-debated cysteine residue in apoB-100. Guevara *et al.* demonstrated Cys<sup>3734</sup> as the apoB-100 cysteine residue in question using molecular modelling and fluorescent labelling of potential candidate residues<sup>11</sup>, while Callow *et al.* posit that Cys<sup>4326</sup> is the residue involved in disulfide bond formation with apo(a) as determined using mutagenesis<sup>12</sup>.

Finally, the KIV<sub>10</sub> domain of apo(a) possesses two characteristics that make it unique with respect to the other KIV domains, and of most relevance to this thesis: a high-affinity, “strong” lysine binding site (sLBS), and an amino acid residue to which an oxidized phospholipid (oxPL) is covalently bound<sup>13,14</sup>. The covalent oxPL modification of apo(a) has been determined empirically to absolutely require the functionality of the sLBS of KIV<sub>10</sub> for addition. The proposed roles for the sLBS and covalent oxPL are described in detail Section 1.1.6.

In addition to the unique covalently-bound oxPL, Lp(a) has been shown to be the preferential carrier of oxPL in the plasma over LDL, an important factor in the context of inducing inflammatory phenotypes in vascular cells and subsequent development of cardiovascular pathologies<sup>15</sup>.



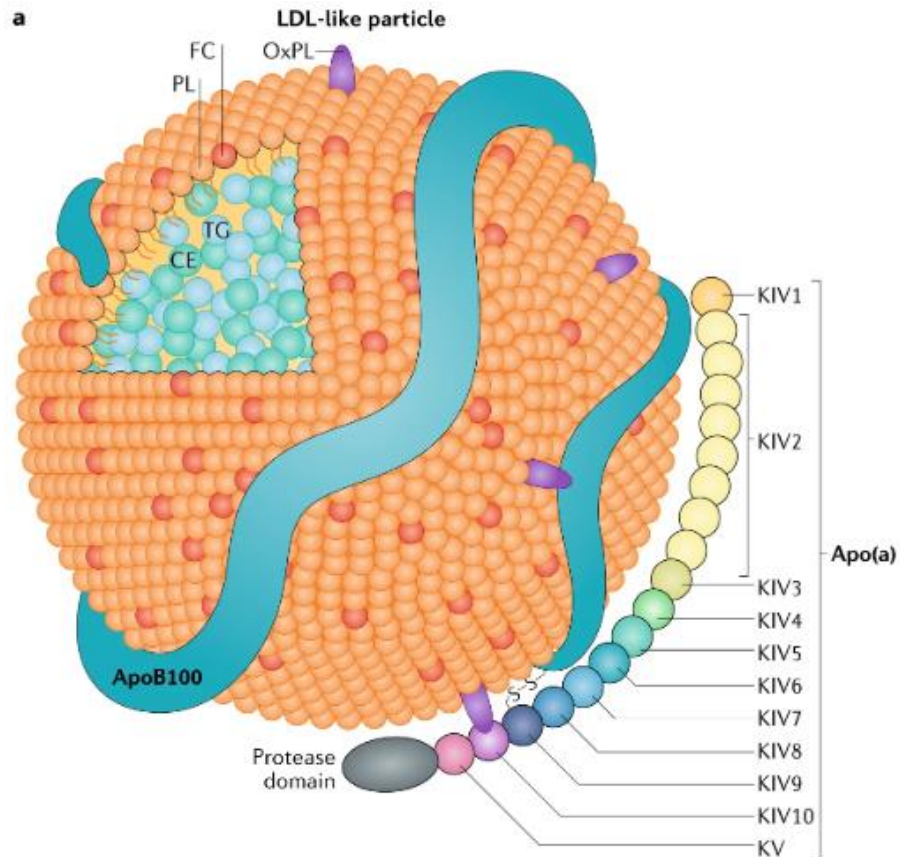


**Figure 1.1. Schematic representation of the Lp(a) particle.**

Lp(a) is a unique lipoprotein owing to its inclusion of apolipoprotein(a). Sharing many characteristics with LDL, Lp(a) possesses a lipoprotein core comprised of triglycerides (TG) and cholesteryl esters (CE), surrounded by a monolayer of phospholipids (PL) and unesterified free cholesterol (FC), all associated with a single copy of apoB-100. In addition to its bulky lipoprotein core, Lp(a) possesses a single copy of apo(a) covalently bound to apoB-100 by a disulfide bridge involving the single free cysteine residue present in the apo(a) KIV<sub>9</sub> domain. Apo(a) contains ten kringle domains homologous to plasminogen KIV, each present in a single copy with the exception of KIV<sub>2</sub>, which varies from 3 to >35 identical repeats corresponding to the number of KIV<sub>2</sub> sequences encoded in the *LPA* gene, and determines the overall size of the apo(a) molecule. The specific characteristics and functions of the various kringle domains comprising apo(a) are described in Section 1.1.2. Also shown are oxidized phospholipids (OxPL) associated with the lipid core as well as covalently bound to KIV<sub>10</sub>. [Boffa & Koschinsky, 2019].

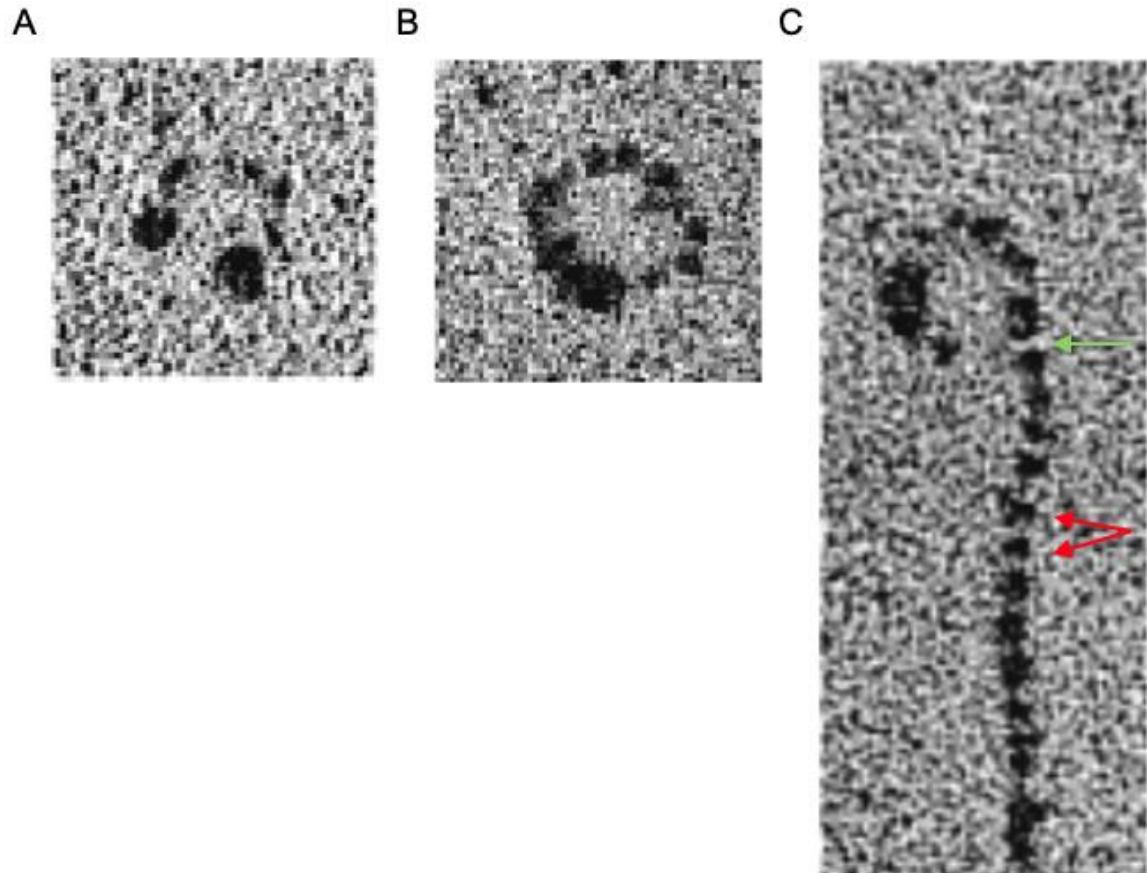


**Figure 1.2. Electron micrographs of LDL and Lp(a).**

LDL can be visualized using electron microscopy as (A) a tightly clustered lipoprotein particle, exhibiting regions of high electron density corresponding to its apoB-100 component. Lp(a) exhibits lysine-dependent interactions between apo(a) and apoB-100, similarly yielding (B) a tightly clustered lipoprotein particle with more electron-dense regions compared with LDL due to the presence of apo(a), or (C) as an “open” conformation with a “ball-and-chain” appearance upon the addition of the lysine analog  $\epsilon$ -ACA. In the open conformation, individual kringle domains of apo(a) can be visualized as “beads on a string” (red arrows), and the single covalent bond involving KIV<sub>9</sub> near the C-terminus of apo(a) can be inferred (green arrow). [Weisel *et al.*, 2001].

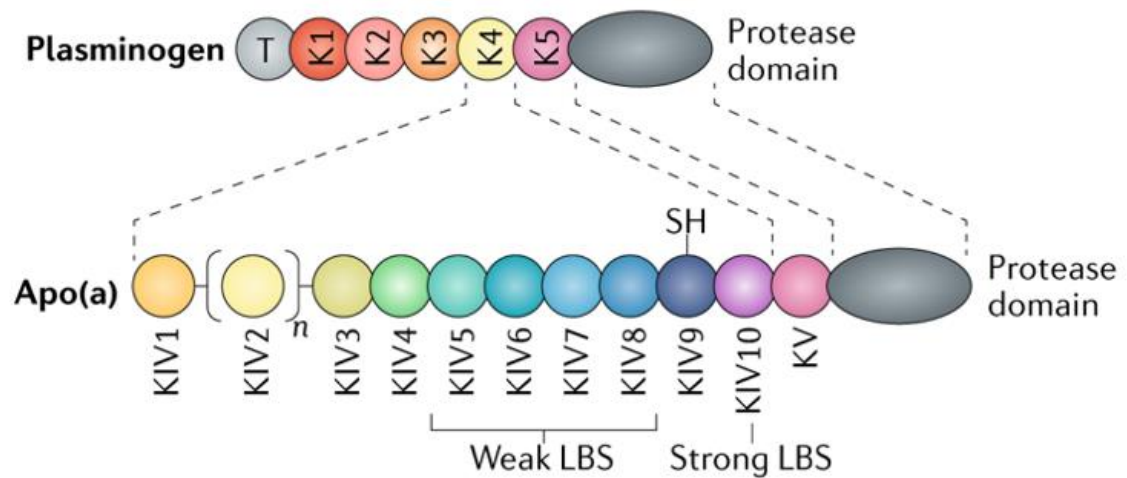


**Figure 1.3. Schematic representation of apo(a).**

Apo(a) strongly resembles plasminogen, sharing substantial sequence and structural homology. Both apo(a) and plasminogen contain multiple kringle domains; the kringles that make up apo(a) include ten unique subtypes sharing extensive sequence identity with plasminogen K4 (KIV<sub>1</sub>-KIV<sub>10</sub>), each found in a single copy with the exception of KIV<sub>2</sub>, which is a repeating domain ranging from 3 to >35 identical copies. In addition to its KIV domains, apo(a) also possesses domains similar in sequence to the plasminogen K5 and protease domains; in apo(a), the protease domain is not enzymatically active. Apo(a) lacks sequences corresponding to the plasminogen tail, K1, K2, and K3 domains. Certain apo(a) KIV domains possess characteristics that are important for the assembly and pathogenicity of Lp(a): the weak lysine binding sites found in KIV<sub>7</sub> and KIV<sub>8</sub> are essential for initial non-covalent interaction between apo(a) and apoB-100, the unpaired Cys<sub>4057</sub> found in KIV<sub>9</sub> is required for covalent linkage to apoB-100, and KIV<sub>10</sub> contains both a strong lysine binding site (strong LBS) as well as a covalently-bound oxPL. Full function of the strong lysine binding site found in KIV<sub>10</sub> is necessary for covalent oxPL modification to occur. [Boffa & Koschinsky, 2019].

### 1.1.2 Apolipoprotein(a)

Apo(a) distinguishes Lp(a) from LDL both structurally and functionally, imparting Lp(a) with unique characteristics. Apo(a) is approximately 28% carbohydrate by weight<sup>16</sup>. As previously stated, apo(a) is composed of repeating domains homologous to the KIV domain of plasminogen. In fact, it has been determined that the existence of *LPA* in humans, apes, and Old World Monkeys, is the result of a gene duplication of *PLG*, and that gene divergence of what we now know as *LPA* and its parent gene *PLG* occurred relatively recently during primate evolution (approximately 40 million years ago)<sup>4,17</sup>. The kringle domains found in apo(a) and plasminogen are so named for their physical resemblance to a traditional Danish pastry of the same name. Kringles form a characteristic tri-looped structure composed of about 80 amino acids, wherein three invariant disulfide bonds are formed between the six invariant cysteine residues present in each kringle (**Figure 1.4**). KIV<sub>9</sub> is the only domain possessing a seventh cysteine; nascently unpaired, this cysteine is the residue through which apo(a) links covalently to apoB-100 in the covalent assembly of the Lp(a) holoparticle<sup>10</sup>. Between each apo(a) kringle domain, there is an inter-kringle linker region of approximately 30 amino acids, rich in serine and threonine residues and thus representing the major proposed sites of O-linked glycosylation<sup>18</sup>. Each KIV domain also possesses at least one site for N-linked glycosylation<sup>19</sup>. Kringle domains are largely considered to serve as protein-binding domains, suggesting that the presence of apo(a) on Lp(a) allows interactions with a variety of ligands with which LDL is unable to interact.

Due to its KIV<sub>10</sub> lysine-binding sites and covalently bound oxPL, it has been hypothesized that apo(a) confers pathogenic potential to Lp(a) beyond that which can be attributed to LDL. The lysine-binding ability of apo(a) allows it to bind exposed lysine residues on a wide variety of ligands, including fibrin and cell-surface receptors<sup>20-22</sup>. The previously mentioned zymogen, plasminogen, also bears lysine-binding kringle domains, the binding interactions of which facilitate its cleavage and activation to the fibrinolytic enzyme plasmin which, in turn, promotes the dissolution of fibrin clots<sup>23,24</sup>. The presence of apo(a) on Lp(a) slows the action of plasmin by inhibiting plasminogen cleavage in a number of contexts<sup>25,26</sup>, thereby evoking a net anti-fibrinolytic/pro-thrombotic effect. A second mechanism by which apo(a) slows the action of plasmin has been demonstrated as well: apo(a) has been shown to participate in the

formation of a plasminogen-tissue plasminogen activator (tPA)-fibrin-apo(a) complex which exhibits a reduced rate of plasmin activation compared with the same complex lacking apo(a)<sup>5</sup>.

The covalently bound oxPL of KIV<sub>10</sub> is implicated in stimulating the production of a variety of pathogenic stimuli, as oxidized lipids have been shown to induce inflammatory processes in vascular cell types<sup>14,27-30</sup>. Plasma oxPL/apoB-100 ratio has a strong correlation with Lp(a) concentration in humans, and further, oxPL/apoB-100 has been found to correlate with the presence and extent of coronary artery disease (CAD)<sup>31,32</sup>. Elevated oxPL/apoB-100 has also been shown to correlate with prevalence of carotid and femoral artery diseases<sup>33</sup>. The covalent oxPL moiety of apo(a) has been shown to induce apoptosis in endoplasmic reticulum (ER)-stressed macrophages in a CD36- and toll-like receptor 2 (TLR2)-dependent manner<sup>34</sup>, a key step in the formation of the necrotic core in atherosclerotic lesions. Based on this information, a strong role for apo(a), and Lp(a) by extension, is suggested in the initiation of endothelial dysfunction, vascular cell inflammation, and necrotic core formation – key processes in the initiation and progression of atherosclerosis.

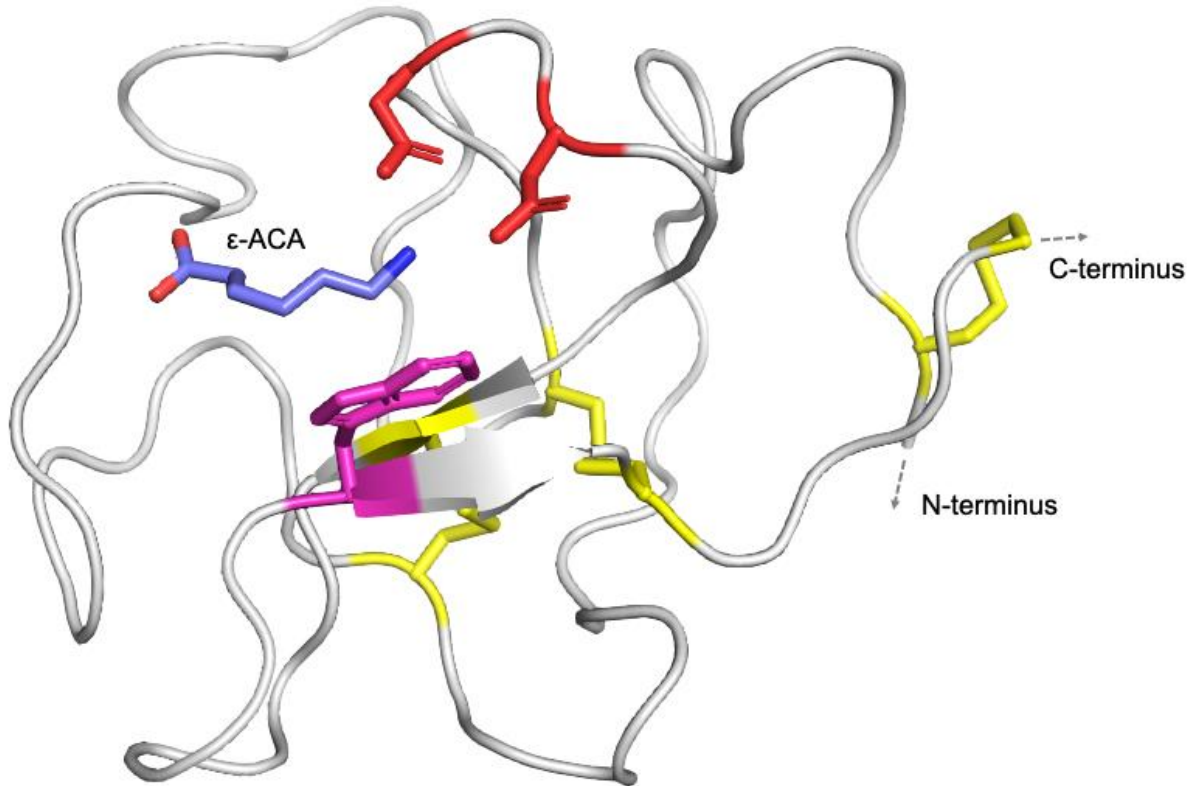


**Figure 1.4. Crystal structure of KIV<sub>10</sub>.**

Kringle domains are found in both plasminogen and apo(a), as well as other proteins involved in thrombotic and fibrinolytic processes. Kringle domains possess a hallmark tri-looped structure stabilized by three invariant disulfide linkages, shown in yellow. Kringles represent important domains for protein-ligand interactions; KIV<sub>10</sub> possesses a strong lysine binding site which facilitates interactions between apo(a) and fibrin, cell surface receptors, and other ligands. The lysine analog  $\epsilon$ -ACA is shown as the bound ligand. Two aspartic acid residues (red) and one tryptophan residue (magenta) that are crucial to the function of the sLBS are shown. Figure generated using PyMOL version 2.3.2, pdb: 3KIV, produced by Mochalkin *et al.*<sup>35</sup>.

### 1.1.3 Lp(a) metabolism

#### 1.1.3.1 Apo(a) secretion

Up to 90% of the variability seen in human plasma Lp(a) concentrations can be attributed to *LPA*<sup>36</sup>, the gene encoding apo(a), which is found on human chromosome 6q25.3-q26<sup>4</sup>. The size of the *LPA* gene itself varies widely within the population, reflecting differences in the number of KIV<sub>2</sub>-encoding sequences present. In general, an inverse correlation exists between the isoform size encoded by a given *LPA* allele and the corresponding plasma Lp(a) concentration observed<sup>7,37</sup>. It is believed that more time is required for cells to process larger apo(a) isoforms due to the greater total number of kringles present, the complex folding required for each, and extensive post-translational modification in the form of N- and O-linked glycosylation. This extended processing stage results in longer periods of ER retention and subsequent ER-associated degradation, the end result of which is reduced levels of secreted protein species and circulating Lp(a)<sup>38-40</sup>. In light of this, it is important to note that Lp(a) levels are generally agreed to be determined primarily at the level of what can broadly be termed “production”, rather than uptake and catabolism of the particle from circulation. *In vivo* kinetic studies in humans have ascribed differences in apo(a) production rates for different isoform sizes (slowest production rates for largest isoform sizes), while failing to show such a relationship for fractional catabolic rates<sup>41</sup>.

Biosynthesis of Lp(a) begins in a similar fashion to many secreted proteins: transcription of the gene, in this case *LPA*, and subsequent apo(a) protein translation/ER translocation, processing, and passage through the constitutive secretory pathway. Several transcription-regulating elements have been identified for *LPA*, including an inductive interleukin (IL)-6 response element in the *LPA* promoter region<sup>42</sup>, a repressive DR-1 promoter element which is bound by the bile acid-bound farnesoid X receptor (FXR)<sup>43</sup>, an Ets motif that has been shown to mediate repression of *LPA* transcription by fibroblast growth factor 19 (FGF-19) via Elk-1 binding<sup>44</sup>, and several cAMP response elements thought to play a role in niacin-mediated Lp(a) reduction<sup>45</sup>. However, the transcriptional control of *LPA* is not fully understood, with evidence suggesting a gene-repressing role for estrogens based on studies in men undergoing estrogen therapy for prostate cancer<sup>46</sup>, as well as post-menopausal women receiving estrogen replacement<sup>47</sup>. Finally, apo(a) secretion is intrinsically regulated by intracellular processing requirements according to the isoform size in question. The proportionally increased ER

retention time observed in apo(a) isoforms of increasing size results in increased proteasomal degradation and, accordingly, reduced secretion efficiency<sup>39</sup>.

With respect to apo(a) secretion, the importance of the processes underlying general protein processing and quality control must be considered thoroughly. Classically, the process of protein secretion involves unidirectional movement of proteins of interest through the ER, the Golgi apparatus, secretory vesicles, and finally culminates in their extracellular release. At the same time, quality control processes typically ensure only properly folded proteins are secreted, targeting misfolded proteins for degradation. Most secreted proteins possess an N-terminal signal sequence that is recognized by cytosolic targeting factors and ER-resident translocation machinery<sup>48</sup>, which directs the translation of that protein/peptide to occur through an ER-embedded Sec61 pore complex following association with the cytosolic ER membrane<sup>49</sup>. The signal recognition particle, a multimeric complex comprised of both protein and RNA components<sup>50</sup>, mediates the targeting of signal peptide-containing polypeptides to the ER, whilst simultaneously slowing protein translation to prevent premature cytoplasmic protein folding that would preclude ER translocation<sup>51</sup>. The N-terminal end of the nascent polypeptide is first inserted into the ER, where a protease complex, usually signal peptidase, cleaves the signal peptide<sup>52</sup>. Protein translation directly into the lumen of the ER then follows, and ER-based quality control of protein folding and post-translational modification occurs. During translation of the protein into the lumen of the ER, sequence recognition by the oligosaccharyltransferase complex occurs, during which N-linked Glc<sub>3</sub>Man<sub>9</sub>GlcNAc<sub>2</sub> glycan motifs are added to Asn in the Asn-X-Thr/Ser consensus sequence<sup>53</sup>; as mentioned previously, each kringle domain of apo(a) possesses at least one such N-glycan attachment site, making this ER-localized stage of protein modification important in the processing of apo(a). It has been demonstrated that the addition and trimming of N-linked glycans is important for the subsequent folding of a great number of secreted protein species, including apo(a)<sup>39,54,55</sup>. This folding process is facilitated by a number of catalytic isomerases (e.g. protein disulfide isomerase), glycosidases, molecular chaperones (e.g. calnexin), and by the oxidizing environment of the ER which favors disulfide bond formation. In the case of properly folded and modified proteins, normal progression to the Golgi apparatus occurs by way of COPII-coated vesicular budding<sup>56,57</sup>. However, in cases of misfolded or improperly processed proteins, the constitutively active ER-associated degradation (ERAD) pathway selectively



recognizes these proteins and exports them for cytosolic degradation by the proteasome<sup>58-60</sup>, blocking their passage to the Golgi.

With respect to the processing and secretion of apo(a), three key studies in cultured baboon hepatocytes are particularly relevant in the context of this thesis. First, a radioactive pulse-chase study revealed that two distinct sizes of apo(a) could be isolated simultaneously from cell lysates: both a mature, glycosylated form of apo(a) and an immature hypo-glycosylated form of apo(a). It is crucial to note that only the mature, fully glycosylated form of the protein was secreted by the cell<sup>61</sup>. The second study revealed that tunicamycin, an indirect inhibitor of N-linked glycosylation, prevented the maturation and secretion of apo(a), and that castanospermine, an inhibitor of N-linked glycan trimming, produced a similar effect<sup>39</sup>. It should be noted that this effect was not observed previously in HEK293 cells stably expressing apo(a)<sup>62</sup>. A third study identified variants of apo(a) that could be isolated from cell lysates but were not secreted; it was determined using immunoprecipitation coupled with pulse-chase analysis and endoglycosidase digests that these apo(a) species were being retained in the ER<sup>40</sup>. Taken together, these data strongly indicate that proper folding as well as N-linked glycosylation are both critical for the secretion of apo(a).

### 1.1.3.2 Lp(a) assembly

Biosynthesis of Lp(a) not only encompasses apo(a) secretion, but also the assembly of the particle, first by initial lysine-dependent non-covalent interaction between apo(a) and apoB-100, and followed by the covalent linkage of apo(a) to apoB-100 (**Figure 1.5**). Until recently, it has been generally accepted that Lp(a) assembly occurs exclusively extracellularly, from newly-secreted apo(a) and either newly-synthesized or circulating LDL; in both cases, the secretion of the apoB-100-containing species is proposed to be unlinked to that of apo(a). This model for Lp(a) assembly has come under scrutiny after an *in vivo* kinetic study in humans showed that the production rate of Lp(a)-associated apoB-100 is quite different than the production rate of apoB-100 found in other lipoprotein species, but matches very closely with the production rate of apo(a)<sup>63</sup>, suggesting a yet uncharacterized relationship between the secretion of apo(a) and Lp(a)-apoB-100. These findings indicate the possibility of intracellular Lp(a) assembly, but the existence of an Lp(a)-destined apoB-100-containing lipoprotein pool must also be considered as a possibility. Regardless of the location of initial noncovalent

interaction, an *in vitro* model of Lp(a) assembly has demonstrated the extracellular activity of an Lp(a)-specific oxidase enzyme involved in catalyzing the formation of the covalent bond between Cys<sup>4057</sup> of apo(a) and Cys<sup>3734</sup> or Cys<sup>4326</sup> of apoB-100<sup>64</sup>. However, the identity of this enzyme and its mechanism of action have not been fully determined. When hypothesizing about the secretion and assembly processes that comprise Lp(a) formation, we must also consider the fact that many therapies known to reduce circulating LDL levels (e.g. mipomersen, lomitapide, anacetrapib, and proprotein convertase subtilisin/kexin type 9 (PCSK9) inhibitors) also reduce Lp(a) levels<sup>65–70</sup>. While much is still unknown about the specifics of Lp(a) assembly in the context of apo(a) secretion and its relationship with apoB-100, it is known that free apo(a) is not simply secreted into the plasma prior to association with an LDL particle; it has been demonstrated that apo(a) species with nonsense mutations N-terminal to Cys4057 (and thereby lacking the ability to form the covalent link to apoB-100 required for Lp(a) assembly) experience rapid degradation in the plasma<sup>71</sup>. Free apo(a) is detectable at very low levels in the plasma, but the vast majority is present in Lp(a) particles<sup>72</sup>.

### 1.1.3.3 Catabolism

Further complicating our incomplete understanding of Lp(a) metabolism, a robust understanding of Lp(a) catabolism remains elusive. Although no definitive receptor for Lp(a) has been identified, it has been established that the liver is the organ for Lp(a) catabolism, while also representing the dominant source of apo(a) secretion. Roles in Lp(a) internalization have been described for a number of receptors including the following: the LDL receptor (LDLR)<sup>73,74</sup> and LDLR family (very low density lipoprotein receptor (VLDLR), LDLR-related protein 1, and gp330/megalin)<sup>75–77</sup>, the plasminogen receptor family (PLG-R<sub>KT</sub>)<sup>78</sup>, and scavenger receptor superfamily (scavenger receptor B1)<sup>79</sup>. The relative contribution of each receptor type to the overall internalization and catabolism of Lp(a) has not been determined. The kidney has also been identified as a minor potential contributor to Lp(a) catabolism owing to its expression of the VLDLR and/or gp330/megalin<sup>80</sup>, but no renal Lp(a) uptake studies have been performed in humans to date.

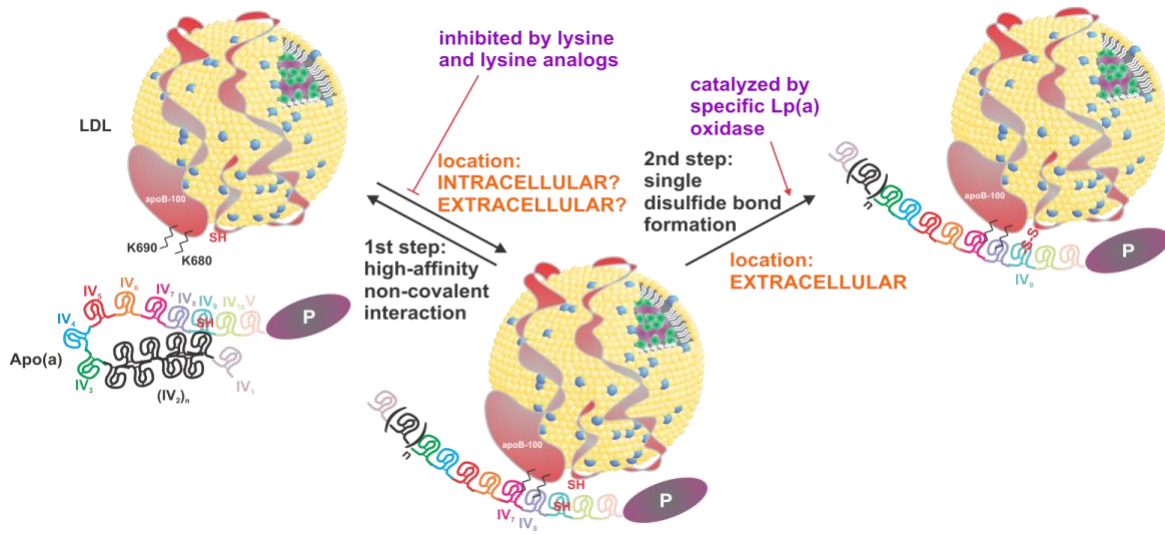


**Figure 1.5. Proposed two-step model for Lp(a) formation.**

The current understanding of Lp(a) formation involves a two-step mechanism. In the first step, apo(a) associates non-covalently with free lysine residues in the N-terminal globular domain of apoB-100 via weak lysine binding sites in the apo(a) KIV<sub>7</sub> and KIV<sub>8</sub> domains. The precise location of initial non-covalent interaction between the two species is unclear; evidence has been presented to suggest that both intracellular and extracellular association are possible. Additionally, it has been demonstrated that the rate of Lp(a)-apoB-100 secretion closely matches that of apo(a). Regardless of the location of this interaction, it has been shown that it can be competitively inhibited with the addition of lysine analogs such as  $\epsilon$ -ACA. The second step of Lp(a) assembly is the formation of a single disulfide bond between Cys<sup>4057</sup> of apo(a) and either Cys<sup>3734</sup> or Cys<sup>4326</sup> (current findings indeterminate)<sup>11,12</sup> of apoB-100. This bond formation is catalyzed by an extracellular Lp(a)-specific oxidase. [Becker *et al.*, 2006].

### 1.1.4 Determinants of plasma Lp(a) concentration

Plasma concentrations of Lp(a) vary widely within the population, from levels that are undetectable to those in excess of 250 nanomolar. It is well established that plasma Lp(a) concentrations are determined predominantly at the stage of production, and that there is a general inverse relationship between concentration of Lp(a) and the size of the *LPA* gene encoding apo(a). The determinants that collectively dictate the level of Lp(a) in the plasma are *LPA* transcription, apo(a) secretion, assembly of Lp(a), and its catabolism.

While *LPA* gene size is the major genetic determinant of apo(a) production and Lp(a) concentration, the general inverse relationship between the two only accounts for about 70% of the observed variation in plasma Lp(a) concentrations. Approximately 22% of this variation has been attributed to *cis*-acting sequences in the gene whose influences have not been fully characterized<sup>36</sup>. There is evidence to suggest that the size of a given *LPA* allele affects not only the plasma concentration of Lp(a) with the corresponding isoform, but that of the second isoform as well<sup>81,82</sup>. Furthermore, there is evidence that single nucleotide polymorphisms (SNPs) influence plasma Lp(a) concentrations as well: rs3798220 (protease-like domain, Ile4399→Met) and rs10455872 (KIV<sub>2</sub>, intronic) are associated with elevated Lp(a) levels and increased incidence of CVD<sup>83</sup>.

At the genomic level, several transcription factor binding sites in the *LPA* promoter region have been identified as modulators of gene transcription. As mentioned previously, these elements include those responsive to 1) IL-6, with a 5-fold enhancement in *LPA* reporter gene activity reported in HepG2 cells treated with IL-6<sup>42</sup>, 2) bile acids, repressing *LPA* transcription via an FXR response element<sup>43</sup>, 3) FGF-19, down-regulating transcription via Elk-1 binding to an Ets motif<sup>44</sup>, and 4) cAMP, up-regulating expression (but depleted by niacin)<sup>45</sup>. In addition to these factors, exogenous estrogen supplementation has been shown to reduce Lp(a) levels<sup>46,47</sup>. However, the exact role of estrogens in this context remains elusive when one considers that there is no significant difference between plasma Lp(a) levels in healthy men and pre-menopausal women, despite a great discrepancy in concentrations of circulating estrogens<sup>84</sup>. Further, it has been demonstrated that Lp(a) levels are higher in post-menopausal women than in pre- or peri-menopausal women, indicating further differences in the handling of Lp(a) in males and females<sup>85</sup>.

Interestingly, it has also been established that a given *LPA* allele may be associated with considerably different concentrations of Lp(a) in the plasma, especially between individuals of different ethnic backgrounds; multiple studies have shown that African Americans have median plasma Lp(a) concentrations significantly exceeding that of Caucasians, and that this discrepancy is not fully accounted for by differences in isoform size distribution<sup>81,86,87</sup>.

#### 1.1.4.1 “Null” *LPA* alleles

Only two null alleles of the *LPA* gene have been identified in humans – both of which result in the generation and secretion of apo(a) species that are unable to participate in Lp(a) assembly. As discussed previously, it has been shown that such unbound apo(a) species are degraded rapidly. A splice site mutation (rs41272114) results in the production of an alternately-spliced *LPA* transcript, the translation of which generates an apo(a) variant that is truncated after KIV<sub>7</sub> and prevents both non-covalent and covalent associations with apoB-100<sup>71</sup>. This SNP is associated with reduced plasma Lp(a) concentrations and reduced CAD risk<sup>88</sup>. The other null allele (rs# unclear, “G4925A”<sup>89</sup>) produces a nonsense mutation in the KIV<sub>2</sub> region; this apo(a) species is believed to be secreted, but, once again, is unable to form Lp(a) and subsequently results in reduced plasma Lp(a) levels<sup>90</sup>. While these two null alleles are the only confirmed variants of this nature, recent findings suggest the discovery of novel non-synonymous mutations in *LPA* that represent null alleles for apo(a), by causing the intracellular retention and degradation of the encoded apo(a) species (unpublished data presented at European Atherosclerosis Society 87<sup>th</sup> Congress by S McCormick, Maastricht, The Netherlands, 2019).

#### 1.1.5 Cardiovascular disease and atherosclerosis

Cardiovascular disease (CVD) is a broad term referring to a class of diseases characterized by dysfunction of the heart and/or vasculature, and collectively represents the leading cause of death in the developed world<sup>91</sup>. While CVD encompasses many specific types of pathologies, the most common is CAD, accounting for the greatest burden of mortality and morbidity of any CVD subtype<sup>92</sup>. CAD is a progressive disease, believed to be initiated by the exposure of the arterial endothelial lining to some form of insult. As a result, endothelial cells undergo structural changes that compromise the integrity of tight junctions between them, increasing the permeability of the lining to circulating particles and allowing the accumulation of

lipoproteins and leukocytes, among other blood components, within the intimal compartment of the vessel<sup>93</sup>. The initial insult to the vessel may take the form of chronically elevated circulating lipids (dyslipidemias), exposure to compounds found in cigarette smoke, shear stress, hyperglycemia, obesity, hypertension, or insulin resistance<sup>94</sup>. Each of the aforementioned insults results in activation of signaling pathways that lead to the generation of excess reactive oxygen species (ROS) and subsequently, an environment within the endothelial cells characterized by high levels of oxidative stress<sup>95,96</sup>. High intracellular levels of oxidative stress activate the NF- $\kappa$ B pathway, and in turn induce the expression of genes under the control of NF- $\kappa$ B-response elements<sup>95,96</sup>. NF- $\kappa$ B-inducible genes encode protein products that serve a wide range of functions including cell surface adhesion molecules (e.g. E- and P-selectins, intercellular adhesion molecule 1 (ICAM-1), and vascular cell adhesion molecule 1 (VCAM-1))<sup>97-100</sup> and pro-inflammatory cytokines (e.g. interferon- $\gamma$  (IFN- $\gamma$ ), IL-1 $\alpha/\beta$ , 6, and 8, tumor necrosis factor  $\alpha$  (TNF $\alpha$ ), and monocyte chemoattractant protein 1 (MCP-1))<sup>101-106</sup>, among others.

Following initial insult and ROS-induced NF- $\kappa$ B signaling, vascular endothelial cells undergo phenotypic changes, resulting in what can broadly be termed “endothelial dysfunction”. Endothelial dysfunction compromises the integrity of intercellular tight junctions, allowing the aberrant efflux of pathogenic factors such as LDL and Lp(a) from the lumen of the vessel into the intimal (sub-endothelial) layer of the vessel wall. It should be noted that upon entering the intimal space of the vessel wall, lipoproteins may be acted upon by enzymes or encounter oxygen radicals, leading to their oxidative modification<sup>107</sup>; the exposure of endothelial cells to oxidized lipoproteins promotes the adhesion and extravasation of immune cell types from the plasma by inducing further production of cell adhesion molecules<sup>29,108,109</sup> and secretion of pro-inflammatory factors<sup>110</sup>. Pro-inflammatory cytokines secreted by the damaged endothelial lining serve to further immune cell convergence and invasion at the site of injury, thereby initiating and propagating a local inflammatory response, initiating the process of atherosclerotic plaque formation<sup>111,112</sup>.

Following the initiation phase resultant from endothelial dysfunction, intimal invasion by immune cells such as monocytes becomes a primary factor in the advancement of local inflammation and atherosclerotic lesion development. Upon their arrival in the intimal space,

monocytes encounter high levels of stimulating growth factors including macrophage colony stimulating factor (M-CSF) and granulocyte-macrophage colony stimulating factor (GM-CSF), inducing their differentiation and maturation to macrophages<sup>113,114</sup>. *In vitro*, M-CSF is constitutively expressed under basal conditions by endothelial cells and smooth muscle cells (SMCs), as well as fibroblasts<sup>115,116</sup>. On the other hand, GM-CSF expression is inducible *in vitro* by TNF $\alpha$  and IL-1 $\beta$  in arterial SMCs<sup>114</sup>, and by oxidized LDL (oxLDL) in endothelial cells and macrophages *in vivo*<sup>117</sup>. This suggests a mechanism by which leukocyte chemoattractants contribute to the propagation of the chronic and non-resolving inflammatory processes ongoing in the developing lesion. As monocyte-to-macrophage differentiation occurs, so too does the up-regulation of TLRs and scavenger receptors in these cells, mediating cell signaling processes that lead to inflammatory cytokine secretion and lipid uptake<sup>118,119</sup>.

Macrophages in the intimal space bind and engulf oxLDL and oxidized Lp(a) via pattern recognition receptors including the TLRs and scavenger receptors mentioned previously, along with CD36. Macrophage uptake of oxidized lipids leads to the formation of lipid-laden foam cells and stimulates their secretion of pro-inflammatory factors<sup>119–122</sup>. These factors propagate further inflammatory responses in vascular cell types while continued uptake of lipoproteins triggers ER stress-mediated apoptotic processes in foam cells, and lead to the formation of the necrotic core in the atherosclerotic plaque<sup>34,123</sup>. In addition to the aforementioned processes, cytokines secreted by activated macrophages induce local migration and proliferation of SMCs<sup>111</sup> and contribute to downstream platelet aggregation<sup>124</sup>; stimulation of both endothelial cell and SMC contraction, migration, and proliferation has also been observed in direct response to apo(a) exposure in an  $\alpha v \beta_3$  integrin- and RhoA/Rho kinase-dependent fashion<sup>125,126</sup>. Platelet aggregation and subsequent activation, mediated by blood-borne von Willebrand factor, promotes the secretion of platelet-derived growth factor (PDGF) and transforming growth factor  $\beta$  (TGF- $\beta$ ), propagating SMC migration and proliferation, as well as synthesis and secretion of extracellular matrix (ECM) components by SMCs, respectively<sup>127–130</sup>. The combination of SMC proliferation and migration, coupled with ECM deposition, leads to the formation of the lesion's fibrous cap<sup>131</sup>, while the contractile response of SMCs to Lp(a) exposure is thought to reduce plaque stability. Overall, the summation of these processes represents the cyclic nature of both the formation as well as the progression of atherosclerotic plaques.

As the deposition of arterial plaques continues over the span of years to decades, blood vessel occlusion gradually obstructs blood flow. In the case of plaque formation in the coronary arteries, (i.e. CAD), blood flow to the myocardium itself becomes reduced and presents symptomatically with feelings of tightness or pain in the chest, clinically termed angina<sup>132</sup>. Over time, chronic exposure of macrophages, endothelial cells, and SMCs to inflammatory factors such as TNF $\alpha$  and decreased nitric oxide levels promotes their secretion of collagenases and matrix metalloproteinases (MMPs)<sup>133,134</sup>. Without intervention, the plaque continues to grow and the stability of the fibrous cap may be compromised by MMP-mediated ECM degradation, reducing the overall stability of the plaque and increasing its risk of rupture. If plaque rupture occurs, exposure of blood to the components of the plaque precipitates the formation of a thrombus which may occlude coronary artery flow completely, resulting in ischemia of the myocardium and subsequent myocardial infarction<sup>131</sup>. Plaque rupture in other vessels can lead to other major events such as ischemic stroke. Recalling the anti-fibrinolytic effect of Lp(a)/apo(a) as an inhibitor of plasmin formation discussed briefly in Section 1.1.2, it is reasonable to speculate that plasma Lp(a) concentration may be a contributing factor in determining the prevalence and severity of cardiovascular events following plaque rupture.

### 1.1.6 Pathophysiology of Lp(a)

The structural duality of the Lp(a) particle, containing both an LDL-like bulky lipid moiety and a plasminogen-like apo(a) molecule, suggests that Lp(a) may participate in both atherogenic and anti-fibrinolytic processes in the vasculature. The potential effects of the KIV<sub>10</sub> sLBS and covalent oxPL on macrophages, endothelial cells, and SMCs are summarized in **Figure 1.6**.

#### 1.1.6.1 Oxidized phospholipid modification of Lp(a)

Oxidized lipoproteins are important drivers of the inflammatory processes involved in the progression of atherosclerosis. In this context, the determination that Lp(a) is the preferential carrier of oxPL in the plasma, compared to LDL, becomes even more relevant. In a study of all lipoprotein-associated oxPL, it was determined that Lp(a) was found to contain approximately 85% of the total quantified oxPL<sup>135</sup>. In fact, it has even been shown *in vitro* that preferential oxPL enrichment of Lp(a), compared to LDL, increases upon oxLDL incubation, suggesting oxPL transfer from oxLDL to Lp(a)<sup>15</sup>. While both LDL and Lp(a) contain non-



covalently associated oxPL, Lp(a) is unique in that it also contains a covalently-bound oxPL. Originally believed to be present within the KV domain<sup>136</sup>, it has since been determined that the oxPL is covalently attached within the apo(a) KIV<sub>10</sub> domain<sup>13</sup>. Interestingly, as discussed previously, this domain also contains a sLBS. The proximity of these two unique features has led to speculation that the sLBS, known to mediate the interaction of Lp(a) with a variety of ligands, may also serve to bring the covalent oxPL in close proximity to these ligands and, in doing so, facilitate the pro-inflammatory and/or oxidative effects associated with exposure to oxPLs. The role of oxPLs in the facilitation of inflammatory processes in the context of atherosclerosis is well understood: it has been shown that exposure of leukocytes to oxPLs activates a variety of pro-inflammatory responses, namely the secretion of pro-inflammatory/chemoattractant cytokines, and macrophage apoptosis<sup>137,138</sup>. OxPLs have been shown to induce transcription of *CXCL8* and secretion of its cytokine product, IL-8, as well as MCP-1 in endothelial cells *in vitro*<sup>139</sup>. Strong evidence for the role of oxPLs in the development of atherosclerosis *in vivo* was published recently, showing that mice overexpressing a single chain variable fragment transgene of the anti-oxPL E06 IgM (E06-scFv) exhibited significantly slower progression of atherosclerosis compared with non-transgenic mice on an identical high cholesterol diet<sup>140</sup>.

With respect to Lp(a) and apo(a), it has been shown that Lp(a)/apo(a) induce apoptosis in ER-stressed macrophages in an oxPL-dependent manner through the TLR2-CD36 heterodimer; removal of the covalent oxPL from apo(a) with phospholipase A<sub>2</sub> (PLA<sub>2</sub>) destroyed its ability to exert pro-apoptotic effects in this study<sup>34</sup>. Furthermore, it has been shown that THP-1 macrophages increase transcription of *CXCL8* and secretion of IL-8 in response to apo(a) exposure, and that these effects are greatly diminished by PLA<sub>2</sub>-mediated oxPL removal<sup>14</sup>.

Taken together, these data strongly implicate a role for Lp(a)/apo(a)-bound oxPL in the induction and propagation of vascular inflammation, the promotion of macrophage/foam cell apoptosis, and the overall development of atherosclerosis.

#### 1.1.6.2 Functional significance of the lysine binding properties of apo(a) KIV<sub>10</sub>

Apo(a) has been shown *in vitro* to stimulate the RhoA/Rho kinase signaling cascade in endothelial cells, dependent on the presence of the KIV<sub>10</sub> sLBS<sup>141</sup>. The result of this signaling

pathway is increased stress fiber formation, endothelial cell contraction, and increased permeability of the vessel wall. Also through the RhoA/Rho kinase pathway, apo(a) has been demonstrated to stimulate vascular SMC migration, proliferation, and chemorepulsion<sup>125,142</sup>. Additionally, the lysine binding activity of apo(a) has been implicated *in vitro* in the disruption of VE-cadherin/ $\beta$ -catenin complexes, increased nuclear  $\beta$ -catenin translocation, and the subsequent stimulation of prostaglandin synthesis through cyclooxygenase 2 (COX-2) up-regulation in human umbilical vein endothelial cells (HUVECs)<sup>110</sup>. Lastly, it has been shown that apo(a) can inhibit tPA-mediated plasminogen cleavage on the cell surface of endothelial cells, monocytes, and macrophages *in vitro*<sup>26</sup>, and within fibrin clots<sup>5,143</sup>. The cell-surface effect was found to be related to the sLBS function of KIV<sub>10</sub>, and was diminished with the addition of the lysine analog  $\epsilon$ -ACA, strongly indicating a role for the lysine-binding properties of apo(a) in the context of inhibiting plasmin activation.

### 1.1.6.3 The role of Lp(a) in thrombosis and fibrinolysis

A growing body of evidence from *in vitro* studies indicates pro-thrombotic/anti-fibrinolytic roles for Lp(a) and apo(a). The striking homology between apo(a) and plasminogen coupled with the lack of apo(a) protease activity suggests a role for apo(a) as an anti-fibrinolytic factor, owing to its ability to act as a inhibitor of plasmin activation by preventing the binding of plasminogen to surface receptors on endothelial cells and monocytes, and by inhibiting tPA-mediated plasminogen cleavage on the cell surface<sup>26</sup>. Apo(a) slows plasmin formation by inhibiting the conversion of Glu<sup>1</sup>-plasminogen to the more readily activated Lys<sup>77</sup>-plasminogen, thereby inhibiting the feed-forward mechanism by which maximal plasmin activation is achieved<sup>143,144</sup>. In addition to the sLBS function of KIV<sub>10</sub>, this process also requires sequences within the KIV<sub>5-8</sub> and KV domains of apo(a)<sup>145,146</sup>. The apo(a) component of Lp(a) has also been shown to participate in the formation of a plasminogen-tPA-fibrin-apo(a) complex, which exhibits a reduced rate of plasmin activation when compared with the same complex lacking apo(a)<sup>5</sup>. Inhibition of tPA-mediated plasmin activation by apo(a) has also been shown to slow thrombolysis *in vivo*, using both transgenic apo(a) mouse and rabbit jugular vein fibrinolysis models<sup>147,148</sup>. Beyond the inhibition of plasminogen cleavage by apo(a), Lp(a) has also been shown to increase synthesis of plasminogen activation inhibitors by endothelial cells and monocytes *in vitro*, providing another mechanism by which Lp(a) can indirectly inhibit plasmin formation<sup>149,150</sup>.

Finally, Lp(a) has also been implicated as a pro-thrombotic contributor due to its ability to bind tissue factor pathway inhibitor (TFPI), suppressing the anti-coagulant effects that TFPI normally exerts as a result upon binding to Factor Xa and the tissue factor/Factor VIIa complex<sup>151</sup>. As TFPI normally acts as a potent inhibitor of the tissue factor-initiated coagulation cascade, binding and inhibition of TFPI by Lp(a) supports a role for Lp(a) as a pro-thrombotic factor in hemostasis.

Taken together, these data along with those presented in Sections 1.1.6.1 and 1.1.6.2 strongly implicate mechanistic roles for Lp(a)/apo(a) in both inflammatory and pro-thrombotic processes, but there remains debate as to the role of elevated Lp(a) concentrations in thrombosis and fibrinolysis *in vivo*<sup>152</sup>.

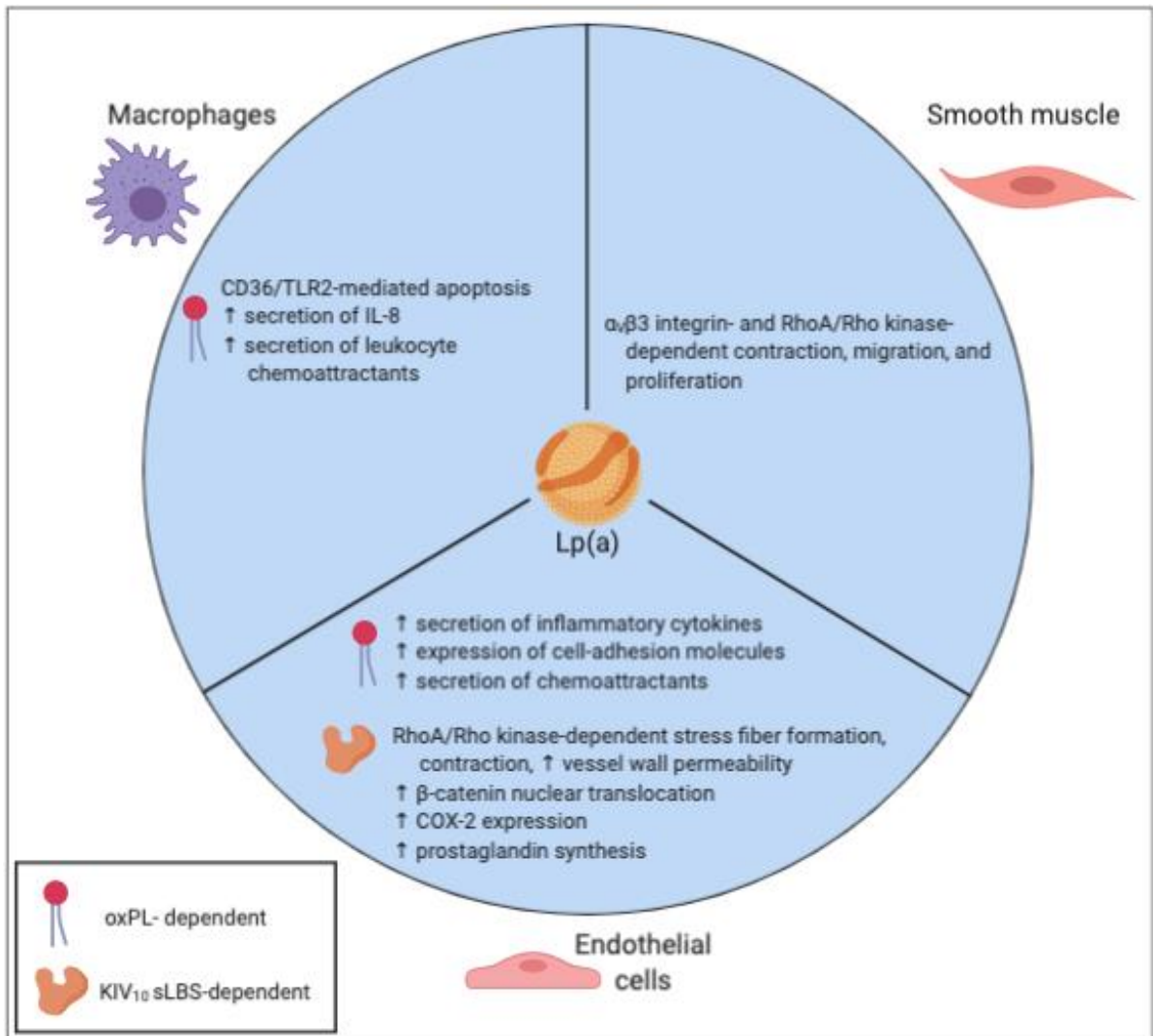


**Figure 1.6. Effects of Lp(a)/apo(a) on vascular cell phenotypes.**

The deleterious effects of Lp(a) and/or apo(a) on a variety of vascular cell types are well documented. These effects importantly include increasing the secretion of IL-8 via NF- $\kappa$ B signaling in macrophages, increasing contraction, migration, and proliferation in smooth muscle cells dependent on  $\alpha_v\beta_3$  integrin and RhoA/Rho kinase signaling, and increasing prostaglandin synthesis in endothelial cells downstream of a sLBS-dependent increase in nuclear translocation of  $\beta$ -catenin and subsequent COX-2 up-regulation. TLR2, toll-like receptor 2; RhoA, Ras homolog gene family, member A; COX-2, prostaglandin-endoperoxidase synthase 2. Figure created with Biorender.com.

### 1.1.7 Lp(a) as a risk factor for CVD

Since its discovery over half a century ago, assessing the role of Lp(a) in the development of CVD *in vivo* remains a daunting challenge. The *LPA* gene, and therefore Lp(a) itself, exists only in humans, apes, and Old World Monkeys. As such, the *in vivo* study of Lp(a) is severely hindered by the unavailability of relevant animal models in determining the role of elevated Lp(a) in CVD. For example, to study Lp(a) in a murine model of disease, mice must 1) be transgenic for human apo(a), 2) produce human apoB-100 as opposed to murine apoB-48, and 3) be bred onto an atherogenic background i.e. *Ldlr*<sup>-/-</sup> or *ApoE*<sup>-/-</sup>.

Assessment of a 58,000-subject meta-analysis of 40 studies showed that individuals with <22 total KIV repeats exhibited increased CAD risk in excess of 2-fold compared to individuals with >22 KIV<sup>153</sup>; the effect of apo(a) isoform size itself on pathogenicity has not been definitively resolved. It is difficult to assess whether these findings are a true representation of the effects of apo(a) isoform size rather than Lp(a) concentration, as many of the studies involved in this meta-analysis did not control for Lp(a) concentration. While studies such as this have reported Lp(a) as a risk factor for CVD for decades, distinguishing Lp(a) as a causal risk factor versus a disease marker had not been possible due to the study designs utilized. A Mendelian randomization study in 2009 confirmed the inverse relationship between *LPA* gene size and Lp(a) plasma levels, and also established a causal role for such “genetically elevated” Lp(a) concentrations in the incidence of CVD<sup>154</sup>. Since then, genome-wide association studies have also determined *LPA* gene size to be a major determinant of CVD risk<sup>155,156</sup>, and other genetic studies have associated two SNPs in the *LPA* gene with increased plasma Lp(a) concentration as well as increased CVD risk<sup>83</sup>. Further genetic studies have allowed us to draw a causal relationship between elevated plasma Lp(a) levels (>50 mg/dL) and >2-fold increased risk for CAD, and indeed that approximately 20% of the global population falls into this risk category<sup>157</sup>. Lp(a) has also been determined to be a causal and independent risk factor for other CVDs such as peripheral vascular disease, ischemic stroke, and calcific aortic valve stenosis<sup>83,154,158–161</sup>.

Despite substantial evidence implicating Lp(a) as an independent and casual risk factor for CVD, current research is still addressing a definitive resolution to the question underlying the “Lp(a) hypothesis”: that specifically lowering Lp(a) levels confers a protective effect with

respect to CVD risk. Findings from recent large-scale clinical trials of anti-PCSK9 antibodies do suggest a benefit associated with Lp(a) reduction independent of other factors<sup>69,70</sup>, but conclusive evidence for such a phenomenon will likely remain beyond reach until therapies targeting Lp(a) specifically, and effectively, can be assessed in large prospective studies.

### 1.1.8 Lipoprotein(a)-lowering therapies

Since its discovery in 1963, a number of therapies have been shown to reduce Lp(a) levels but until recent years there have been few options that are effective beyond modest reduction – and fewer still that are specific for Lp(a). The most well-established class of lipoprotein-lowering drug, the statin, while highly effective at reducing plasma levels of LDL, exhibits a complete lack of efficacy in reducing Lp(a)<sup>162,163</sup>, with some trials even reporting increases in Lp(a) with statin treatment<sup>164</sup>. These reports call our understanding of the mechanism of Lp(a) catabolism through the LDLR into question<sup>73,74</sup>. The therapeutic options that are known to lower Lp(a) fall into four broad categories: antibodies, nucleic acids, small molecules, and non-pharmacological interventions. A summary of drug class, specificity, mechanism of action, and availability can be found in **Table 1.1**.

#### 1.1.8.1 Antibodies that lower Lp(a) concentration

There are two targets to which FDA-approved antibody therapy is available with secondary effects on Lp(a) lowering: PCSK9 and the IL-6 receptor. While they are not specific for Lp(a), monoclonal antibody inhibitors of PCSK9 (evolocumab, alirocumab) and the IL-6 receptor (tocilizumab) have been shown to reduce plasma Lp(a) levels by up to 30% and 40%, respectively<sup>69,165–167</sup>.

Mechanistically, the interaction of PCSK9 with the LDLR prevents LDLR recycling to the plasma membrane and instead promotes its intracellular degradation<sup>168</sup>. Antibody inhibition of PCSK9 by evolocumab or alirocumab prevents the interaction between PCSK9 and the LDLR, thereby increasing the plasma membrane abundance of the LDLR and enhancing clearance of apoB-100-containing lipoproteins (primarily LDL) from the plasma<sup>169,170</sup>. The finding that anti-PCSK9 antibody therapy is able to reduce Lp(a) levels by up to 30% suggests that there may indeed be a role for the LDLR in Lp(a) internalization under the right circumstances: when circulating LDL is low<sup>171</sup>. On the other hand, there is also evidence of decreased Lp(a)

production in response to antibody blockage of PCSK9<sup>171,172</sup>, suggesting the mechanism of Lp(a) lowering by this approach is complex.

In the case of the IL-6 receptor, Lp(a) reductions of up to 41% have been reported in patients undergoing treatment for rheumatoid arthritis with the IL-6 receptor antibody tocilizumab<sup>166,167</sup>. It is theorized that the blockade of IL-6 signaling prevents the induction of *LPA* expression under control of the IL-6 response element mentioned in Section 1.1.3.

### 1.1.8.2 Nucleic acid-based therapies for Lp(a) lowering

Perhaps most promising in the context of Lp(a) lowering therapy are the recent reports of nucleic acid-based therapies targeted specifically to reduce translation of apo(a). Both antisense oligonucleotide (ASO) and double-stranded RNA-interfering (RNAi) options are currently in development and reduce Lp(a) specifically, rather than reducing Lp(a) as a secondary effect of apoB-100-targeted approaches. The ASO IONIS-Apo(a)-LR<sub>x</sub> binds specifically to *LPA* mRNA and targets it for degradation by RNase H1, with a documented downstream Lp(a) reduction of up to 92%<sup>173</sup>. AMG890 is an RNAi option in development by Amgen, specifically targeting *LPA* mRNA as well. While little is known about this brand new drug, Lp(a) reductions of 85-90% in non-human primates have been reported<sup>174</sup>.

Nucleic acids that are not specific to Lp(a) but still reduce plasma Lp(a) levels include mipomersen<sup>65,66</sup> (ASO targeted against *APOB* mRNA) and inclisiran<sup>175,176</sup> (RNAi against *PCSK9* mRNA). Mipomersen and inclisiran have been reported to reduce circulating Lp(a) by up to 39% and 25%, respectively<sup>65,66,175,176</sup>.

### 1.1.8.3 Small molecule approaches to Lp(a) lowering

To date, no small molecules exist to specifically lower plasma Lp(a). A number of small molecules (on the market, and discontinued) have been shown to reduce Lp(a) as a secondary effect. These include niacin<sup>177</sup>, lomitapide (microsomal triglyceride transport protein inhibitor)<sup>67</sup>, and cholesteryl ester transport protein inhibitors such as anacetrapib<sup>178,179</sup>. At present, niacin is the only pharmacological intervention recommended for lowering Lp(a) by both the European Atherosclerosis Society<sup>157</sup> and the National Lipid Association<sup>180</sup>. Decreases in plasma Lp(a) concentrations as high as 40% have been reported with niacin therapy<sup>181</sup>, but multiple large-scale trials have failed to find reductions in major cardiovascular events despite

the positive impact of niacin on plasma lipid profiles<sup>181–183</sup>. The limited set of small molecules with Lp(a)-reducing effects produce modest effects at best, leaving an open market for orally-active Lp(a)-specific therapeutics.

#### 1.1.8.4 Lipoprotein apheresis

Lipoprotein apheresis (LA) is not dissimilar in principle to hemodialysis: whole blood or plasma is circulated extracorporeally through resins, matrices, or filters designed to extract specific lipoproteins, before it is returned to the vasculature. LA most commonly extracts apoB-100-containing lipoproteins including both LDL and Lp(a). LA is an important therapy in those patients with homozygous familial hypercholesterolemia (HoFH), offering a sustained reduction in Lp(a) of 25-40%<sup>184</sup>, and reducing 5-year risk of major adverse coronary events by up to 86% in long-term studies<sup>185–187</sup>. This decreased risk is due to the simultaneous reduction of LDL and Lp(a) in these studies. As such, it is not possible to properly quantify the relative contribution of lowering Lp(a) to overall risk reduction.



**Table 1.1. Therapies that have been shown to reduce plasma Lp(a) concentrations.**

<b>Agent</b>	<b>Class</b>	<b>% Lp(a) ↓</b>	<b>Lp(a)-specificity?</b>	<b>Mechanism of action</b>
Alirocumab	Monoclonal antibody	30	No	Inhibition of PCSK9; ↑ LDL receptor no.; ↓ apo(a) secretion
E06 †	Monoclonal antibody	N/A	No	Blockade of pro-inflammatory oxPL on Lp(a)
Evolocumab	Monoclonal antibody	30	No	Inhibition of PCSK9; ↑ LDL receptor no.; ↓ apo(a) secretion
Tocilizumab	Monoclonal antibody	30	No	IL-6 receptor blockade; ↓ transcription of <i>LPA</i> mRNA
AMG 890 †	RNAi	85-90 <sup>△</sup>	Yes	↓ translation of <i>LPA</i> mRNA
Inclisiran †	RNAi	14-25	No	↓ translation of <i>PCSK9</i> mRNA
IONIS-Apo(a) <sub>Rx</sub> *	ASO	70	Yes	↓ <i>LPA</i> mRNA
IONIS-Apo(a)-L <sub>Rx</sub> †	ASO	90	Yes	↓ <i>LPA</i> mRNA; targeted to hepatocytes by conjugated GalNAc modification
Mipomersen	ASO	21-39	No	↓ <i>APOB</i> mRNA
Anacetrapib *	Small molecule	36	No	Unknown (secretion of apoB?)
Lomitapide	Small molecule	15-20	No	MTP inhibitor; ↓ secretion of apoB-containing lipoproteins
Niacin	Small molecule	25	No	↓ cAMP-mediated transcription of <i>LPA</i>
Lipoprotein apheresis	N/A	70 (acute) 25-40 (sustained)	No	ApoB- or apo(a) affinity-based extracorporeal removal of lipoproteins from plasma

† Therapy in development

\* Development halted

△ Demonstrated in non-human primates

Adapted with modifications from Borrelli *et al.* (2019)<sup>188</sup>.

## 1.2 Aims, rationale, & hypotheses

It has been shown that there is a clear and substantial role for the KIV<sub>10</sub> sLBS of apo(a) in thrombosis and fibrinolysis, and in the modulation of inflammatory gene expression in vascular cell types<sup>5,110,141</sup>. However, the direct contributions of the KIV<sub>10</sub> covalent oxPL to the observed functions of apo(a)/Lp(a) are less clear, due in part to the difficulty associated with manipulation of a modification that we know relatively little about. Here, we seek to elucidate structure-function relationships attributable to the KIV<sub>10</sub> domain of apo(a), in the context of both the sLBS and the covalent oxPL modification, as well as the structural requirement of sLBS function for oxPL addition. The aims of our work are targeted toward 1) expanding our understanding of the specific functions of the covalent oxPL addition to KIV<sub>10</sub> *in vitro*, and 2) characterizing the lysine binding and oxPL status of recombinant apo(a) variants bearing nonsynonymous human-derived polymorphisms in the KIV<sub>10</sub> sequence. We hypothesize that amino acid substitutions in the KIV<sub>10</sub> domain of apo(a) will influence the functional characteristics of this kringle, by modulating its ability to bind lysine and/or host a covalent oxPL modification. Additionally, we hypothesize that the KIV<sub>10</sub> sLBS and covalent oxPL are both relevant in the ability of apo(a) to induce inflammatory phenotypes in vascular cells, as reported previously<sup>14,189</sup>.

### 1.2.1 Aim 1: generation of 17K apo(a) containing the KIV<sub>10</sub> His33→Ala substitution

Identifying the precise amino acid residue in apo(a) that contains the covalent oxPL modification was an aim of a previous student from our group, following the determination that the oxPL is covalently bound within the KIV<sub>10</sub> domain<sup>13</sup>, rather than within the KV domain as previously reported<sup>136</sup>. In order to identify the residue in question, a site-directed mutagenesis approach was used to substitute candidate residues in the KIV<sub>10</sub> domain to alanine, generate recombinant KIV<sub>10</sub>KV proteins containing these mutations, and then assess the sLBS status (Section 2.7) and oxPL status (Section 2.8) of these proteins following purification. Candidate residues were determined based on the type of addition reaction required for covalent oxPL modification. Residues that could participate in a Michael addition reaction (His; Cys residues ruled out due to characteristic saturated disulfide bonding in kringle domains) or form a Schiff base (Arg, Lys) were each mutated individually using this approach. Following generation of these protein species and subsequent assessment of their sLBS and

oxPL status, it was determined that KIV<sub>10</sub> His33 is likely the residue containing the covalent oxPL<sup>190</sup>. Of note, KIV<sub>10</sub> His33→Ala was the only variant that retained its lysine binding ability, but lost reactivity with the E06 anti-oxPL antibody. Based on this information, the first aim was to generate and purify a variant of apo(a) with KIV<sub>10</sub> His33→Ala in the context of 17 KIV domains (17K H33A; corresponds to a naturally occurring apo(a) isoform size). Our goal was to use RNA-Seq to compare the transcriptome of differentiated THP-1 macrophage-like cells treated with 17K H33A to that of cells treated with the wildtype version of recombinant apo(a) (17K). We hypothesized that 17K H33A would induce only sLBS-dependent changes in gene expression, while 17K would induce both sLBS- and oxPL-dependent changes. Using this information, we sought to determine which effects of apo(a) treatment of these cells are due to the covalent oxPL exclusively, furthering our understanding of the potential contributions of Lp(a)/apo(a) to the progression of atherosclerosis.

### 1.2.2 Aim 2: characterize the KIV<sub>10</sub> mutations Met64→Thr and Arg10→Gln

In a large-scale screening study performed by our Dutch collaborator Dr. Erik Stroes (University of Amsterdam), two patients were determined to possess unexpectedly low oxPL despite high Lp(a) levels. Blood samples from these patients were sent to our group, and the KIV<sub>10</sub>-encoding regions of their *LPA* alleles were sequenced. Each patient was heterozygous for a non-synonymous base substitution; one patient had an *LPA* variant encoding Thr at position 64 rather than Met (M64T), and the other, a Gln at position 10 rather than Arg (R10Q). In an effort to understand the contributions of these variants to the properties of KIV<sub>10</sub>, we sought to generate recombinant apo(a) variants containing M64T and R10Q substitutions and determine their lysine binding and oxPL status. We hypothesized that these substitutions would, in some way, influence the ability of KIV<sub>10</sub> to bind lysine and/or be modified with a covalently-bound oxPL.

## 2 Materials and Methods

### 2.1 Cell culture

All cells were cultured in humidified atmosphere with 5% CO<sub>2</sub> and 95% humidity, at 37 °C.

Human embryonic kidney 293 (HEK293) cells as described by Russel *et al.*<sup>191</sup> were cultured in Minimum Essential Medium (MEM; Gibco) supplemented with 5% (v/v) fetal bovine serum (FBS; VWR International) and 1% (v/v) antibiotic/antimycotic (anti-anti; Gibco). HEK293 cells were passaged at a ratio of 1:5 upon reaching 80% confluence.

Human hepatocellular carcinoma (HepG2) cells were purchased from American Type Culture Collection (ATCC; HB-8065™) cultured in Dulbecco's Modified Eagle Medium Nutrient Mixture F-12 (DMEM/F12; Gibco), supplemented with 10% (v/v) FBS and 1% (v/v) anti-anti. HepG2 cells were passaged at a ratio of 1:5 upon reaching 80% confluence.

Human THP-1 acute monocytic leukemia cells (THP-1 monocytes) were purchased from ATCC (TIB-202™) and cultured in Roswell Park Memorial Institute 1640 medium (RPMI-1640; Gibco) supplemented with 10% (v/v) FBS, 1% (v/v) anti-anti, and 55 μM β-mercaptoethanol (complete medium). THP-1 cells were cultured to maintain a density between 3x10<sup>5</sup> and 1x10<sup>6</sup> cells/mL.

### 2.2 Generation of apo(a) expression plasmids

Wildtype apo(a) expression plasmids encoding 17-kringle IV (17K), 14-kringle IV (14K), 6-kringle IV (6K), and a construct containing KIV<sub>10</sub>, KV, and the protease-like domain (10-P) in the pRK5 plasmid, and a wildtype apo(a) expression construct encoding only the KIV<sub>10</sub> and KV domains of apo(a) (KIV<sub>10</sub>KV) in the pcDNA.4c plasmid, were all generated prior to this thesis<sup>13,14,190,192</sup>. Schematic diagrams of these apo(a) species can be found in **Figure 2.1**. All mutagenesis reactions were prepared according to manufacturers' protocols and carried out in a BioRad T100 thermocycler. Sequences of primer pairs used can be found in **Table 2.1**. Mutations were verified via Sanger sequencing performed at the London Regional Genomics Centre (Robarts Research Institute, London, Ontario, Canada) using primer pair A/B for pRK5 plasmids, and an in-house T7 promoter primer for pcDNA.4c plasmids.

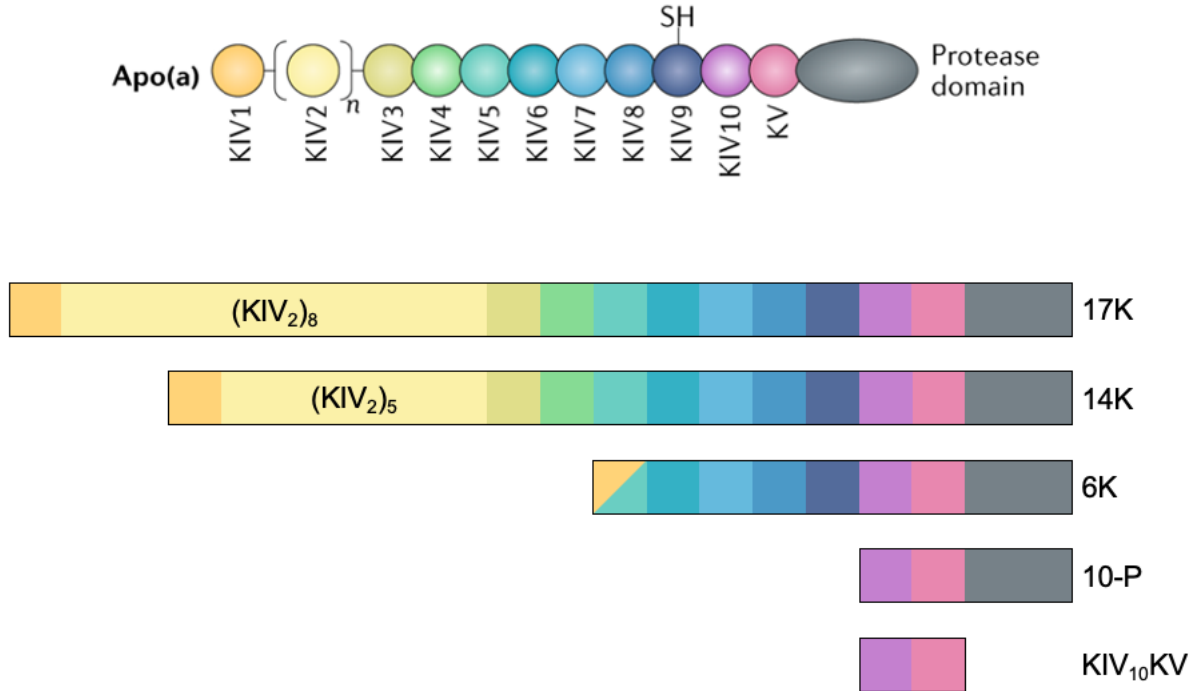


**Figure 2.1. Schematic representations of recombinant apo(a) species.**

Two full-length apo(a) variants were utilized in this thesis, along with three truncated variants. The full-length variants, 17K and 14K, contain one copy of each of the KIV domains, with the exception of KIV<sub>2</sub>, which is found in 8 and 5 copies, respectively. Additionally, these variants contain one copy of the KV and protease-like domains. The 6K apo(a) variant contains a fusion kringle of KIV<sub>1</sub> and KIV<sub>5</sub>, along with one copy of each of KIV<sub>6</sub> through KIV<sub>10</sub>, and one copy of the KV and protease-like domains. The 10-P variant contains only the KIV<sub>10</sub>, KV, and protease-like domains, while KIV<sub>10</sub>KV contains only the KIV<sub>10</sub> and KV domains. Critically, all variants utilized in this thesis contain the KIV<sub>10</sub> domain.

**Table 2.1. Primer pairs used for KIV<sub>10</sub> sequencing and mutagenesis reactions.**

<b>Primer pair</b>	<b>Forward (5'→3')</b>	<b>Reverse (5'→3')</b>
A/B	CCTAGAGACTCCCCTGTTGT	CCCAGTAACAGTGGTTGCCTT
C/D	CATGACACCACACCGG <b>gcg</b> CAGAGGACCCAG	CTGGGGTCCTCTG <b>cg</b> cCCGGTGTGGTGTGTCAG
E/F	GGCCAGAGTTATC <b>a</b> AGGCACATTCTC	GAGAATGTGCCT <b>t</b> GATAACTCTGGCC
G/H	GGCCAGAGTTAT <b>g</b> cAGGCACATTCTC	GAGAATGTGCCT <b>g</b> cATAACTCTGGCC
I/J	GTTTTACCA <b>c</b> GGACCCAGCATC	GATGCTGGGGTCC <b>g</b> TGGTAAAAC
K/L	CAGAGTTATC <b>a</b> AGGCACATTCTC	GCCATTACCATGGTAGCA
M/N	ACCACACCGG <b>a</b> ATCAGAGGAC	GTCATGGATGACCAAGATTGAC
O/P	ACCACACCGG <b>g</b> cTCAGAGGACC	GTCATGGATGACCAAGATTG
Q/R	CACACCGG <b>C</b> aCAGAGGACCC	GTGTCATGGATGACCAAGATTGAC
S/T	ACCACACCGG <b>t</b> ATCAGAGGAC	GTCATGGATGACCAAGATTGAC
U/V	TGTTTTACCA <b>c</b> GGACCCAGC	CCAAGGGCCTGTATCGGC

\*Bold-faced, lower-case letters indicate mismatched bases required for mutagenesis.

### 2.2.1 17K H33A

A 17K plasmid containing the KIV<sub>10</sub> His33→Ala substitution (pRK5.17K.H33A) was generated by site-directed mutagenesis using the QuikChange II XL Site-Directed Mutagenesis Kit (Agilent Technologies Inc.) with primer pair C/D under the following conditions: initial denaturation at 95 °C (1 min), followed by denaturation at 95 °C (50 sec), annealing at 60 °C (50 sec), and extension at 68 °C (11 min, 36 sec) for a total of 18 cycles, followed by a final elongation at 68 °C (7 min).

### 2.2.2 14K mutants

14K plasmids containing the KIV<sub>10</sub> substitutions Arg10→Gln (pRK5.14K.R10Q), Arg10→Ala (pRK5.14K.R10A), and Met64→Thr (pRK5.14K.M64T) were generated using the QuikChange II XL Site-Directed Mutagenesis Kit with primer pairs E/F, G/H, and I/J, respectively, under the same conditions indicated in Section 2.2.1 with the exception of extension for 10 min, 36 sec rather than 11 min, 36 sec. All three reactions were conducted with annealing at 60 °C.

### 2.2.3 6K mutants

6K plasmids containing the KIV<sub>10</sub> substitutions Arg10→Gln (pRK5.6K.R10Q) and His33→Asn (pRK5.6K.H33N) were generated using the Q5 Site-Directed Mutagenesis Kit with primer pairs K/L and M/N, respectively, under the following conditions: initial denaturation at 98 °C (30 sec), followed by denaturation at 98 °C (10 sec), annealing at 62 °C and 67 °C (30 sec), respectively, and extension at 72 °C (4 min) for a total of 25 cycles, followed by a final elongation at 72 °C (2 min).

### 2.2.4 10-P mutants

10-P plasmids containing the KIV<sub>10</sub> substitutions His33→Ala (pRK5.10-P.H33A), His33→Asn (pRK5.10-P.H33N), His33→Gln (pRK5.10-P.H33Q), His33→Tyr (pRK5.10-P.H33Y), and Arg10→Gln (pcDNA.4c.KIV<sub>10</sub>KV.R10Q) were generated using the Q5 Site-Directed Mutagenesis Kit with primer pairs O/P, M/N, Q/R, S/T, K/L, respectively, under the following conditions: initial denaturation at 98 °C (30 sec), followed by denaturation at 98 °C (10 sec), annealing at 69 °C, 67 °C, 69 °C, 67 °C, and 62 °C (30 sec), respectively, and

extension at 72 °C (3 min) for a total of 25 cycles, followed by a final elongation at 72 °C (2 min).

### 2.2.5 KIV<sub>10</sub>KV mutants

KIV<sub>10</sub>KV plasmids containing the KIV<sub>10</sub> substitutions Arg10→Gln (pcDNA.4c.KIV<sub>10</sub>KV.R10Q) and Met64→Thr (pcDNA.4c.KIV<sub>10</sub>KV.M64T) were generated using the Q5 Site-Directed Mutagenesis Kit with primer pairs K/L and U/V, respectively, under the following conditions: initial denaturation at 98 °C (30 sec), followed by denaturation at 98 °C (10 sec), annealing at 62 °C and 69 °C (30 sec), respectively, and extension at 72 °C (3 min) for a total of 25 cycles, followed by a final elongation at 72 °C (2 min).

## 2.3 Generation of stably-expressing cell lines

### 2.3.1 17K H33A

HEK293 cells were co-transfected with the pRK5.17K.H33A and pRSVNeo plasmids (10 µg and 0.5 µg/100 mm culture dish, respectively) using MegaTran 1.0 transfection reagent (Origene) according to the manufacturer's protocol. After 24 hours, transfected cells were exposed to 0.8 mg/mL Geneticin® selection antibiotic (ThermoFisher Scientific) until a viable population of cells was observed. Cells were then trypsinized, counted, and diluted to 8 cells/mL in MEM, and 100 µL of this cell suspension was then plated in each well of a 96-well plate. Once clonal populations of cells were observed, conditioned medium (CM) from each clone was assessed for the presence of apo(a) using an enzyme-linked immunosorbent assay (ELISA). An apo(a)-positive clonal population was selected for use after assessing expression and protein size by immunoblot of CM. ELISA reactivity and immunoblot signal obtained from CM from these clones was exceptionally weak in comparison to control CM from established lines. This process of stable line generation was repeated multiple times for 17K H33A, but apo(a) was only ever detectable in extremely small amounts.

### 2.3.2 KIV<sub>10</sub>KV R10Q and KIV<sub>10</sub>KV M64T

Separate populations of HEK293 cells were transfected with pcDNA.4c.KIV<sub>10</sub>KV.R10Q and pcDNA.4c.KIV<sub>10</sub>KV.M64T plasmids (10 µg/100 mm culture dish) using MegaTran 1.0 transfection reagent according to the manufacturer's protocol. After 24 hours, cells were



exposed to 250  $\mu\text{g}/\text{mL}$  Zeocin™ selection antibiotic (ThermoFisher Scientific) until viable populations of cells were observed.

## 2.4 Preparation of conditioned medium and cell lysates from stable- and transiently-transfected cells

### 2.4.1 Stably-expressing cell lines

HEK293 cells stably expressing proteins of interest were seeded with  $5 \times 10^5$  cells/well in each well of a 6-well plate. Once the cells had formed a confluent monolayer, growth medium was removed and replaced with 750  $\mu\text{L}$  of serum-free Opti-MEM™ medium (Gibco). Serum-free medium was used in order to prevent serum proteins from interfering with immunoblot analysis. After 48 hours of incubation, CM was collected, supplemented with 1% (v/v) Protease Inhibitor Cocktail (PIC; Sigma), and frozen at  $-20\text{ }^\circ\text{C}$  until use. Cells were then lysed by the addition of 300  $\mu\text{L}$  V4 lysis buffer (50 mM Tris-HCl pH 7.4, 1% (v/v) NP-40, 0.25% (w/v) sodium deoxycholate, 150 mM NaCl, 1 mM EDTA). Whole cell lysates were collected and supplemented with 1% (v/v) PIC, homogenized by repeated shearing with a 20g needle, sonicated for 10 minutes at 40 kHz, and centrifuged at  $21,000 \times g$  for 10 minutes to pellet debris. Supernatants were collected and frozen at  $-20\text{ }^\circ\text{C}$  until use. Total protein concentrations of lysate samples were determined by bicinchoninic acid (BCA; Pierce™, ThermoFisher) assay prior to freezing.

### 2.4.2 Transiently transfected cells

Wildtype cells (HEK293 or HepG2) were seeded with  $5 \times 10^5$  cells/well, in a 6-well plate. At approximately 65% confluency, cells were transfected using MegaTran 1.0 transfection reagent (Origene) according to the manufacturer's protocol, using 2  $\mu\text{g}$  DNA/well. Cells were incubated with the transfection mixture for 24 hours, after which the transfection mixture was removed, cells were washed once with sterile 1X phosphate-buffered saline (PBS), and 750  $\mu\text{L}$  of serum-free Opti-MEM™ was added. Collection of CM and whole cell lysates was then performed after 48 hours as described in Section 2.4.1.

## 2.5 Purification of recombinant apo(a)

Recombinant apo(a) was purified from the CM of stably-expressing cell lines. Opti-MEM™ was used for this purpose, and was collected/replaced every 48 hours. After CM was collected, it was supplemented with 1 mM phenylmethylsulfonyl fluoride (PMSF), and stored at -20 °C until purification. Prior to purification, CM was thawed, modified if necessary (i.e. for Ni<sup>2+</sup> Sepharose® purifications), and passed through a 0.2 µm asymmetric polyethersulfone (aPES) vacuum filtration system.

### 2.5.1 Purification of recombinant 17K apo(a) species

As previously described<sup>14</sup>, filtered CM was passed over a column containing Lysine Sepharose® 4B chromatography resin (GE Healthcare Life Sciences). The column was then washed extensively with wash buffer (0.5 M NaCl in 1X PBS), and then bound apo(a) was eluted with wash buffer supplemented with 200 mM ε-ACA. Eluted fractions were analyzed for light absorption at 280 nm ( $A_{280}$ ), and fractions with  $A_{280} > 0.100$  were dialyzed extensively against 1X HEPES-buffered saline (HBS; 20 mM HEPES, 150 mM NaCl, pH 7.4), and concentrated using an Amicon® 10 kDa cutoff centrifugal filter unit (Millipore Sigma).

### 2.5.2 Purification of recombinant KIV<sub>10</sub>KV apo(a) species

Recombinant KIV<sub>10</sub>KV apo(a) species contained a His6 tag encoded by the pcDNA.4c plasmid, thereby allowing these proteins to be purified using Ni<sup>2+</sup> Sepharose® chromatography resin. Prior to vacuum filtration, harvested CM was adjusted to 0.5 M NaCl and supplemented with 0.2 mM β-mercaptoethanol, 5 mM imidazole, 2% (v/v) glycerol, pH 8.0. The modified CM was passed over a column containing Ni<sup>2+</sup> Sepharose® excel chromatography resin (GE Healthcare Life Sciences). The column was washed extensively with KIV<sub>10</sub>KV wash buffer (50 mM NaH<sub>2</sub>PO<sub>4</sub>, 0.5 M NaCl, 1 mM β-mercaptoethanol, 12 mM imidazole, pH 8.0), and then bound KIV<sub>10</sub>KV was eluted with KIV<sub>10</sub>KV wash buffer adjusted to 300 mM imidazole, pH 8.0. Eluted fractions were analyzed for  $A_{280}$ , and fractions with  $A_{280} > 0.010$  were dialyzed extensively against 1X HBS, and concentrated using an Amicon® 10 kDa cutoff centrifugal filter unit.

## 2.6 Purification of plasma-derived Lp(a)

Lp(a) was purified with informed consent from the plasma of a fasted volunteer with high plasma Lp(a) levels and a single 16K apo(a) isoform as described previously<sup>26</sup>, with modifications. Up to 100 mL of whole blood was collected from the donor into EDTA-coated vacutainers® (BD Life Sciences). Plasma was isolated by centrifugation at 4 °C and then supplemented with 100 µM PMSF. Plasma density was adjusted to 1.02 g/mL with the addition of solid NaBr, the volume was adjusted to 40 mL with the addition of sterile 1X PBS, and the modified plasma was loaded into Quick-Seal centrifuge tubes (Beckman-Coulter) and heat-sealed. Sealed tubes were centrifuged at 257,320 x g (50,000 rpm) using a Type 70 Ti rotor in a Beckman-Coulter Optima™ L-100 XP Ultracentrifuge for 18 hours at 10 °C. The top layer of supernatant containing chylomicrons and VLDL was removed (these particles have a density of  $\rho < 1.02$  g/mL), and the infranatant was collected. The infranatant density was then adjusted to 1.21 g/mL with the addition of solid NaBr, the volume was adjusted to 40 mL with the addition of 1X PBS, and the modified plasma was loaded into new Quick-Seal centrifuge tubes and heat-sealed. Sealed tubes were centrifuged as indicated in the previous step. After centrifugation, the top layer of the supernatant (the remaining lipoprotein fraction including Lp(a); these lipoproteins have a density of  $1.02 \text{ g/mL} < \rho < 1.21 \text{ g/mL}$ ) was extracted and dialyzed extensively against Buffer A (20 mM Tris-HCl containing 150 mM NaCl, 0.01% (w/v) NaN<sub>3</sub>, 0.01% (w/v) EDTA, pH 7.4). After dialysis, the lipoprotein fraction was diluted 3-fold with 20 mM Tris-HCl, pH 7.4, and passed over a column containing DEAE-Sepharose® chromatography resin (GE Healthcare Life Sciences) that had been equilibrated with DEAE wash buffer (20 mM Tris-HCl, 50 mM NaCl, pH 7.4). The column was then washed extensively with DEAE wash buffer adjusted to 150 mM NaCl, 7.4, and Lp(a) was then eluted with DEAE wash buffer adjusted to 250 mM NaCl, pH 7.4. Eluted Lp(a) fractions were then pooled and dialyzed extensively against 1X HBS. Purified Lp(a) concentration was measured by BCA assay (Pierce, ThermoFisher Scientific), and purity was analyzed by sodium dodecyl sulfate polyacrylamide gel electrophoresis (SDS-PAGE) followed by silver staining. Aliquots of the purified material were stored at -80 °C.

## 2.7 Determination of lysine binding status of recombinant apo(a) using a lysine binding assay

A chromatography column containing 1 mL of Lysine Sepharose® 4B chromatography resin was prepared. Next, 15 µg of the purified protein of interest was diluted to 1.0 mL in wash buffer (Section 2.5.1) and passed over the column. The column was then washed five times with 1.0 mL of wash buffer to elute unbound material; these wash fractions were collected. Next, the column was subjected to a multi-step ε-ACA elution (100 nM, 1 µM, 10 µM, 100 µM, 1 mM, 10 mM, 100 mM, and 200 mM ε-ACA) in wash buffer. Elution fractions (12 fractions of 1.0 mL each) were collected from this gradient elution. All fractions were assessed for the presence of apo(a) by immunoblot analysis using a polyclonal anti-apo(a) antibody (Affinity Biologicals, 1:10,000) following SDS-PAGE under reducing conditions. SDS-PAGE was conducted using a 12% polyacrylamide gel, and resolved proteins were transferred to a PVDF membrane in 1X transfer buffer (25 mM Tris-HCl containing 192 mM glycine and 10% (v/v) methanol). Proteins were defined as lysine binding-positive if they were eluted during the ε-ACA gradient elution, and lysine binding-negative if they were eluted during the wash steps.

## 2.8 Determination of covalent oxPL modification of apo(a) by E06 immunoblotting

KIV<sub>10</sub>KV apo(a) species (1 µg) were resolved by SDS-PAGE using a 12% polyacrylamide gel, then transferred to a polyvinylidene difluoride (PVDF) membrane (Millipore Sigma) in 1X transfer buffer. The membrane was then blocked for 6 hours in E06 blotting buffer (20 mM Tris-HCl containing 150 mM NaCl, 1% (w/v) bovine serum albumin, 0.1% (w/v) NaN<sub>3</sub>, and 0.27 mM EDTA, pH 7.4) at room temperature. The membrane was then incubated with E06 primary antibody (Avanti Polar Lipids; 1:1000) for 12 hours at room temperature. Next, the membrane was washed with E06 blotting buffer before incubation with an anti-IgM HRP-conjugated secondary antibody (Sigma; 1:7500) for 1 hour at room temperature, followed by another round of washing with E06 blotting buffer. Immediately prior to incubation with chemiluminescent substrate, the membrane was rinsed once with 1X Tris-buffered saline (TBS; 20 mM Tris-HCL containing 150 mM NaCl, pH 7.4). Immunoreactive bands were

visualized using SuperSignal West Femto Maximum Sensitivity Substrate (ThermoFisher Scientific) with a Bio-Rad ChemiDoc™ MP Imaging System.

## 2.9 Detection of apo(a) by immunofluorescence microscopy

### 2.9.1 Sample preparation

HEK293 cells stably expressing 17K apo(a) or 17K H33A apo(a) were seeded at a density of  $2 \times 10^5$  cells/well in 6-well plates containing gelatin-coated 24 mm square glass coverslips. Cells were grown to approximately 65% confluency at which time they were fixed with 85% v/v ethanol, 5% (v/v) glacial acetic acid, and 10% (v/v) 37% formaldehyde for 1 minute and permeabilized for 5 minutes with 0.2% (v/v) Triton X-100 in 1X PBS. Following permeabilization, coverslips were blocked for 1 hour with immunofluorescence blocking buffer (5% (w/v) BSA and 0.1% (v/v) polysorbate 20 in 1X PBS). After blocking, coverslips were incubated in immunofluorescence blocking buffer containing  $\alpha$ 1-4 mouse primary monoclonal antibody against apo(a) (1:200) and a rabbit primary antibody against one intracellular marker of interest (calnexin, Abcam ab22595, 1:2000; *trans*-Golgi network integrated membrane protein 2 (TGN46), Abcam ab50595 1:100; early endosome antigen 1 (EEA1), Abcam ab2900, 1:500; lysosomal-associated membrane protein-1 (LAMP-1), Abcam ab24170, 1:100) for 1 hour at 37 °C. Coverslips were then washed with 0.1% (v/v) polysorbate 20 in 1X PBS. Next, coverslips were incubated in immunofluorescence blocking buffer containing Alexa Fluor® 488-conjugated goat anti-mouse antibody and Alexa Fluor® 568-conjugated goat anti-rabbit antibody (ThermoFisher Scientific; 1:125) for 30 minutes at 37 °C. Finally, coverslips were washed with 0.1% (v/v) polysorbate 20 in PBS, incubated with DAPI (1:3000) in 1X PBS for 5 minutes at room temperature, washed with 1X PBS, and then mounted on glass microscope slides using Shandon™ Immu-Mount™ (Fisher Scientific).

### 2.9.2 Imaging of apo(a)-expressing cells

For the purpose of qualitatively assessing the presence of apo(a) in stable cell lines, slides were imaged using a Zeiss Imager.Z2 microscope with AxioVision Rel. 4.8 software. Images were acquired using a 20 times magnification objective.

To determine intracellular localization of apo(a) in 17K and 17K H33A stable lines, slides were imaged using a Leica Sp8 scanning confocal microscope with Leica Application Suite X (LASX) software. Images were acquired at 2048 x 2048 resolution using a 63 times magnification objective with 1.518 refractive index immersion oil, as well as six times digital zoom.

Co-localization of apo(a) with organelle markers was quantified using LASX, with background and threshold set at 10% and 70%, respectively, for both channels.

## 2.10 Illumina MiSeq Next Generation Sequencing: characterizing the apo(a) transcriptome in human macrophage-like cells

THP-1 monocytes were suspended at a density of  $8 \times 10^5$  cells/mL in RPMI-1640 medium supplemented with 100 nM phorbol-12-myristate-13-acetate (PMA) to induce protein kinase C-mediated differentiation to macrophages<sup>193</sup>. 24-well plates were seeded with 1 mL/well of this suspension. After 36 hours, cells were supplied with fresh PMA-supplemented medium. After a further 36 hours, this medium was replaced with serum-free complete medium (Section 2.1) and incubated for 16 hours (starvation conditions); this was done in order to maximize sensitivity to treatments as previously described<sup>14</sup>. Following starvation, the medium was replaced with fresh serum-free medium supplemented with 250 nM Lp(a), 17K apo(a), 17K D56A apo(a), or no supplement. Each of the aforementioned treatments was performed in the absence of presence of 200 mM  $\epsilon$ -ACA (to inhibit lysine binding) for a total of 8 treatment groups, performed in duplicate. This represented a single biological replicate for each treatment. Cells were incubated with the treatments for 6 hours, after which total RNA was isolated using the QIAGEN RNeasy Mini Kit according to the manufacturer's protocol.

RNA was submitted to the London Regional Genomics Centre (LRGC) for analysis using the Illumina NextSeq 500 (Illumina Inc.). Total RNA samples were quantified using the Qubit 2.0 Fluorometer (ThermoFisher Scientific). Quality was assessed using the Agilent 2100 Bioanalyzer (Agilent Technologies Inc.) and the RNA 6000 Nano kit (Caliper Life Sciences). Samples were then processed using the Vazyme VAHTS Total RNA-seq (H/M/R) Library Prep Kit for Illumina (Vazyme) which includes ribosomal RNA reduction. Samples were depleted and fragmented prior to cDNA synthesis, then cDNA was indexed, cleaned-up and

amplified via polymerase chain reaction. Biological replicate libraries were pooled into one library per treatment. The pooled library size distribution was assessed on an Agilent High Sensitivity DNA Bioanalyzer chip (Agilent Technologies Inc.), and quantified using the Qubit 2.0 Fluorometer. The library was sequenced as a single end run, 1 x76 bp, using a High Output v2 kit (75 cycles). Fastq data files were downloaded from BaseSpace and analyzed using Partek Flow. After importation, data was aligned to hg19 using STAR 2.5.3a and annotated using RefSeq Transcripts 90. Features with more than 5 reads were normalized using counts per million (CPM), then -fold change and p-values were determined using Partek Flow's Gene Specific Analysis (GSA).

## 2.11 Statistical methods for data analysis

Data are presented as mean  $\pm$  standard error of the mean (SEM). Apo(a)-organelle colocalization was determined using LASX, and analyzed using two-tailed students t-tests with significance set at  $p < 0.05$ . Relative E06 reactivity of KIV<sub>10</sub>KV species was determined by densitometric analysis using BioRad Image Lab™ Software 6.0.1, and analyzed using a two-tailed Welch's t-test with significance set at  $p < 0.05$ . Significance for next generation sequencing output was set at  $p < 0.05$  unless indicated otherwise, and determined using Partek Flow's GSA.

### 3 Results

#### 3.1 The amino acid residues KIV<sub>10</sub> His33 and KIV<sub>10</sub> Arg10 are required for processing and secretion of apo(a)

Previous work has shown that the *LPA* gene contains several “null” alleles, wherein no apo(a) protein is detectable in the plasma that corresponds to the null. Null alleles for *LPA* have been shown to exist in both “transcript-negative” and “transcript-positive” forms in cultured baboon hepatocytes: transcript-negative null alleles are either not transcribed or generate a highly unstable transcript, and typical transcript-positive null alleles generate apo(a) species that are translated into the ER but are unable to be secreted, as defined by White *et al.*<sup>40</sup>. Additionally, a different variety of null allele leads to the secretion of apo(a) species that are unable to form Lp(a) due to truncations prior to the kringle domains required for Lp(a) assembly<sup>71,88</sup>. Unfortunately, the White *et al.* report<sup>40</sup> of ER-retained apo(a) species preceded the wide availability of high-throughput DNA sequencing methods, and, as such, DNA sequences corresponding to the transcript-positive null apo(a) species described previously were not determined. At the time of publication, however, the authors speculated that DNA mutations may have given rise to “rogue” kringles that are unable to properly fold, and cause apo(a) species containing them to be retained in the ER. This is of key interest to the results presented herein, as we have demonstrated a molecular basis for ER-retained apo(a) species corresponding to the transcript-positive null allele expression phenotype described previously<sup>40</sup>. In our study, we have identified two key amino acid residues in apo(a) KIV<sub>10</sub> that are absolutely required for the normal processing and secretion of apo(a): Arg10 and His33.

##### 3.1.1 17K H33A is translated, but not secreted by HEK293 cells

Substitution of the His33 residue in KIV<sub>10</sub> was originally conceived as a means of generating an apo(a) protein species that would retain KIV<sub>10</sub> sLBS function, but would be incompatible for covalent oxPL addition. This proposal was based on previous findings from our group indicating that KIV<sub>10</sub> His33 may serve as the site of oxPL modification<sup>190</sup>. As such, the first step was to generate and purify 17K H33A apo(a) to characterize the functional role of the covalent oxPL in KIV<sub>10</sub>. In order to achieve this, a plasmid encoding this apo(a) variant (pRK5.17K.H33A) was generated using site-directed mutagenesis. A line of HEK293 cells stably expressing 17K H33A was established using the method described in Section 2.3.1. CM



from this cell line was collected, but no apo(a) was detectable in this medium by immunoblot. This result was consistently reproduced over a number of attempts made to generate this stable line, prompting immunofluorescent staining to determine if the cells were able to produce the protein, but unable to secrete it, as described previously<sup>40</sup> (**Figure 3.1**). After observing that apo(a) was abundant within the 17K H33A-expressing cells using immunofluorescence, but undetectable in CM from these cells, an immunoblot of CM and cell lysates was performed to compare the wildtype 17K cell line to the 17K H33A line (**Figure 3.2**). Two distinct sizes of apo(a) were present in the lysates of 17K-expressing cells, but only the larger size (corresponding to mature apo(a)) was detected in CM. In the lysates from the 17K H33A-expressing cells, only the smaller size (corresponding to unprocessed/immature apo(a)) was detected, and no apo(a) was detected in the corresponding CM.

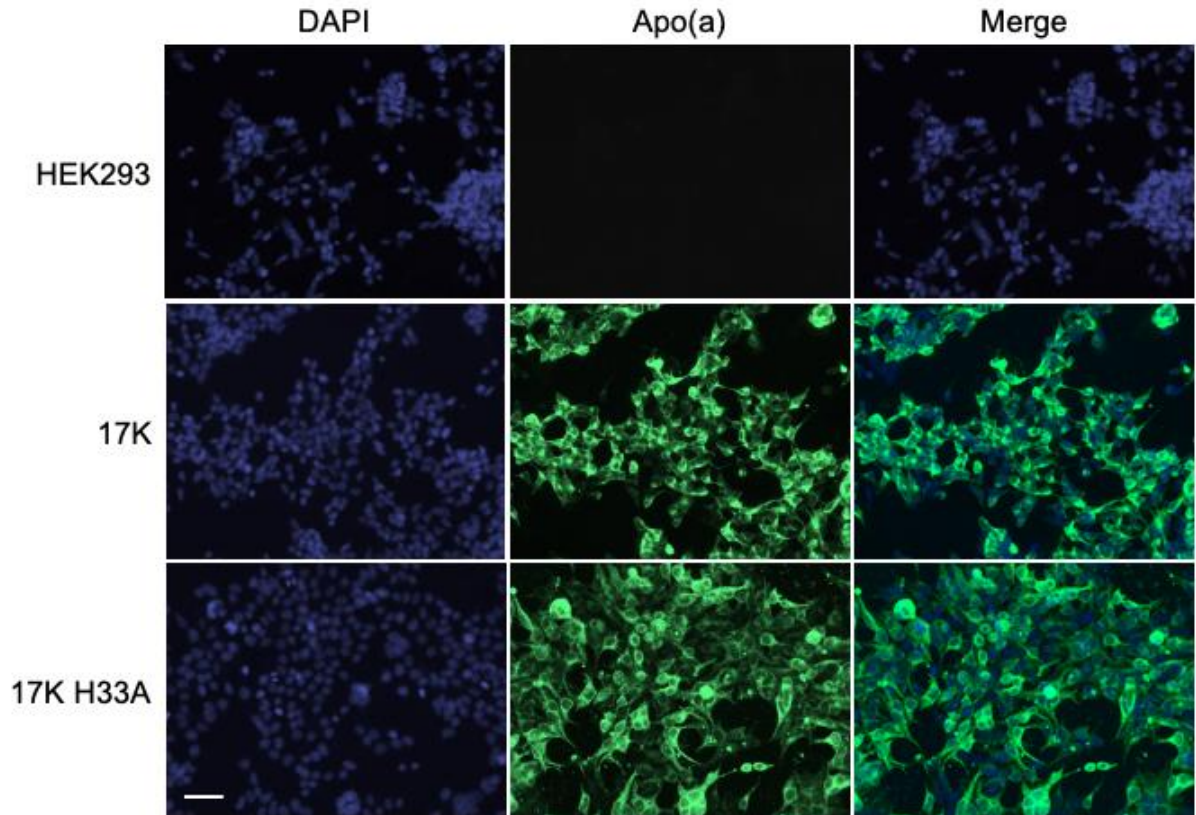


**Figure 3.1. HEK293 17K H33A cells exhibit abundant apo(a) content.**

Wildtype, 17K, and 17K H33A (stably-expressing) HEK293 cells were prepared for imaging as described in Section 2.9, and were stained for apo(a) using the  $\alpha$ 1-4 mouse monoclonal primary antibody and Alexa Fluor® 488-conjugated anti-mouse secondary antibody (green), and nuclei using DAPI (blue). Cells were imaged at 20 times magnification in all cases using a Zeiss Imager.Z2 microscope with AxioVision Rel. 4.8 software. Scale bar = 50  $\mu$ m.

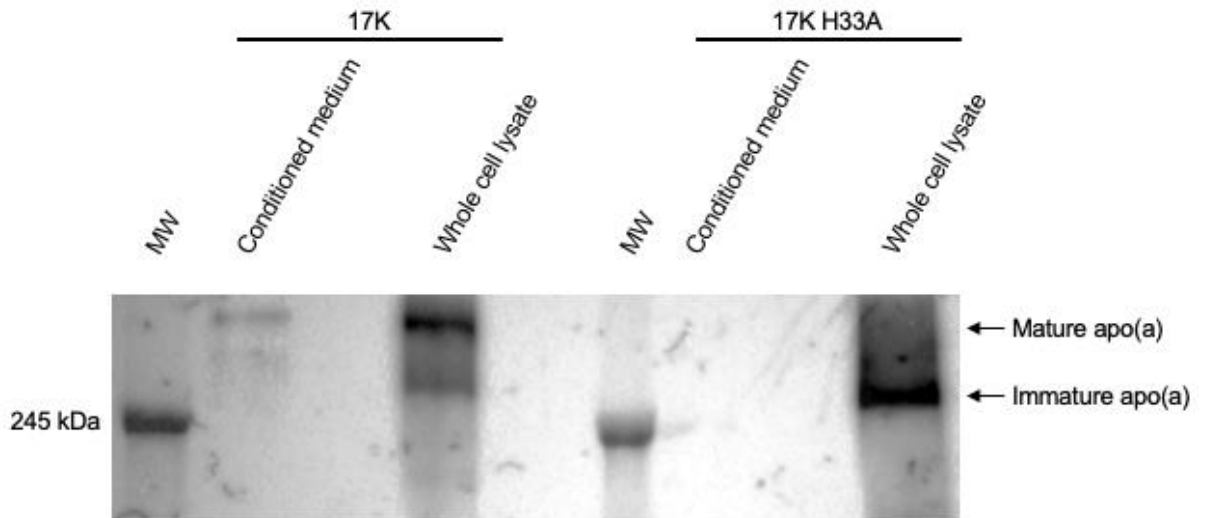


**Figure 3.2. 17K H33A is not secreted, and is found at a reduced molecular weight in cell lysates.**

CM and whole cell lysates were collected from HEK293 cells stably expressing 17K and 17K H33A variants of apo(a). Lysate samples contained a total of 15  $\mu$ g protein as determined by BCA assay. Each CM sample was prepared using a volume of CM that was proportional to the volume of lysate used for the corresponding lysate sample, to approximately control for cell number. Samples were analyzed by SDS-PAGE using a 7% polyacrylamide gel under non-reducing conditions, and resolved proteins were transferred to a PVDF membrane and immunoblotted for apo(a) using the mouse  $\alpha$ 1-4 monoclonal antibody. Band sizes corresponding to mature and immature forms of apo(a) are indicated. MW = molecular weight marker.

### 3.1.2 Truncated apo(a) species with additional KIV<sub>10</sub> His33 substitutions are translated, but not secreted by HEK293 cells

After identifying that 17K H33A apo(a) was present within cells but not secreted, different apo(a) variants were explored, as well as different substitutions to replace His33. The goals of this process were to determine 1) if the apo(a) isoform used, in this case 17K, was a factor in the observed lack of secretion, and 2) if residues other than alanine, and more similar to histidine, would be less disruptive at position 33. Initially, plasmids encoding substitutions of H33N, H33Q, and H33Y (based on similarity to histidine, without the potential for oxPL addition) were generated by site-directed mutagenesis in the context of pRK5.10-P – a plasmid expressing a truncated variant of apo(a) that contains the critical KIV<sub>10</sub> domain, as well as the KV and protease-like domains. Apo(a) was detectable in CM from cells transfected with the wildtype 10-P plasmid, but not the mutant variants (**Figure 3.3**). No apo(a) was detectable in the lysates of the transfected cells corresponding to either wildtype or mutant plasmids. In light of the low abundance of recombinant 10-P species, further experiments utilized the pRK5.6K plasmid, which exhibits very high expression levels of the corresponding recombinant protein and possesses the critical KIV<sub>10</sub> domain.

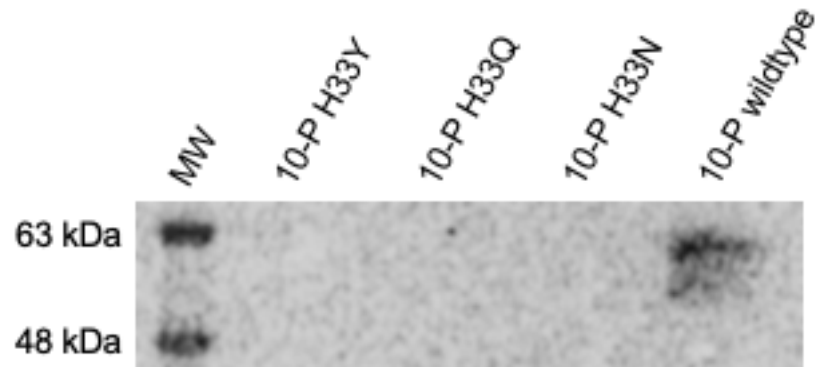


**Figure 3.3. 10-P apo(a) variants with substitutions to KIV<sub>10</sub> His33 are not secreted.**

CM was collected from HEK293 cells transiently transfected with variants of the 10-P apo(a)-encoding vector. All samples were prepared under non-reducing conditions, and an equal volume of CM was used to make up each sample. Samples were analyzed using SDS-PAGE with a 12% polyacrylamide gel, resolved proteins were transferred to a PVDF membrane, and immunoblotted for apo(a) using the mouse a34 monoclonal antibody. MW = molecular weight marker.

In the context of pRK5.6K, an H33N substitution was introduced to further test the effects of His33 substitution on apo(a) secretion using an apo(a) variant that exhibits a relatively high level of expression, and, as such, was expected to be detectable in both CM and cell lysates. In order to also address the possibility that previous observations of non-secretion were cell type-specific, transient transfections of 6K and 6K H33N were performed in HepG2 cells in addition to HEK293, since human hepatocytes synthesize apo(a) *in vivo*. In this experiment, the 6K H33N apo(a) variant showed the same pattern of expression as 17K H33A: in both cell types, no apo(a) was detectable in CM, and only a smaller-sized, incompletely processed apo(a) species was detectable in lysates from cells transiently transfected with this plasmid (compared with both sizes present in cells transfected with wildtype 6K) (**Figure 3.4**).

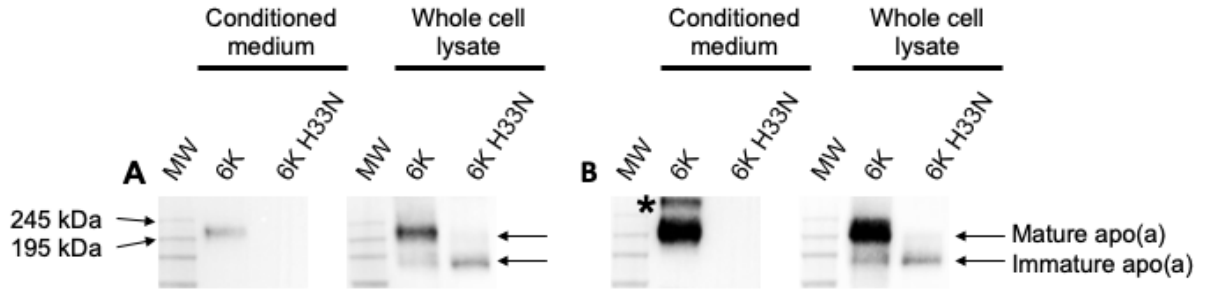


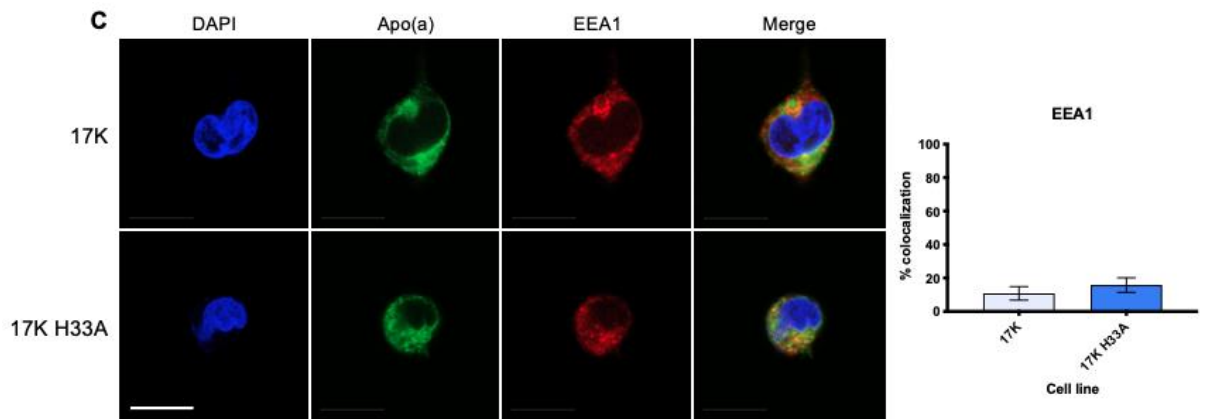
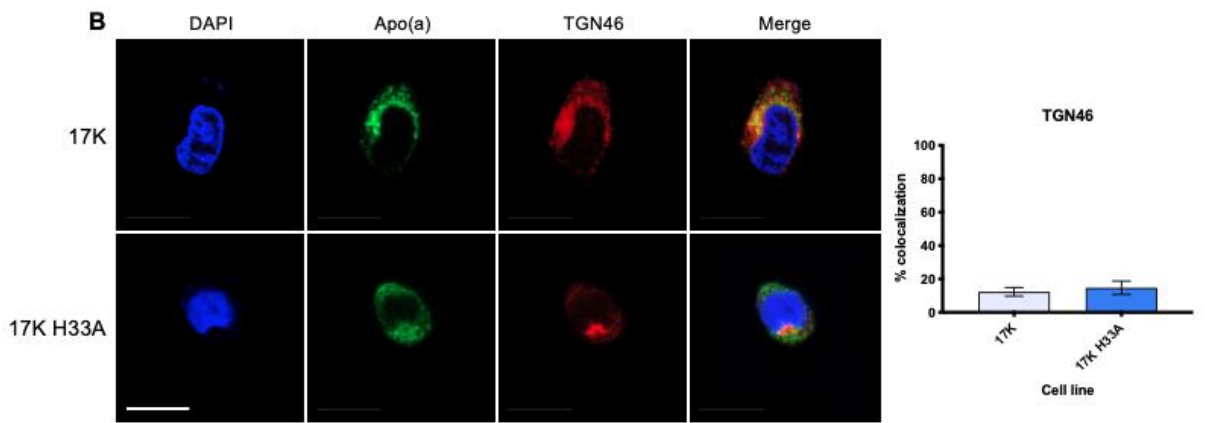
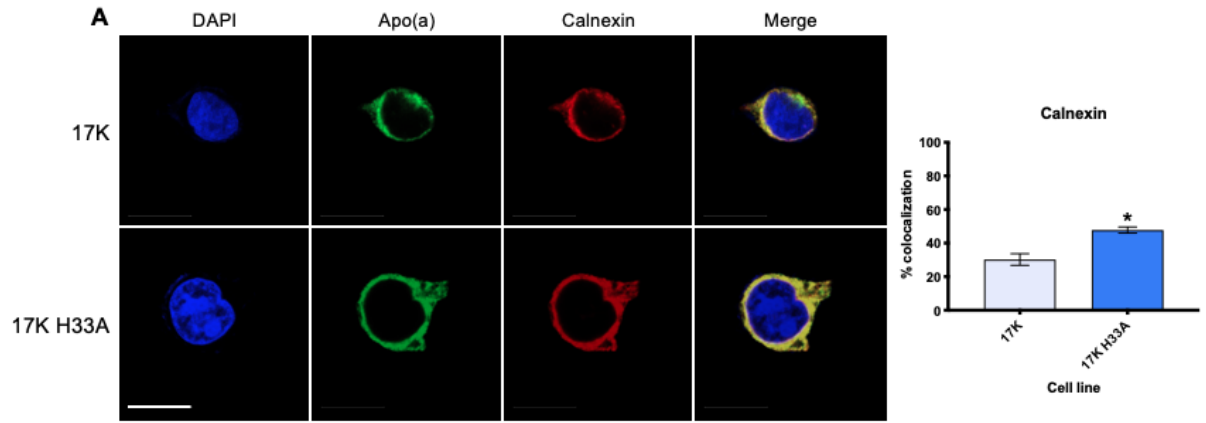
**Figure 3.4. 6K H33N apo(a) is not secreted by HEK293 or HepG2 cells.**

CM and whole cell lysates were collected from (A) HEK293 and (B) HepG2 cells transiently transfected with recombinant 6K apo(a). All samples were prepared under non-reducing conditions. Lysate samples contained a total of 15  $\mu$ g protein as determined by BCA assay. CM samples were prepared using volumes of CM that were proportional to the volume of lysate used for the corresponding lysate sample, to approximately control for cell number. Samples were analyzed by SDS-PAGE using 4-20% polyacrylamide gradient gels (ThermoFisher Scientific), transferred to a PVDF membrane, and immunoblotted for apo(a) using a sheep  $\alpha$ -Lp(a) polyclonal antibody (Affinity Biologicals). Band sizes corresponding to mature and immature forms of apo(a) are indicated. Asterisk = proposed homodimer of 6K, MW = molecular weight marker.

### 3.1.3 17K H33A is retained in the endoplasmic reticulum in HEK293 cells

Histidine is present at position 33 in all apo(a) and plasminogen kringle domains<sup>4</sup>, and amino acid substitution at this position has never been reported. As such, no mechanisms have been proposed for the intracellular retention we have observed for protein species containing substitutions at this position. In an attempt to explain these observations in the context of previous work showing ER-retained species of apo(a) with the same expression phenotype<sup>40</sup>, confocal immunofluorescence microscopy was performed to assess the co-localization of mutated and wildtype apo(a) with a number of subcellular structures: ER (calnexin), *trans*-Golgi (TGN46), early endosomes (EEA1), and lysosomes (LAMP-1), as described in Section 2.9. It was determined that 17K H33A exhibits higher co-localization with calnexin than does wildtype 17K (**Figure 3.5**).





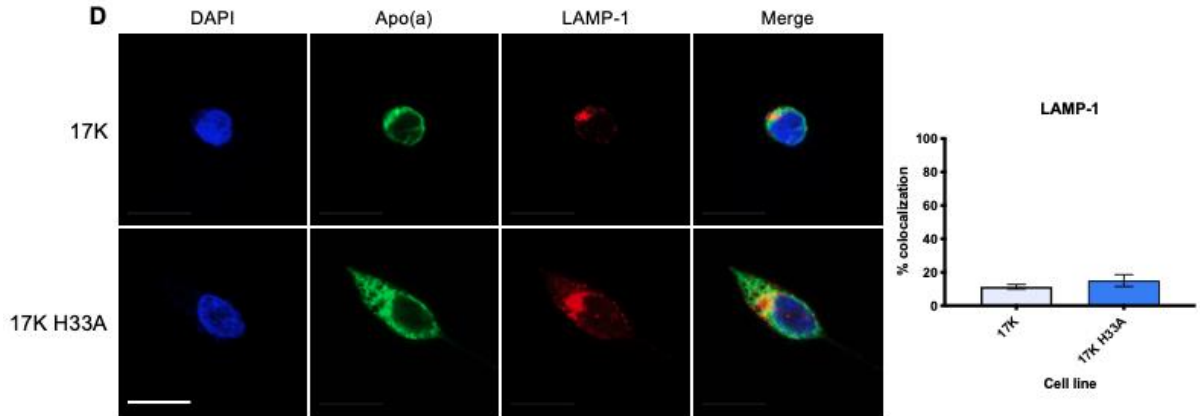


**Figure 3.5. 17K H33A apo(a) exhibits increased co-localization with calnexin compared with wildtype 17K.**

HEK293 cells stably expressing 17K apo(a) (17K) or 17K H33A apo(a) (17K H33A) were immunostained for apo(a) (green) and intracellular markers of interest (red). Apo(a) was co-stained alongside (A) calnexin, ER; (B) TGN46, *trans*-Golgi (C) EEA1, early endosomes; (D) lysosomes, LAMP-1; representative images are shown. The 17K H33A apo(a) variant (n=3) exhibited greater co-localization with calnexin than the 17K wildtype (n=3) ( $p=0.01$ ). Each biological replicate represents the set of values obtained from analysis of organelle co-localization in 3 individual cells from a single experiment. Data are shown as mean  $\pm$  SEM ( $*p=0.01$ ) determined by two-tailed students t-test. Cells were imaged at 63 times magnification with 1.518 refractive index oil and six times digital zoom, in all cases, using a Leica Sp8 scanning confocal microscope with Leica Application Suite X software. Scale bar = 10  $\mu\text{m}$ .

### 3.1.4 6K R10Q is translated, but not secreted by HEK293 and HepG2 cells

In collaboration with Dr. Erik Stroes (University of Amsterdam), the substitution of Arg10→Gln (R10Q) in apo(a) KIV<sub>10</sub> was first proposed as a potential modulator of apo(a) function after it was observed that an individual with high Lp(a) levels, but unexpectedly low oxPL, was heterozygous for this substitution. In order to characterize any functional differences imparted to apo(a) by Gln at KIV<sub>10</sub> position 10, we sought to generate recombinant apo(a) species bearing this change, and to subsequently assess lysine binding and oxPL status of these variants in comparison to wildtype apo(a). Initially, this substitution was generated in the context of pcDNA.4c.KIV<sub>10</sub>KV and pRK5.10-P, but no apo(a) was detectable in the CM or cell lysates from HEK293 cells transfected with these plasmids. As such, a pRK5.6K.R10Q plasmid was generated by site-directed mutagenesis with the goal of increasing overall abundance. A transient transfection experiment was conducted with pRK5.6K.R10Q in the same way as for the pRK5.6K.H33N plasmid, using both HepG2 and HEK293 cells. A similar pattern of expression was observed for the R10Q variant as we observed for the H33X variants: no apo(a) was detectable in CM, and only a smaller protein, corresponding to an incompletely processed apo(a) species, was observed in cell lysates (**Figure 3.6**).

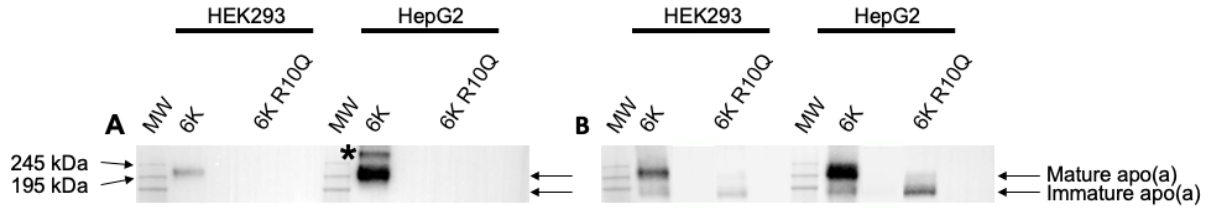


**Figure 3.6. 6K R10Q apo(a) is not secreted by HEK293 or HepG2 cells.**

(A) CM and (B) whole cell lysates were collected from HEK293 and HepG2 cells transiently transfected with variants of 6K apo(a). All samples were prepared under non-reducing conditions. Lysate samples contained a total of 15  $\mu$ g protein as determined by BCA assay. CM samples were prepared using volumes of CM that were proportional to the volume of lysate used for the corresponding lysate sample, to approximately control for cell number. Samples were analyzed by SDS-PAGE using 4-20% polyacrylamide gradient gels (ThermoFisher Scientific), transferred to a PVDF membrane, and immunoblotted for apo(a) using a sheep  $\alpha$ -Lp(a) polyclonal antibody (Affinity Biologicals). Band sizes corresponding to mature and immature forms of apo(a) are indicated. Asterisk = proposed homodimer of 6K, MW = molecular weight marker.

### 3.1.5 14K R10Q and 14K R10A recombinant apo(a) variants are translated, but not secreted by HEK293 and HepG2 cells

While the 6K apo(a) minigene generally mimics the characteristics of its full-length apo(a) counterpart, it has been reported previously that results from experiments using this apo(a) variant do not always yield the same results as full-length apo(a)<sup>192,194,195</sup>. It was therefore important in our studies to verify that the observed pattern of non-secretion with 6K R10Q was also observed using a full-length apo(a) species. To test this, the R10Q mutation was introduced in pRK5.14K, as 14K apo(a) is a full-length, physiologically relevant isoform with high expression levels in cultured cells owing to its relevantly low number of KIV domains. With respect to the R10Q substitution, it is imperative to consider that this is a naturally occurring mutation in the human population (rs776662773, prevalence 0.01-0.03%), meaning that the implications of our *in vitro* characterization of this substitution, and of the importance of Arg10 in general, are of direct relevance to the study of apo(a) in humans. A 14K R10A variant was also generated in order to determine whether the observed characteristics from the R10Q version were the result of the presence of Gln10. A transient transfection experiment was conducted in HEK293 and HepG2 cells using wildtype, R10Q, and R10A variants of 14K apo(a). CM and cell lysates were collected and immunoblotted for apo(a). The wildtype 14K apo(a) was observed in lysates at two distinct sizes. The larger size was the only species detectable in CM. It was observed that only the smaller size of the R10Q variant was present in cell lysates; this was also observed for the R10A variant. These findings were consistent in both HepG2 and HEK293 cells (**Figure 3.7**).

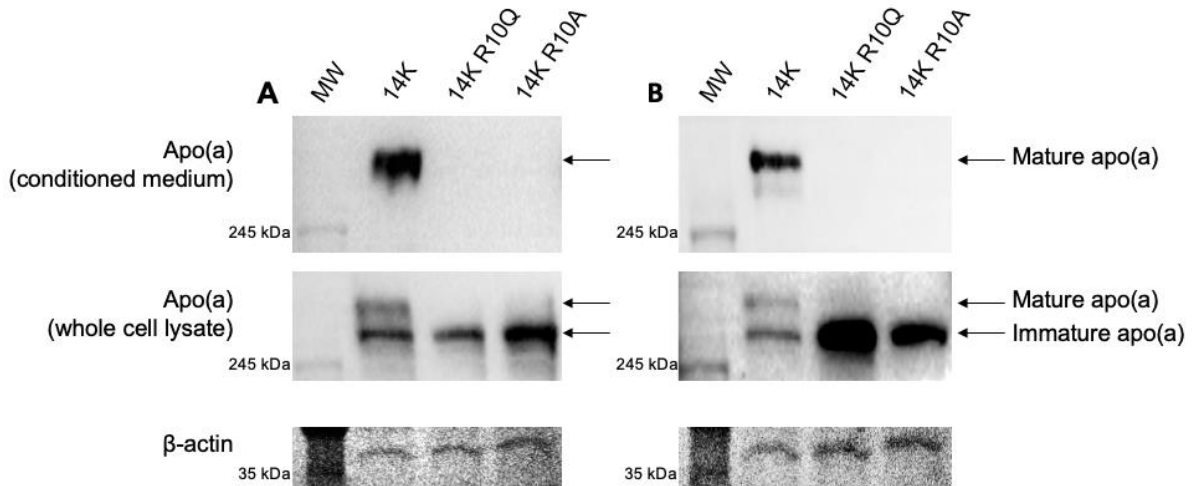


**Figure 3.7. R10Q and R10A variants of 14K apo(a) are not secreted by HEK293 or HepG2 cells.**

CM and whole cell lysates were collected from (A) HEK293 and (B) HepG2 cells transiently transfected with variants of 14K apo(a). All samples were prepared under non-reducing conditions. Lysate samples contained a total of 15  $\mu$ g protein as determined by BCA assay. CM samples were prepared using volumes of CM that were proportional to the volume of lysate used for the corresponding lysate sample, to approximately control for cell number. Samples were analyzed by SDS-PAGE using split 7/15% polyacrylamide gels. Resolved proteins were transferred to a PVDF membrane, and immunoblotted for apo(a) using a sheep  $\alpha$ -Lp(a) polyclonal antibody (Affinity Biologicals). Band sizes corresponding to mature and immature forms of apo(a) are indicated.  $\beta$ -actin was visualized by Imperial<sup>TM</sup> protein stain (ThermoFisher Scientific). MW = molecular weight marker.

### 3.2 Met/Thr at KIV<sub>10</sub> position 64 modulates the degree of covalent oxPL modification, but not sLBS function

As described in Section 1.2.2, a second patient was identified by our collaborator Dr. Erik Stroes (University of Amsterdam) as possessing unusually low oxPL levels despite high Lp(a); upon KIV<sub>10</sub> exon sequencing of this patient, a non-synonymous Met64→Thr (M64T) substitution was identified. Interestingly, despite both patients being classified as possessing unusually low oxPL, the M64T patient had nearly 50-fold greater apo(a)-associated oxPL than the R10Q patient. Further, most apo(a) alleles contain threonine at position 64 (“major allele”), and methionine replaces it in only 25-35% of alleles (“minor allele”). The apo(a) sequence our group has used historically encodes the minor allele<sup>4</sup>, so while the Thr64 substitution was not particularly rare (as was R10Q), it presented an opportunity to probe these two common variants for potential differences in KIV<sub>10</sub> functionality. The M64T substitution was generated by site-directed mutagenesis in pcDNA.4c.KIV<sub>10</sub>KV. A line of HEK293 cells stably expressing this variant was generated, and recombinant protein was purified from the CM of these cells as described in Section 2.5.2. First, the lysine binding ability of the apo(a) KIV<sub>10</sub>KV M64T variant was characterized using the lysine binding assay described in Section 2.7, comparing it to the Met64 positive control, and a non-lysine binding negative control which contains a KIV<sub>10</sub> Asp56→Ala substitution (**Figure 3.8**). Here, we found that the M64T variant binds lysine in a manner comparable to the corresponding Met64 variant.

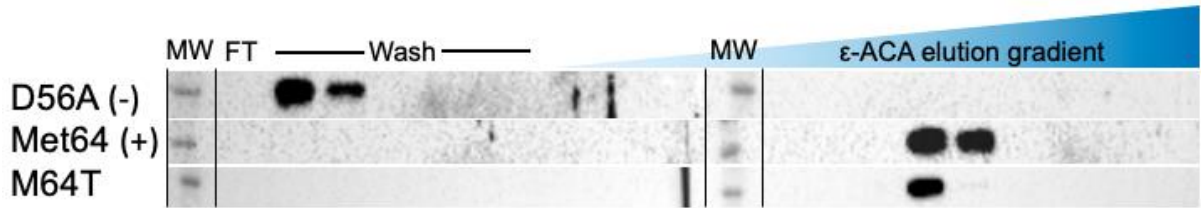


**Figure 3.8. The KIV<sub>10</sub>KV M64T apo(a) variant binds Lysine Sepharose® in a comparable manner to the Met64 variant.**

Lysine binding assays were conducted for each variant (D56A, negative control; Met64, minor allele, positive control; M64T, major allele) as described in Section 2.7. The D56A variant did not bind to the resin, and was eluted non-specifically during the wash steps. The Met64 variant remained bound to the resin and was specifically eluted by the lysine analog  $\epsilon$ -ACA. Similar to the Met64 variant, the M64T variant remained bound to the resin and was eluted with  $\epsilon$ -ACA. MW = molecular weight marker, FT = flow-through fraction.



After determining that the lysine binding function of the KIV<sub>10</sub>KV M64T variant was not different from the corresponding Met64 variant, the presence of covalently-bound oxPL was assessed by E06 immunoblot as described in Section 2.8. Initially, the M64T variant was compared to the oxPL-deficient D56A variant to qualitatively determine its oxPL status (**Figure 3.9a**). After confirming that the M64T variant was oxPL-positive, we compared it to the Met64 variant to assess relative amounts of oxPL modification (**Figure 3.9b**). The relative amount of covalent oxPL associated with the M64T variant compared to the Met64 variant was determined by immunoblot densitometry to be approximately 2.8-fold (**Figure 3.10**).

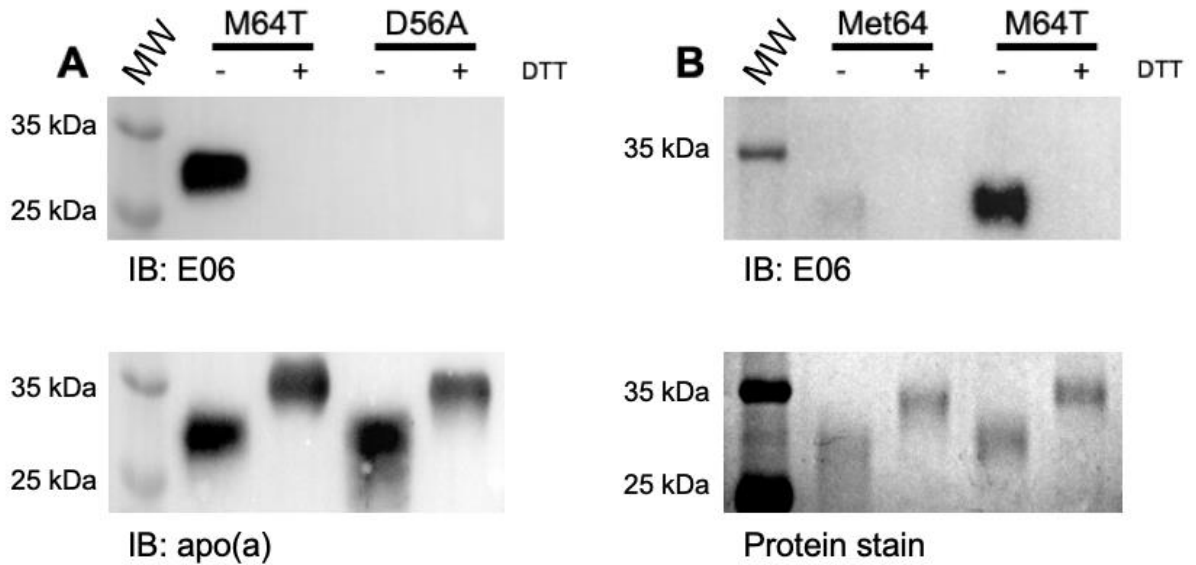


**Figure 3.9. Representative immunoblots comparing E06 reactivity of apo(a) KIV<sub>10</sub>KV M64T to KIV<sub>10</sub>KV D56A and Met64 KIV<sub>10</sub>KV.**

Purified KIV<sub>10</sub>KV proteins (1  $\mu$ g) were analyzed by SDS-PAGE using a 12% polyacrylamide gel. Resolved proteins were transferred to a PVDF membrane and immunoblotted for oxPL using the E06  $\alpha$ -oxPL IgM (Avanti Polar Lipids). **(A)** KIV<sub>10</sub>KV M64T and D56A variants were compared to qualitatively assess the presence of covalent oxPL in the M64T variant, using the D56A variant as a negative control. Membrane was stripped using 0.5 M NaOH and re-blotted for apo(a) using a sheep  $\alpha$ -Lp(a) polyclonal antibody (Affinity Biologicals). **(B)** The KIV<sub>10</sub>KV M64T variant was compared to the Met64 variant to quantitatively assess relative E06 reactivity, and an Imperial™ protein stain (ThermoFisher Scientific) was conducted to control for mass of loaded proteins. In both **(A)** and **(B)**, sample reduction using 10 mM dithiothreitol (DTT) abrogated E06 signal. MW = molecular weight marker.

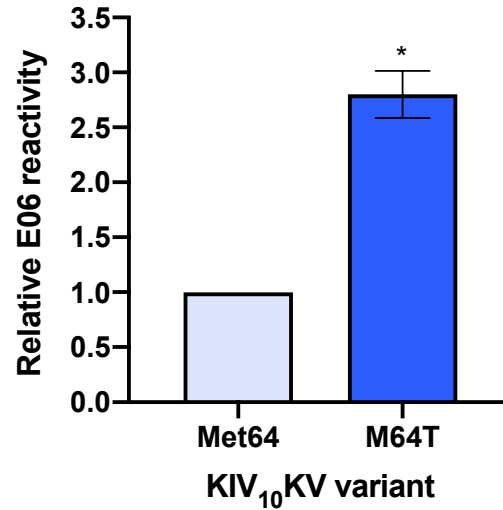


**Figure 3.10. Relative oxPL signal abundance determined by E06 immunoblot densitometry of apo(a) KIV<sub>10</sub>KV Met64 and M64T variants.**

KIV<sub>10</sub>KV M64T exhibited a mean oxPL immunoblot signal intensity that is 2.8 ( $\pm 0.2$ )-fold greater than the Met64 variant ( $n=3$ ). Each biological replicate represents the densitometric comparison of E06 signal for each protein variant after controlling for mass of loaded protein using the Met64 band as the reference point in each case. Data are shown as mean  $\pm$  SEM (\* $p = 0.01$ ); analysis of significance was determined by two-tailed Welch's t-test.

### 3.3 The structure and functions of apo(a) KIV<sub>10</sub> are implicated in the induction of pro-atherogenic phenotypes in macrophage-like cells

The covalent oxPL of apo(a) has previously been implicated by multiple sources as an important contributor to the induction of inflammatory phenotypes in vascular cells<sup>14,140,189</sup>. However, the exact contributions of the covalent oxPL to these inflammatory phenotypes have not been extensively characterized. At the outset of this project, we sought to directly assess gene induction effects attributable exclusively to the covalent oxPL by comparing the transcriptome of THP-1 macrophages treated with wildtype apo(a) (17K; sLBS- and oxPL-positive) to that of cells treated with KIV<sub>10</sub> His33-substituted apo(a) (17K H33A; sLBS-positive, oxPL-negative). It was important to maintain the integrity of the KIV<sub>10</sub> sLBS in this context since it has been shown that this functionality can contribute to the induction of pro-inflammatory effects in vascular cell types<sup>110</sup>. Apo(a) species containing the covalent oxPL but lacking sLBS activity is not possible, as covalent oxPL addition cannot occur without lysine binding. After determining that substitution of KIV<sub>10</sub> His33 results in a transcript-positive null allele for the *LPA* gene and, in turn, that purification and experimental use of this recombinant species would not be possible, our approach was modified to assess the effects of both the sLBS and the oxPL indirectly. We did this by utilizing the lysine analog  $\epsilon$ -ACA to selectively eliminate lysine binding-dependent gene induction/repression in THP-1 macrophages treated with apo(a). To assess the effects that are solely attributable to the presence of the KIV<sub>10</sub> oxPL, we compared the transcriptomes of THP-1 macrophages treated with 17K to those treated with a 17K version of the D56A variant (sLBS- and oxPL-negative), both in the presence of 200 mM  $\epsilon$ -ACA. We also compared the transcriptomes of THP-1 macrophages treated with 17K alone or 17K in the presence of 200 mM  $\epsilon$ -ACA, to assess effects that are contingent on lysine binding, but represent the co-operative effects of apo(a) lysine binding and covalent oxPL (henceforth “LBS-facilitated effects”).

Overall, these experiments included 8 treatments, as follows: 250 nM of either Lp(a), 17K apo(a), 17K D56A apo(a), or no treatment (NT) – each in the presence or absence of 200 mM  $\epsilon$ -ACA (**Figure 3.11**). A t-distributed stochastic neighbour embedding (t-SNE) plot is shown to demonstrate the consistency we observed between biological replicates for each treatment (**Figure 3.12**). This variety of treatments yielded a very large data set and the opportunity to

make many comparisons, but only those comparisons which we felt were most relevant to the scope of this thesis were explored herein.

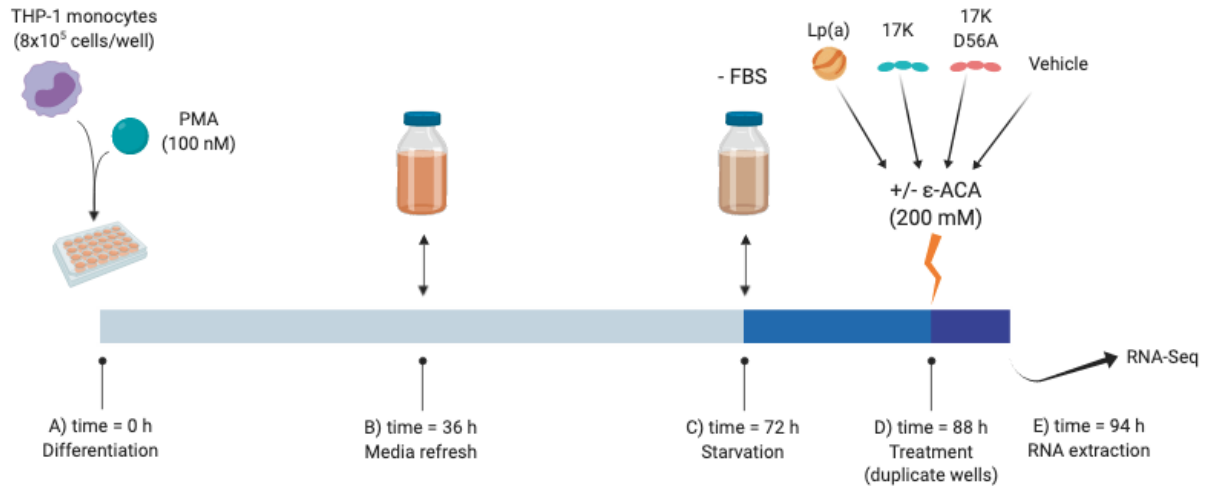


**Figure 3.11. Experimental design of functional assay used to generate RNA for RNA-Seq analysis.**

(A) THP-1 monocytes were suspended at a density of  $8 \times 10^5$  cells/mL in RPMI-1640 medium supplemented with 100 nM PMA. 24-well plates were seeded with 1 mL/well of this suspension. (B) After 36 hours, cells were supplied with fresh medium. (C) After a further 36 hours, medium was replaced with serum-free medium and incubated for 16 hours (starvation conditions). (D) Following starvation, the medium was replaced with fresh serum-free medium supplemented with either 250 nM Lp(a), 17K apo(a), 17K D56A apo(a), or no supplement. Each of the aforementioned treatments was performed in the absence of presence of 200 mM  $\epsilon$ -ACA (to inhibit lysine binding) for a total of 8 treatment groups, each performed in duplicate. Cells were incubated with the treatments for 6 hours. (E) Total RNA was isolated using the QIAGEN RNeasy Mini Kit according to the manufacturer's protocol and sent to LRGC for RNA-Seq analysis. Figure created with Biorender.com.

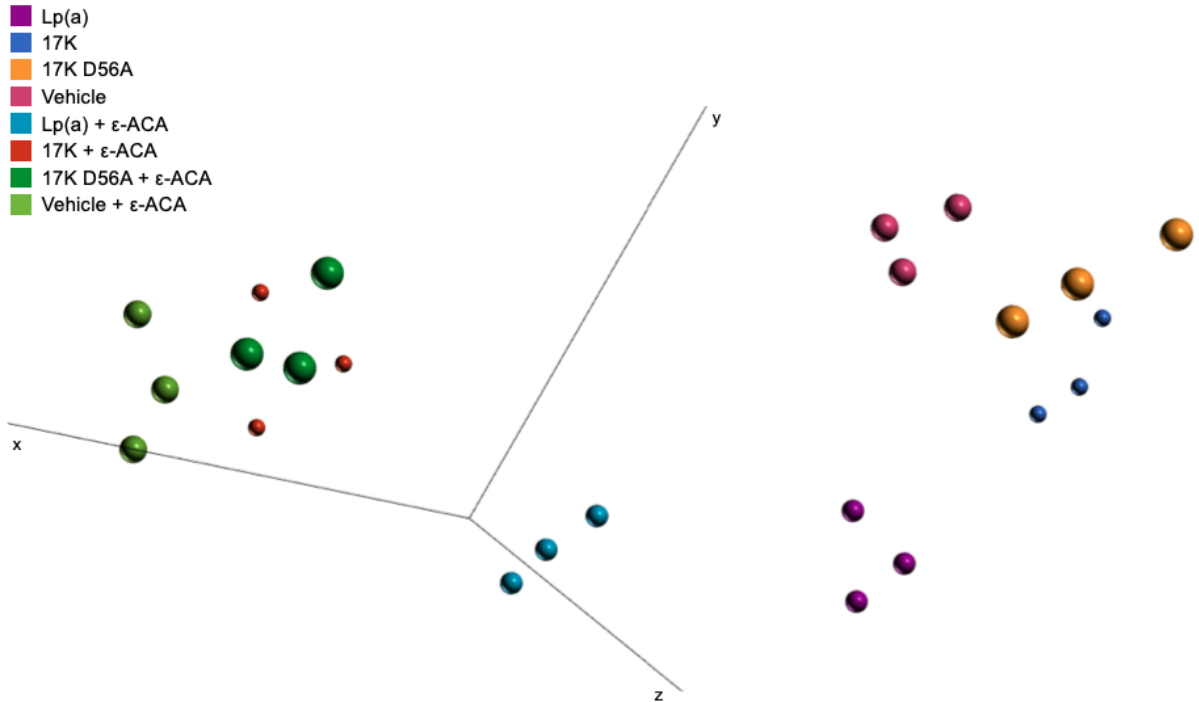


**Figure 3.12. t-SNE plot of biological replicates for RNA sequencing samples.**

t-distributed stochastic neighbour embedding converts a data set with many dimensions (i.e. expression for thousands of genes) to a data set with far fewer dimensions (in this case, three), while preserving the degree of similarity (or dissimilarity) between any given points. Each point in this t-SNE plot represents the gene expression attributable to a single biological replicate for the treatment corresponding to the colour of the point. The spatial clustering of biological replicates demonstrated in by t-SNE plot is indicative of high consistency within replicates for any given treatment, while the spatial separation of clusters is indicative of the differences in gene induction associated with each treatment.

### 3.3.1 The KIV<sub>10</sub> covalent oxPL has functions in enabling immune function

A number of genes were identified as being differentially regulated in THP-1 macrophages treated with 17K or 17K D56A apo(a), both in the presence of 200 mM  $\epsilon$ -ACA. Since lysine binding-dependent interactions were inhibited in each of these treatments, it can be inferred that changes in gene expression were induced exclusively by the presence of the KIV<sub>10</sub> covalent oxPL in the 17K treatment. Genes with implications in the activity of the immune system, namely by recruitment of leukocytes and priming phagocytic cells to engulf apoptotic cells, were found to be differentially regulated owing to the presence or absence of the covalent oxPL (**Table 3.1**). A total of 127 genes were found to be differentially regulated in this comparison, with  $p < 0.05$  and a -fold change of  $\geq 2$  or  $\leq -2$ .



**Table 3.1. Selected genes differentially expressed in THP-1 macrophages in response to the presence of the KIV<sub>10</sub> covalent oxPL addition to apo(a).**

<b>Gene</b>	<b>-fold change (17K + <math>\epsilon</math>-ACA vs. 17K D56A + <math>\epsilon</math>-ACA)</b>
<i>CCL18</i>	+325.0
<i>GULP1</i>	+5.9
<i>CHN2</i>	+3.9
<i>LAX1</i>	-320.3

### 3.3.2 The lysine-binding function of apo(a) facilitates the induction of inflammatory responses

Next, we assessed the LBS-facilitated effects of apo(a) in gene induction. To do this, we compared the transcriptomes of THP-1 macrophages treated with either 17K apo(a) alone or 17K apo(a) in the presence of 200 mM  $\epsilon$ -ACA. This comparison allowed us to identify which genes were induced, or repressed, *contingent* on the lysine binding functionality of apo(a), representing the effects of both lysine binding and the covalent oxPL. Parameters for determining significance were set more stringently in this comparison, at  $p < 0.001$  and a -fold change of  $\geq 2$  or  $\leq -2$ . Many of the genes found to be differentially regulated have functions in immune activation and regulation; this finding was not explicitly represented in the top gene ontology (GO) terms that were found to be enriched in this comparison (**Table 3.2**), but the top Kyoto Encyclopedia of Genes and Genomes (KEGG) pathways are highly indicative of inflammation (**Table 3.3**). Of the top 15 enriched KEGG pathways, 5 are directly related to the inflammatory processes of infection (bacterial, viral, or parasitic) and autoimmunity. A total of 1602 genes were found to be differentially regulated in this comparison.

**Table 3.2. Top 15 enriched GO terms in THP-1 macrophages treated with 17K apo(a) compared to those treated with 17K apo(a) + 200 mM  $\epsilon$ -ACA.**

<b>GO term</b>	<b>Enrichment score</b>	<b>P-value</b>
DNA-binding transcription factor activity, RNA polymerase II-specific	20.06	1.93E-09
DNA-binding transcription factor activity	19.01	5.53E-09
tRNA modification	13.53	1.33E-06
Transcription regulator activity	12.20	5.05E-06
Regulation of transcription by RNA polymerase II	11.56	9.58E-06
tRNA processing	11.16	1.42E-05
Embryonic limb morphogenesis	11.06	1.58E-05
Embryonic appendage morphogenesis	11.06	1.58E-05
Negative regulation of cell-cell adhesion	10.97	1.72E-05
Regulation of signaling receptor activity	10.56	2.59E-05
Negative regulation of cell population proliferation	10.20	3.73E-05
Regulation of cellular process	9.71	6.10E-05
Regulation of transcription, DNA-templated	9.69	6.19E-05
Cytokine activity	9.69	6.22E-05
Negative regulation of leukocyte cell-cell adhesion	9.59	6.86E-05

**Table 3.3. Top 15 enriched KEGG pathways in THP-1 macrophages treated with 17K apo(a) compared to those treated with 17K apo(a) + 200 mM  $\epsilon$ -ACA.**

<b>KEGG pathway</b>	<b>Enrichment score</b>	<b>P-value</b>
Cytokine-cytokine receptor interaction	13.3	1.67E-06
Neuroactive ligand-receptor interaction	8.37	2.31E-04
Gap junction	6.81	1.10E-03
JAK-STAT signaling pathway	6.77	1.14E-03
<i>Herpes simplex virus 1 infection</i>	6.08	2.29E-03
<i>Salmonella infection</i>	5.30	5.00E-03
<i>Legionellosis</i>	4.86	7.79E-03
MicroRNAs in cancer	4.79	8.29E-03
Toll-like receptor signaling pathway	4.33	1.00E-02
Transcriptional misregulation in cancer	4.25	1.00E-02
<i>Inflammatory bowel disease (IBD)</i>	4.11	2.00E-02
Lipoic acid metabolism	3.81	2.00E-02
Homologous recombination	3.68	3.00E-02
Folate biosynthesis	3.61	3.00E-02
<i>African trypanosomiasis</i>	3.58	3.00E-02

\*Italicized pathways are directly related to infection (bacterial, viral, and parasitic), and autoimmunity.

### 3.3.3 Differential regulation of genes with atherogenic implications

In addition to our assessment of GO terms and KEGG pathways, we examined the differential regulation of specific genes of interest in response to treatment with 17K apo(a) compared to 17K apo(a) + 200 mM  $\epsilon$ -ACA. We identified genes that were not differentially expressed in response to the addition of  $\epsilon$ -ACA by excluding genes that showed differences when comparing the vehicle and vehicle +  $\epsilon$ -ACA treatments (**Figure 3.13a**). Several roles are proposed for apo(a) in the development of atherosclerosis, rationalizing our investigation into the potential mechanisms underlying these effects. Thus, we considered genes from enriched GO terms and KEGG pathways, as well as previously established literature, to identify genes of interest with respect to the development of atherosclerosis. This subset included genes with roles in cell-cell adhesion, cell signaling, and modulation of the extracellular environment (**Figure 3.13b**). The differential regulation of this subset of genes is summarized in **Figure 3.13c**.

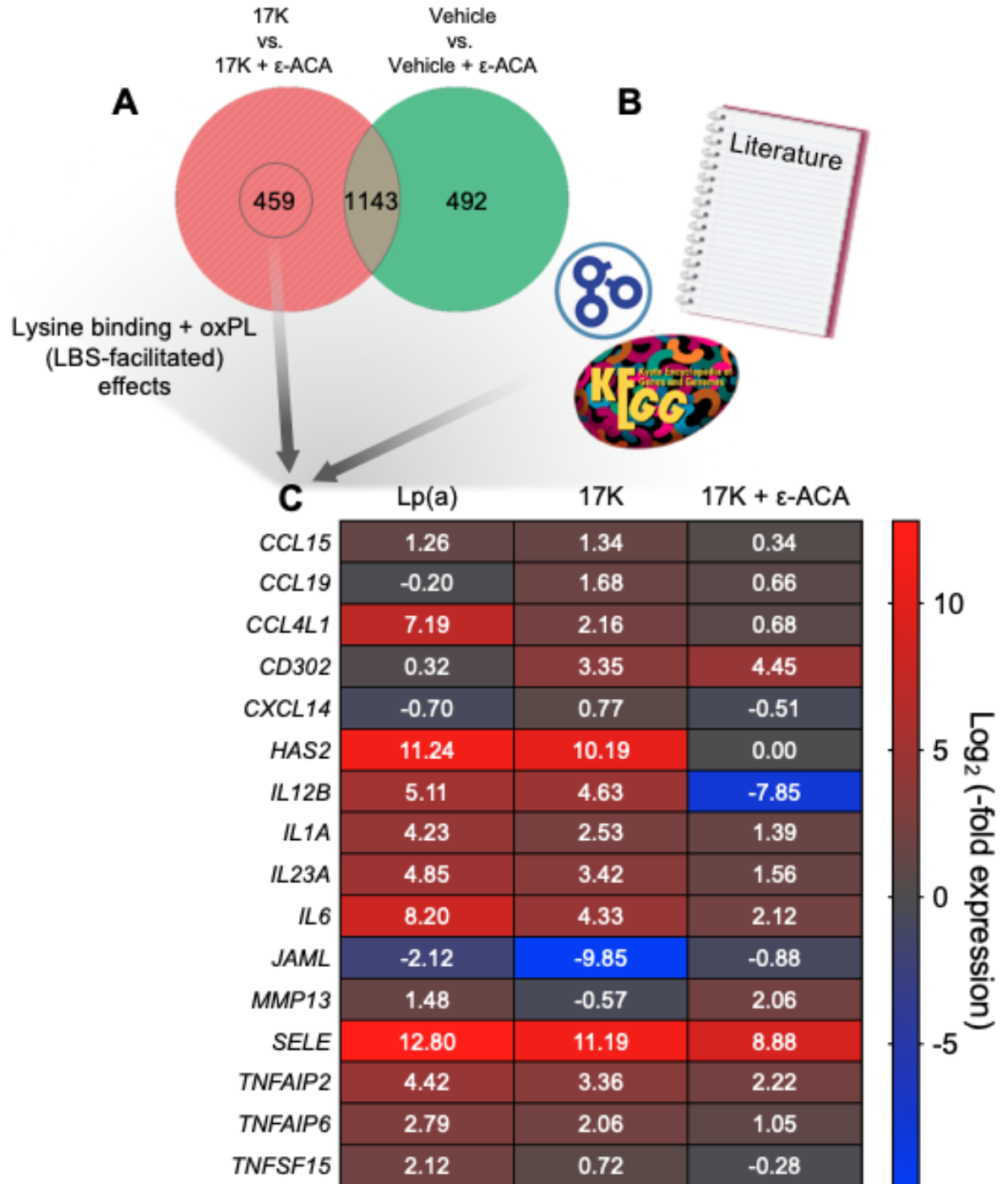


**Figure 3.13. Subset of genes which are differentially regulated by apo(a) dependent on the KIV<sub>10</sub> sLBS and covalent oxPL, rationalized by a potential role in the pathology of inflammation and atherosclerosis.**

(A) Differences in gene expression were assessed in THP-1 macrophages treated with 17K apo(a) or 17K apo(a) + 200 mM  $\epsilon$ -ACA, and also in THP-1 macrophages treated with vehicle or vehicle + 200 mM  $\epsilon$ -ACA. Genes that were found to be differentially regulated in the presence or absence of  $\epsilon$ -ACA were disqualified from further analysis, to prevent confounding. The differential regulation of these genes is deemed to be LBS-facilitated, encompassing both lysine binding- and oxPL-derived effects. (B) Genes appearing in GO terms and KEGG pathways enriched in the 17K vs. 17K +  $\epsilon$ -ACA comparison were considered in the context of literature relating to atherosclerosis; genes with implications in inflammation were of greatest interest. Genes encoding proteins with potential implications in the pathology of atherosclerosis were selected. (C) Visual representation of differential gene regulation in THP-1 macrophages treated with 17K apo(a) or 17K apo(a) + 200 mM  $\epsilon$ -ACA, compared to vehicle. Inclusion of Lp(a) allows comparison to 17K apo(a) to visualize similarities and differences in gene regulation, thereby implying the importance of apo(a) in gene regulation by Lp(a). Heat map represents  $\log_2$  (-fold expression) corresponding to the indicated treatment, compared to vehicle.

## 4 Discussion

Elevated plasma Lp(a) concentration is now considered the single most prevalent heritable risk factor in the development of CVD<sup>196</sup>. Approximately 20% of the population is classified in a high-risk category, owing to plasma Lp(a) levels in excess of 50 mg/dL<sup>196</sup>; this classification alone predisposes this demographic to a >2-fold increased risk of myocardial infarction, when compared with the remaining 80% of the population<sup>154</sup>. Though an understanding of Lp(a) as a contributor to the development of CVD has been established by determining the risks associated with its elevation, our understanding of the specific mechanisms by which Lp(a) contributes to disease progression remains incomplete. Our imprecise understanding of the specific functionalities that underlie the robust pathogenicity of Lp(a) has no doubt given way to the bleak therapeutic landscape we are faced with today: there remains a complete lack of therapies available to specifically reduce Lp(a) levels, and further still, no approved therapies are available to specifically reduce its pathogenic potential. Indeed, the outlook for individuals with genetically elevated Lp(a) levels has been poor until recent years, which has brought an explosion of prospective Lp(a)-specific drugs into pre-clinical and clinical investigation<sup>188</sup>.

A multifaceted approach to treating elevated Lp(a) levels – including specifically-targeted reduction of circulating particles – will be important moving forward. In light of this, however, exciting findings from a recent publication assessing oxPL blockade have provided important proof of principle to the notion that the pathogenicity of Lp(a) can be limited not only by reducing its abundance in the circulation, but also by masking key structural and/or functional components<sup>140</sup>. This study demonstrated that an anti-oxPL antibody fragment, E06-scFv, was able to reduce the severity and slow the progression of atherosclerosis in *Ldlr*<sup>-/-</sup> mice fed a high-cholesterol diet<sup>140</sup>. While this study did not make assessments with respect to Lp(a) specifically, the non-fragment version of the E06 antibody has been shown in numerous studies to bind to the covalent oxPL of Lp(a)/apo(a) in the same way as it binds to oxPLs found in oxLDL<sup>15,122,197</sup>. Further experiments using Lp(a) will be necessary to directly assess the effects of Lp(a)-oxPL blockade in this context, but a similar benefit is expected. Insights into the importance of oxPLs in CVD from both *in vitro* and *in vivo* studies continue to rationalize further investigation of structure-function relationships in Lp(a) and apo(a), especially those that may influence the presence, exposure, or abundance of the KIV<sub>10</sub> covalent oxPL.



## 4.1 A molecular basis for novel transcript-positive apo(a) null alleles

We have demonstrated that *LPA* alleles encoding substitutions for KIV<sub>10</sub> Arg10 or His33 are able to be transcribed, but that the protein products of these transcripts are unable to be secreted by either HEK293 or HepG2 cells. These observations are consistent across different isoforms and truncated variants of apo(a) (e.g. 6K), indicating that we have indeed identified two amino acid residues that are absolutely necessary for the secretion of apo(a). Our findings match those of White *et al.* in baboon hepatocytes, who made identical observations of transcript-positive apo(a) species that were unable to be secreted<sup>40</sup>. A molecular basis for these ER-retained apo(a) species was not indicated by White *et al.*, presumably due to limited access to DNA sequencing at the time of publication. At this time, White *et al.* postulated that spontaneous mutations may have led to the evolution of “rogue” kringles which are unable to fold properly and result in ER-retained apo(a) species. Our findings have both recapitulated these observations, and provided a molecular basis for them. Indeed, we have identified two independent nonsynonymous mutations in the KIV<sub>10</sub>-encoding region that are sufficient to generate a null expression phenotype for apo(a).

Prior to our study, two null alleles were identified in the *LPA* gene. The first of which (SNP rs41272114) introduces a splice site mutation. This leads to an alternatively-spliced transcript whose protein product is truncated by a nonsense mutation in the KIV<sub>7</sub> domain<sup>71</sup>. The other null allele (rs# unclear, “G4925A”<sup>89</sup>) generates a nonsense mutation within the repeating KIV<sub>2</sub>-encoding sequence, specifically in the exonic donor splice site of the second KIV<sub>2</sub> exon<sup>90</sup>. These null alleles share common characteristics: both truncated apo(a) variants are able to be secreted, neither can participate in the formation of Lp(a), and both are the result of nonsense mutations. In contrast, the novel null alleles we have identified lead to the translation of apo(a) species that are unable to be secreted, each the result of a unique nonsynonymous substitution. It is unclear whether these species are capable of covalent Lp(a) formation since they are not secreted, making Lp(a) assembly assays, as described previously<sup>64</sup>, impossible. While evidence of intracellular Lp(a) assembly has been demonstrated using the 6K apo(a) variant<sup>192</sup>, experiments using full-length apo(a) have not yielded the same result, suggesting that attempting similar experiments with KIV<sub>10</sub> Arg10- and His33-substituted apo(a) species would be unreliable<sup>194,195</sup>. That being said, the inclusion of all kringles required for Lp(a) assembly

in these retained species suggests their hypothetical compatibility in the Lp(a) assembly process, further distinguishing them from previously reported *LPA* null alleles.

## 4.2 Substitutions of apo(a) KIV<sub>10</sub> Arg10: a double-edged sword?

In terms of null alleles, KIV<sub>10</sub> Arg10 may be considered even more interesting than His33 as a critical residue for apo(a) secretion given that it was originally rationalized for investigation after it was found to be substituted for glutamine (R10Q) in a human subject. As such, our finding that KIV<sub>10</sub> Arg10-substituted apo(a) species are unable to be secreted can be assumed to hold true in humans, since this was the case in the context of 14K apo(a), which represents an isoform that naturally occurs in the population (unlike truncated constructs like 10-P or 6K). In collaboration with Dr. James Gault (Windsor University), comprehensive *in silico* molecular modeling of the KIV<sub>10</sub> R10Q domain is underway to more closely examine the structural changes that this substitution introduces in the KIV<sub>10</sub> domain. This may, in the future, allow us to theorize about the possible mechanisms contributing to the intracellular retention of this variant that we have shown. In a purely speculative context, with the structure of KIV<sub>10</sub> in mind, Arg10 may act to coordinate the position of other amino acids during the folding of KIV<sub>10</sub>, a critical function that could explain why it is essential for the secretion of apo(a).

Regardless of underlying mechanisms, the physiological implications for non-secreted apo(a) species such as the KIV<sub>10</sub> R10Q variant are difficult to determine, largely owing to the fact that subjects bearing this particular substitution are too rare to allow studies *in vivo*. The SNP corresponding to the R10Q substitution (rs776662773) is found in 0.01-0.03% of *LPA* alleles, meaning that only one individual in every 2,500, on average, is a heterozygous carrier of this allele, and that one in 6.25 million individuals is homozygous. Until a cohort can be assembled that is large enough to sufficiently power a study of rs776662773 carriers, we are left little choice but to theorize about the implications associated with these types of null alleles. In this context, two key findings should be considered: 1) apo(a) species with the KIV<sub>10</sub> R10Q substitution are translated, but not secreted, and as such are unable to participate in Lp(a) assembly, and 2) null alleles corresponding to apo(a) species which are unable to participate in Lp(a) assembly are associated with reduced Lp(a) levels and reduced risk of CVD<sup>71,88–90,198</sup>. While the mechanisms preventing these null apo(a) species from participating in Lp(a)

formation are markedly different, it is a hypothetical possibility that rs776667223 may be associated with reduced plasma Lp(a) concentrations and reduced CVD risk, similarly to other *LPA* null alleles.

While cardiovascular health may stand to benefit in individuals expressing an R10Q-substituted apo(a) variant, one must also consider the fate of the non-secreted apo(a) species. As we have shown in the HEK293 and HepG2 cell lines, transcript-positive null apo(a) species are retained intracellularly, and we have demonstrated that this retention occurs in the ER in HEK293 cells for KIV<sub>10</sub> H33A-substituted apo(a). Further experiments are planned to determine if this is the case for KIV<sub>10</sub> R10Q-substituted apo(a), and if this finding is recapitulated in HepG2 cells as well. A similar observation has been reported previously in a study of cultured primary baboon hepatocytes<sup>40</sup>, suggesting that this finding is likely to hold true across secretory cell types. Together, these findings suggest that R10Q-substituted apo(a) species may accumulate within the ER of hepatocytes in human rs776667223 carriers.

Accumulation of misfolded proteins in the ER triggers their degradation via the ERAD pathway<sup>58-60</sup>, and chronic activity of the ERAD pathway gives way to the unfolded protein response (UPR)<sup>199,200</sup>. The UPR is characterized by global repression of protein synthesis and can eventually trigger apoptosis<sup>199</sup>. ER stress/UPR activation in hepatocytes has been characterized with respect to diseases of the liver such as non-alcoholic fatty liver disease (NAFLD)/non-alcoholic steatohepatitis (NASH), with our current understanding of the role of ER stress in NAFLD/NASH centered on dysregulation of lipid homeostasis in the liver<sup>201,202</sup>. Previous studies have demonstrated the ER stress-mediated activation of sterol regulatory element-binding proteins (SREBPs), transcription factors with roles in cholesterol metabolism, LDLR expression, and *de novo* lipogenesis<sup>203,204</sup>. For example, SREBP-1 plays an important role in fatty acid and triglyceride biosynthesis<sup>205</sup>. Additionally, one arm of the UPR increases nuclear localization of pro-apoptotic CHOP, a C/EBP-homologous protein<sup>206</sup>; this homology facilitates the interference of CHOP with C/EBP $\alpha$ , a transcription factor whose normal function involves the regulation of gluconeogenesis and lipid homeostasis<sup>207</sup>. The combination of UPR-induced hepatocyte apoptosis with dysregulation of SREBP and C/EBP $\alpha$  signaling, among other factors, seems to contribute to the ER stress-mediated disruption of hepatic lipid metabolism and sets the stage for fatty liver-related pathologies. Based on this understanding of the role of ER stress in fatty liver, it is reasonable to posit that without some means of gene

silencing, chronic ER retention of transcript-positive *LPA* null species may compromise the overall health of the liver in individuals who are carriers. Similar to the potential cardioprotective effect proposed above, this hypothesis is difficult to test since the population of KIV<sub>10</sub> R10Q apo(a) variant carriers is very small. However, *in vitro* methods may shed light on the likelihood of increased NAFLD/NASH in such carriers; comparing the expression and/or activity of UPR markers such as CHOP, SREBP-1, or p-eIF2 $\alpha$  in HepG2 cells stably expressing either wildtype or R10Q apo(a) may indicate if such an outcome is possible in human hepatocytes.

### 4.3 Implications of the requirement of KIV<sub>10</sub> His33 for apo(a) secretion

In the context of this thesis, the substitution of His33 was rationalized as a means to investigate the identity of this residue as the site of covalent oxPL addition to apo(a), and to subsequently assess the functional contributions of the oxPL directly. In all kringles of apo(a) and in plasminogen K4, position 33 is indeed occupied by a histidine residue<sup>4</sup>; such an extreme degree of sequence conservation, coupled with our reported observations, suggests that this residue is truly indispensable for proper KIV kringle folding and/or function. It should, however, be noted that other kringles in plasminogen do contain substitutions at this position<sup>4</sup>. Unfortunately, this negates the idea of KIV<sub>10</sub> His33 substitution as an *in vitro* tool for obtaining a more complete understanding of the structure-function relationships in KIV<sub>10</sub> of apo(a), such as the mechanism of covalent oxPL addition. Future attempts to this end will require different approaches. Despite the highly conserved nature of His33, natural His33 substitution cannot yet be ruled out; reports of substitutions at this position may not exist simply because, until now, the relevance of such an observation has not been established, and we have not “looked” for it in humans. Additionally, the scarcity of rs776662773 (R10Q) suggests that transcript-positive null alleles including those involving Arg10 or His33 substitution could be incredibly rare. However, for the time being, the obligate requirement for KIV<sub>10</sub> His33 in the secretion of apo(a) is not applicable to humans beyond our *in vitro* findings in human-derived cell lines.

#### 4.4 KIV<sub>10</sub> Thr64 and the implications of enriched covalent oxPL modification

We have shown, in the context of KIV<sub>10</sub>KV, that KIV<sub>10</sub> Thr64 enriches covalent oxPL modification by nearly 3-fold in comparison with the same species that contains a methionine at this position. This finding is exciting in and of itself, as it is the first report of two apo(a) species that are both covalently modified with oxPL, but to differing extents. In addition to demonstrating this effect, we have provided a concrete molecular basis for it, solely attributable to the naturally occurring polymorphism resulting in a methionine/threonine substitution at KIV<sub>10</sub> position 64. Additionally, there is potential significance in this finding as KIV<sub>10</sub> Thr64 and Met64 represent the major (~65%) and minor (~35%) alleles in the human population, respectively. This discrepancy in oxPL modification may represent a determinant of CVD risk that is currently not accounted for. The relationship between the M64T substitution and the increase in covalent oxPL modification we observe is currently unclear, but molecular modeling in collaboration with Dr. Murray Junop (University of Western Ontario) has shown subtle differences between the Met64 and Thr64 versions of KIV<sub>10</sub>, despite the overall shape of the domain remaining virtually identical (**Figure 4.1**). When comparing the Thr64 and Met64 versions of KIV<sub>10</sub>, the most obvious difference is that the Arg71 side chain is repositioned closer to His33, the residue where covalent oxPL addition has been proposed. Arg71 is one of seven amino acids required for KIV<sub>10</sub> sLBS function, and as such we see that the orientation of the sLBS is changed slightly, rotating the modeled ligand's carboxyl group. Currently, the mechanism by which the covalent oxPL is added to KIV<sub>10</sub> is unknown. If His33 is indeed the oxPL-modified residue, Thr64-mediated repositioning of Arg71 and reorientation of the lysine binding site may in turn change the electrochemical microenvironment of the His33 side chain in such a way that covalent oxPL modification is favoured more-so in the Thr64 variant than in the M64 variant.

While we are only able to make educated guesses about the physiological implications of R10Q-substituted apo(a) species, the RNA-Seq-derived gene regulation data presented in **Table 3.1** allow us to make more concrete hypotheses about the potential effects attributable directly to increased apo(a)-bound oxPL. We have shown that the oxPL alone induces strong up-regulation of the *CCL18* gene which encodes CCL18 (aka pulmonary activation-regulated chemokine; PARC), a chemokine whose primary function is the recruitment of a wide variety

of immune cell types<sup>208–210</sup>. In addition to attracting immune cells, CCL18 exerts immunomodulatory effects in many of these cells, playing roles in both pro-inflammatory<sup>211</sup> and anti-inflammatory<sup>212</sup> processes. Expression of *CCL18* has been shown in human atherosclerotic plaques, and *in situ* RNA hybridization suggests that *CCL18* expression is restricted to CD68<sup>+</sup> macrophages<sup>213</sup>. What is very interesting in the context of our results is the expression pattern of *CCL18* that has been demonstrated *in vitro*: while no differences in *CCL18* expression were found in naïve THP-1 monocytes or PMA-differentiated THP-1 macrophages incubated with oxLDL<sup>213</sup>, we have clearly shown that the covalent oxPL of apo(a) is capable of strongly inducing *CCL18* expression under similar experimental conditions. In addition to inducing *CCL18* expression, we have also shown that the covalent oxPL strongly represses the expression of *LAX1*, which encodes lymphocyte transmembrane adapter 1. This adapter protein is involved in the negative regulation of antigen-receptor signaling in both T- and B-cells<sup>214</sup>, implying that the covalent oxPL acts to facilitate a maximal inflammatory response in these cell types. This effect may synergize with that of CCL18, which potentially acts to recruit both T- and B-cells to the site of oxPL exposure. The sum of these effects would be to recruit various immune cell types to sites of atherosclerotic plaque development and enable a maximal inflammatory response, providing evidence for the role of the covalent oxPL in the initiation and propagation of atherosclerosis. These effects alone are enough to hypothesize that added oxPL enrichment of apo(a) may contribute to accelerated atherogenesis *in vivo* by increasing the potency of *CCL18* induction and *LAX1* repression. It is uncertain if these regulatory effects are threshold-based or if a proportional dose-response may be observed. *In vitro* comparisons of gene expression in macrophages exposed to Met64 and Thr64 variants of apo(a) may give further perspective with respect to the nature of these relationships. It is important to note that the Met64 variant of 17K apo(a) was used in the RNA-Seq experiment we conducted, and that studies comparing Met64 and Thr64 variants of full-length apo(a) represent a strong candidate for further investigation into the functional significance of the KIV<sub>10</sub> covalent oxPL.

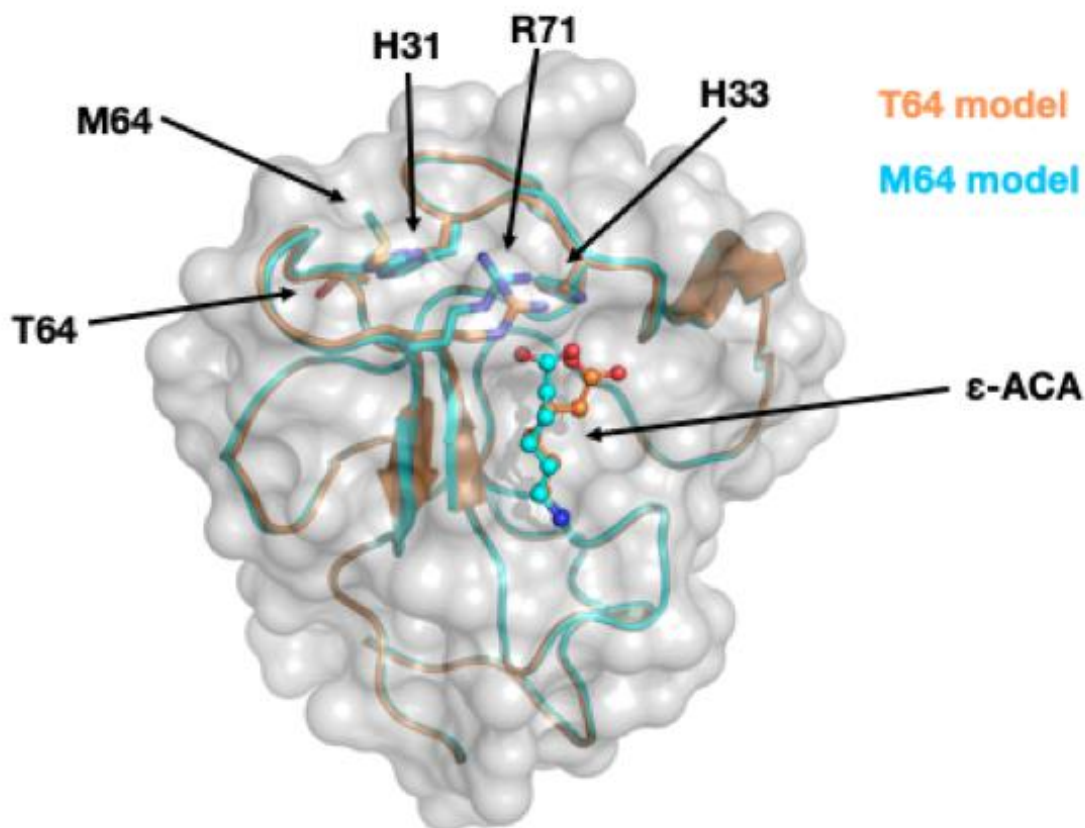


**Figure 4.1. Molecular modeling overlay of Met64 (blue) and Thr64 (orange) variants of apo(a) KIV<sub>10</sub>, with ε-ACA as the bound ligand.**

The orientation of the peptide backbone is nearly identical between the Met64 and Thr64 (M64T) variants of apo(a) KIV<sub>10</sub>, as shown. However, differences are apparent in the two variants: the orientation of the Arg71 (R71) side chain and the orientation of the carboxyl group of the bound ligand are altered. In comparison to the Met64 variant, the Thr64 variant Arg71 side chain is closer to the side chain of His33 (H33). Arg71 is one of seven amino acids forming the sLBS of KIV<sub>10</sub> (Arg71 being a component of the cationic center), and this repositioning in turn alters the orientation of the carboxyl group of the bound ligand. Additionally, if His33 is indeed the site of covalent oxPL addition as proposed<sup>190</sup>, the microenvironment of this residue as altered by the aforementioned differences may be more favourable for covalent oxPL addition in the Thr64 variant than in the Met64 variant, thereby explaining our observations. Figure created by Dr. M Junop and R Szabla using Rosetta Relax for energy minimization and PyMOL for structure visualization.

## 4.5 Apo(a) LBS-facilitated gene regulation effects have atherogenic implications

Multiple *in vitro* studies have demonstrated potentially atherogenic KIV<sub>10</sub> sLBS-dependent effects of apo(a) treatment in both endothelial cells<sup>110,141</sup> and SMCs<sup>125,142</sup>. While endothelial cells and SMCs both have distinct roles in the development of atherosclerosis, cells of the immune system, such as macrophages, are critical in propagating the chronic inflammatory response that has been characterized within atherosclerotic plaques<sup>215,216</sup>. Thus, we sought to identify LBS-facilitated (lysine-binding *and* covalent oxPL-dependent) gene regulation effects of apo(a) in THP-1 macrophages in order to gain further understanding of the influence of apo(a) on cells involved in the inflammatory response. In this study, and in previous studies, the lack of an oxPL-negative/sLBS positive apo(a) species has prevented us from discerning effects that are attributable exclusively to the KIV<sub>10</sub> oxPL versus those that rely on the physical interaction facilitated by the KIV<sub>10</sub> sLBS. Indeed, we must consider that these lysine binding-dependent effects, while requiring lysine binding, are not necessarily due to lysine binding. The close spatial proximity of the KIV<sub>10</sub> sLBS and oxPL may facilitate the interaction of the covalent oxPL with ligands of the sLBS. In this context, while it has been demonstrated that the KIV<sub>10</sub> sLBS has roles in thrombotic/fibrinolytic balance by way of physical interaction with fibrin and other substrates<sup>5,26,144,151</sup>, it is unclear whether these same types of physical interactions are capable of inducing signaling pathways in cells. We believe it is most reasonable to assume that apo(a)-mediated signaling that is contingent on lysine binding represents a co-operative process involving both the physical lysine binding process, as well as the exposure of bound ligands to the covalent oxPL. As such, we deem these effects to be “LBS-facilitated”.

We utilized RNA sequencing to expand our understanding of structure-function relationships of the apo(a) KIV<sub>10</sub> domain, and the data presented are focused on LBS-facilitated effects. While some downstream effects that require the lysine binding functionality of apo(a) have been characterized in other vascular cell types, this newer approach has provided us an opportunity to explore many potential mechanisms by which apo(a)/Lp(a) may contribute to atherosclerosis via modulation of the immune system. In order to acquire a broad understanding of these LBS-facilitated effects, we first considered the enriched GO terms and KEGG pathways associated with lysine binding-facilitated interactions of apo(a). Here, we



observed 5 entries directly related to infection (bacterial, viral, and parasitic) within the top 15 enriched KEGG pathways, complimented by enrichment of the *cytokine activity* GO term and the *cytokine-cytokine receptor interaction* KEGG pathway. These GO terms and KEGG pathways share a common theme – signaling in inflammatory processes – which supplies evidence for the proposed pro-inflammatory roles for apo(a)/Lp(a) in facilitating the initiation and progression of atherosclerosis. In this study, we have demonstrated the enrichment of numerous inflammation-associated GO terms and KEGG pathways, as well as the differential regulation of individual genes with atherogenic implications.

In addition to the enriched GO terms and KEGG pathways we have identified in **Table 3.2** and **Table 3.3**, we assessed a subset of genes fitting the following criteria: 1) LBS-facilitated (i.e. differential regulation between 17K and 17K +  $\epsilon$ -ACA treatments), 2) rationalization for a role in atherosclerosis, and 3) no differential regulation between vehicle and vehicle +  $\epsilon$ -ACA treatments. For these genes, we compared expression in response to Lp(a), 17K, and 17K +  $\epsilon$ -ACA; these data are shown in **Figure 3.13**. These genes have ascribed functions in inflammatory mediation, immune cell chemotaxis, cell-cell adhesion, and modulation of the extracellular matrix.

#### 4.5.1 LBS-facilitated effects in inflammation and chemotaxis: roles for *CCL4L1*, *CCL15*, *CCL19*, *CXCL14*, *IL1A*, *IL6*, *IL12B*, *IL23A*, *TNFAIP2*, *TNFAIP2*, and *TNFSF15*

The genes listed in the heading have established roles in modulating the function and activity of the immune system. Members of the CC and CXC chemokine families largely serve as immune cell chemoattractants and induce convergence of various leukocyte subtypes at sites of injury<sup>215,216</sup>. Interleukins serve a wide variety of functions, each individual member exerting numerous physiological effects; however, the interleukins we found to be differentially expressed – interleukins 1 $\alpha$ , 6, 12 $\beta$ , and 23 $\alpha$  – are all considered to be pro-inflammatory in nature<sup>215</sup>. The LBS-facilitated up-regulation of these interleukins, and of the CC and CXC chemokines, supports a role for the function of the apo(a) KIV<sub>10</sub> domain in the inflammatory properties of apo(a)/Lp(a). The TNF $\alpha$ -induced proteins (*TNFAIP2* and *TNFAIP6*) have anti-inflammatory roles<sup>217,218</sup>, so the increased expression of these factors that we have reported may indicate protective autoregulation of the inflammatory response evoked in response to

apo(a). Finally, TNF superfamily member 15 (*TNFSF15*) is the only known ligand for death receptor 3<sup>219</sup>, suggesting a potential role for apo(a)/Lp(a) in T cell apoptosis. Additionally, high expression of *TNFSF15* has been demonstrated to correlate positively with prevalence of CAD in humans<sup>220</sup>. Overall, these findings support the proposed identity of Lp(a) as a potent pro-inflammatory stimulus in the vasculature, and suggest that the lysine binding properties of apo(a), along with its covalently-bound oxPL have roles in mediating this effect.

#### 4.5.2 LBS-facilitated effects in cell-cell adhesion and extravasation: roles for *CD302*, *JAML*, and *SELE*

The adhesion of leukocytes to the endothelial lining is a critical step in the development of atherosclerotic lesions, facilitating leukocyte extravasation from the plasma into the intimal compartment of the blood vessel<sup>216</sup>. We demonstrate lysine binding-dependent repression of *CD302* and Junctional Adhesion Molecule-Like (*JAML*) expression in response to apo(a), but increased expression of E-selectin (*SELE*). At first glance, the down-regulation of cell-adhesion molecules may seem counterintuitive, but when the cell-specific expression of these proteins is considered, these results are logical. *CD302* and *JAML* are naturally found on monocytes and macrophages, with evidence supporting roles for these receptors in the adhesion, migration, and extravasation of these cells<sup>221,222</sup>. In this context, one must consider that we have exposed macrophage-like cells to a type of inflammatory stimulus that would normally be encountered only after atherosclerotic plaque invasion. It is therefore understandable that the expression of cell-adhesion molecules is repressed in response, as such factors would serve no further function at this stage. On the other hand, the massive up-regulation of E-selectin expression we have observed, while not relevant in leukocytes, suggests that apo(a)/Lp(a) may up-regulate E-selectin in endothelial cells by a similar mechanism. Indeed, it has been shown previously that Lp(a) stimulates E-selectin production in human coronary artery endothelial cells<sup>223</sup>. Our finding that *SELE* expression in macrophage-like cells is enhanced when comparing 17K to 17K +  $\epsilon$ -ACA (but not absent in the 17K +  $\epsilon$ -ACA treatment) allows us to speculate that this effect is partially, but not fully LBS-facilitated in endothelial cells as well.

#### 4.5.3 LBS-facilitated effects in extracellular matrix remodeling: roles for *HAS2* and *MMP13*

The simultaneous up-regulation of hyaluronan synthase 2 (HS2; *HAS2*) and repression of matrix metalloproteinase 13 (collagenase 3, *MMP13*) indicates a net increase of hyaluronic acid deposition in the atherosclerotic plaque microenvironment. Hyaluronic acid has been identified as a component of human atherosclerotic plaques at all stages of lesion development<sup>224,225</sup>. Hyaluronic acid deposition may serve to facilitate macrophage recruitment, as it has been demonstrated that macrophages bind hyaluronic acid on the endothelial surface and within the arterial wall in a CD44-mediated fashion<sup>226,227</sup>. While invasive immune cells such as macrophages act to degrade ECM in order to migrate into the atherosclerotic lesion, rather than to secrete ECM, it should be considered that apo(a)/Lp(a) exposure may elicit a HS2-mediated secretory response in other nearby vascular cells, such as SMCs. The relevance of *HAS2* expression in atherosclerosis is clear: hyaluronic acid is an ECM component found in human atherosclerotic plaques<sup>224,225</sup>, and has established implications in inflammatory modulation and promotion of cell migration<sup>228,229</sup>.

In the context of inflammatory modulation, apo(a) has been shown previously to up-regulate COX-2 (*PTGS2*) expression in endothelial cells, an effect that was demonstrated to require KIV<sub>10</sub> sLBS function<sup>110</sup>. COX-2 mediates the conversion of arachidonic acid to prostaglandin H<sub>2</sub>, a precursor for prostaglandin E<sub>2</sub> (PGE<sub>2</sub>), which has been shown to be abundant in human atherosclerotic plaques<sup>230,231</sup>. In addition to its effects as an inflammatory mediator, PGE<sub>2</sub> has been found to induce *HAS2* expression in human SMCs<sup>232</sup>. Taken together, these findings comprise a multi-step, LBS-facilitated pathway through which apo(a)/Lp(a) may elicit 1) increased prostaglandin synthesis, and 2) increased *HAS2* expression/hyaluronic acid synthesis, within atherosclerotic plaques. This does not directly address implications of increased *HAS2* expression in THP-1 macrophages treated with apo(a)/Lp(a), but proposes a mechanism by which the same effect may be evoked in SMCs as a consequence of apo(a)/Lp(a) exposure.

In the context of cell migration, hyaluronic acid has been demonstrated to decrease PDGF-induced SMC proliferation and increase PDGF-induced SMC migration in cultured human pulmonary vascular SMCs, suggesting a role for hyaluronic acid in fibrous cap formation<sup>224</sup>.

## 4.6 Study limitations and future directions

The greatest limiting factor of this work was our inability to generate an apo(a) species with intact KIV<sub>10</sub> lysine binding function that also lacked the covalently bound oxPL. While we have shown that KIV<sub>10</sub> His33-substituted apo(a) species are able to be translated, the intracellular retention of such variants within the ER prevented their purification and functional characterization as part of this work. Similarly, the intracellular retention we have shown for KIV<sub>10</sub> Arg10-substituted apo(a) species has limited our ability to functionally characterize these variants in the same way. While we believe that the *in vitro* findings we have shown are translatable to *in vivo* systems, we must consider that this is not always the case, and that our use of *in vitro* systems is an inherent limitation of our work. However, identical reports of ER-based intracellular retention of apo(a) species has been reported in cultured primary baboon hepatocytes<sup>195</sup>, suggesting that our findings are indeed a true representation of the secretory pathway *in vivo*. In order to further demonstrate the ER-based intracellular retention of R10Q-substituted apo(a), we plan to assess organelle co-localization of full-length wildtype and R10Q apo(a) variants in both HEK293 and HepG2 cells, in a similar fashion to that shown in Section 3.1.3. This approach will add a second dimension to the immunoblot data shown in Section 3.1.5, by demonstrating intracellular retention of R10Q-substituted apo(a) using confocal immunofluorescence microscopy. In future investigations of the KIV<sub>10</sub> R10Q substitution, mass spectrometry of Lp(a) isolated from the plasma of rs776662773 carriers should demonstrate the absence or presence of apo(a) species containing this substitution in humans, thereby supporting or refuting our assertion that this polymorphism represents a null *LPA* allele. Further, an assessment of the potential contribution of chronically ER-retained apo(a) in hepatocytes to fatty liver-related pathologies should be conducted using an experimental approach like the one proposed to address this in Section 4.2.

Our finding that the KIV<sub>10</sub> M64T substitution enriches oxPL abundance was demonstrated in the truncated KIV<sub>10</sub>KV construct, which is not a physiologically relevant apo(a) species. To date, however, the characteristics of the structural components of KIV<sub>10</sub> (oxPL, sLBS) have been translatable from KIV<sub>10</sub>KV to full-size apo(a) variants<sup>13,190</sup>. While this strongly implies that M64T-mediated oxPL enrichment will be present in full-size apo(a) species, this must be confirmed before we can propose its relevance with respect to human physiology. If this effect is confirmed in recombinant variants of naturally-occurring apo(a) isoforms (e.g. 14K, 17K),

future studies may aim to retrospectively analyze previous population studies in order to determine whether the rs1801693 polymorphism (KIV<sub>10</sub> T64M; recall that Thr64 is the major allele in the population) is associated with reduced CVD risk and/or mortality. An additional approach to directly assess the functional effects of covalent oxPL enrichment will be the use of Met64 and Thr64 apo(a) variants, in parallel, for *in vitro* experiments using the methods described in Section 2.10.

## 4.7 Summary and conclusions

In summary, we have shown that the KIV<sub>10</sub> domain is a highly sensitive structural component of apo(a) with important implications in the processing and secretion of apo(a) itself, as well as a critical role in the facilitation of apo(a)-induced pro-atherogenic effects in vascular cell types.

We have shown that single substitutions of either Arg10 or His33 in KIV<sub>10</sub> are sufficient to cause intracellular retention of apo(a) species containing these substitutions, and have provided evidence that this retention occurs in the ER, in agreement with the findings of a previous group. The R10Q substitution is the result of a rare, naturally occurring SNP (rs776667223) in the *LPA* gene, with a prevalence of 0.01-0.03% in the human population. Since previously established *LPA* null alleles result in premature truncation of the encoded apo(a) species, we propose that this SNP represents a novel type of null allele for the *LPA* gene, derived from a single amino acid substitution (rather than a nonsense mutation). The implications of this finding are relevant only to the small proportion of the human population who are rs776667223 carriers, but we hypothesize that this SNP may correlate with decreased plasma Lp(a) concentration, decreased CVD risk, and/or increased prevalence of fatty liver.

Using the truncated KIV<sub>10</sub>KV apo(a) variant, we have shown that the identity of the residue at KIV<sub>10</sub> position 64 is able to influence the degree of oxPL modification the protein undergoes. This, in itself, is a novel finding, as this is the first demonstration of oxPL-positive apo(a) species that differ in the relative extent of oxPL modification. The major and minor *LPA* alleles contain KIV<sub>10</sub> Thr64 and Met64, respectively, with the threonine-containing allele found at approximately twice the prevalence as the methionine-containing allele in the human population. We have demonstrated that the Thr64 variant of KIV<sub>10</sub>KV contains approximately 2.8 times the covalent oxPL per mass quantity of protein than the Met64 variant does. Based

on the roles which have been proposed for oxPLs in atherosclerosis, along with the atherogenic gene regulation effects we have shown to be oxPL-dependent in THP-1 macrophages, we hypothesize that Thr64-containing apo(a) species may be associated with increased CVD risk compared to Met64-containing species.

The complex structure-function relationships of apo(a) KIV<sub>10</sub> are exemplified by the gene regulation effects we have shown in THP-1 macrophages that are contingent on the lysine binding ability of apo(a), as well as those that are exclusively due to the presence of the covalently bound oxPL. Our overall understanding of the results presented herein is that apo(a) elicits a wide variety of LBS-facilitated gene regulatory effects in THP-1 macrophages, implicating both the KIV<sub>10</sub> sLBS and covalent oxPL in this process. We have demonstrated that apo(a)/Lp(a) have the potential to drastically alter the microenvironment of atherosclerotic plaques by altering the expression of genes related to leukocyte convergence/chemotaxis, cell-adhesion, pro-inflammatory signaling, and ECM deposition.

In conclusion, the KIV<sub>10</sub> domain is a key domain in apo(a) with complex structure-function relationships. We have shown that single-residue substitutions in the primary sequence of KIV<sub>10</sub> can alter the extent to which this domain is modified covalently with oxPLs, or even prevent the secretion of apo(a) entirely. We have also shown that sub-structures of KIV<sub>10</sub>, namely the sLBS and oxPL, are strongly implicated in the pathogenicity of apo(a)/Lp(a). Taken together, these findings support our hypotheses and supply evidence indicating critical roles for the structure and function of the apo(a) KIV<sub>10</sub> domain in the pathologies associated with Lp(a) *in vivo*.

## References

1. Berg, K. A new serum type system in man--the Lp system. *Acta Pathol. Microbiol. Scand.* **59**, 369–82 (1963).
2. Ellis, K. L., Boffa, M. B., Sahebkar, A., Koschinsky, M. L. & Watts, G. F. The renaissance of lipoprotein(a): Brave new world for preventive cardiology? *Prog. Lipid Res.* **68**, 57–82 (2017).
3. Weisel, J. W. *et al.* The structure of lipoprotein(a) and ligand-induced conformational changes. *Biochemistry* **40**, 10424–10435 (2001).
4. McLean, J. W. *et al.* cDNA sequence of human apolipoprotein(a) is homologous to plasminogen. *Nature* **330**, 132–137 (1987).
5. Hancock, M. A., Boffa, M. B., Marcovina, S. M., Nesheim, M. E. & Koschinsky, M. L. Inhibition of plasminogen activation by lipoprotein(a): critical domains in apolipoprotein(a) and mechanism of inhibition on fibrin and degraded fibrin surfaces. *J. Biol. Chem.* **278**, 23260–9 (2003).
6. Gabel, B. R. & Koschinsky, M. L. Analysis of the proteolytic activity of a recombinant form of apolipoprotein(a). *Biochemistry* **34**, 15777–15784 (1995).
7. Brunner, C. *et al.* The number of identical kringle IV repeats in apolipoprotein(a) affects its processing and secretion by HepG2 cells. *J. Biol. Chem.* **271**, 32403–32410 (1996).
8. Becker, L., Cook, P. M., Wright, T. G. & Koschinsky, M. L. Quantitative evaluation of the contribution of weak lysine-binding sites present within apolipoprotein(a) kringle IV types 6-8 to lipoprotein(a) assembly. *J. Biol. Chem.* **279**, 2679–88 (2004).
9. Becker, L., McLeod, R. S., Marcovina, S. M., Yao, Z. & Koschinsky, M. L. Identification of a critical lysine residue in apolipoprotein B-100 that mediates noncovalent interaction with apolipoprotein(a). *J. Biol. Chem.* **276**, 36155–62 (2001).
10. Koschinsky, M. L., Côté, G. P., Gabel, B. & van der Hoek, Y. Y. Identification of the cysteine residue in apolipoprotein(a) that mediates extracellular coupling with apolipoprotein B-100. *J. Biol. Chem.* **268**, 19819–25 (1993).
11. Guevara, J. *et al.* Proposed mechanisms for binding of apo[a] kringle type 9 to apo B-100 in human lipoprotein[a]. *Biophys. J.* **64**, 686–700 (1993).
12. Callow, M. J. & Rubin, E. M. Site-specific mutagenesis demonstrates that cysteine 4326 of apolipoprotein B is required for covalent linkage with apolipoprotein (a) in vivo. *J. Biol. Chem.* **270**, 23914–7 (1995).
13. Leibundgut, G. *et al.* Determinants of binding of oxidized phospholipids on apolipoprotein (a) and lipoprotein (a). *J. Lipid Res.* **54**, 2815–2830 (2013).
14. Scipione, C. A. *et al.* Mechanistic insights into Lp(a)-induced IL-8 expression: a role for oxidized phospholipid modification of apo(a). *J. Lipid Res.* **56**, 2273–2285 (2015).
15. Bergmark, C. *et al.* A novel function of lipoprotein [a] as a preferential carrier of

- oxidized phospholipids in human plasma. *J. Lipid Res.* **49**, 2230–2239 (2008).
16. Fless, G. M., ZumMallen, M. E. & Scanu, A. M. Physicochemical properties of apolipoprotein(a) and lipoprotein(a-) derived from the dissociation of human plasma lipoprotein (a). *J. Biol. Chem.* **261**, 8712–8 (1986).
  17. Lawn, R. M., Schwartz, K. & Patthy, L. Convergent evolution of apolipoprotein(a) in primates and hedgehog. *Proc. Natl. Acad. Sci.* **94**, 11992–11997 (1997).
  18. Kratzin, H., Armstrong, V. W., Niehaus, M., Hilschmann, N. & Seidel, D. Structural relationship of an apolipoprotein (a) phenotype (570 kDa) to plasminogen: homologous kringle domains are linked by carbohydrate-rich regions. *Biol. Chem. Hoppe. Seyler.* **368**, 1533–44 (1987).
  19. Garner, B. *et al.* Structural elucidation of the N- and O-glycans of human apolipoprotein(a): role of o-glycans in conferring protease resistance. *J. Biol. Chem.* **276**, 22200–8 (2001).
  20. Harpel, P. C., Gordon, B. R. & Parker, T. S. Plasmin catalyzes binding of lipoprotein (a) to immobilized fibrinogen and fibrin. *Proc. Natl. Acad. Sci. U. S. A.* **86**, 3847–51 (1989).
  21. Hoover-Plow, J. & Huang, M. Lipoprotein(a) metabolism: potential sites for therapeutic targets. *Metabolism.* **62**, 479–91 (2013).
  22. Hughes, S. D. *et al.* Lipoprotein(a) vascular accumulation in mice. In vivo analysis of the role of lysine binding sites using recombinant adenovirus. *J. Clin. Invest.* **100**, 1493–1500 (1997).
  23. Godier, A. & Hunt, B. J. Plasminogen receptors and their role in the pathogenesis of inflammatory, autoimmune and malignant disease. *J. Thromb. Haemost.* **11**, 26–34 (2013).
  24. Medcalf, R. L. Fibrinolysis, inflammation, and regulation of the plasminogen activating system. *J. Thromb. Haemost.* **5**, 132–142 (2007).
  25. Liu, L., Boffa, M. B. & Koschinsky, M. L. Apolipoprotein(a) inhibits in vitro tube formation in endothelial cells: identification of roles for kringle V and the plasminogen activation system. *PLoS One* **8**, e52287 (2013).
  26. Romagnuolo, R., Marcovina, S. M., Boffa, M. B. & Koschinsky, M. L. Inhibition of plasminogen activation by apo(a): role of carboxyl-terminal lysines and identification of inhibitory domains in apo(a). *J. Lipid Res.* **55**, 625–34 (2014).
  27. Chisolm, G. M. & Steinberg, D. The oxidative modification hypothesis of atherogenesis: an overview. *Free Radic. Biol. Med.* **28**, 1815–26 (2000).
  28. Kume, N. & Kita, T. Roles of lectin-like oxidized LDL receptor-1 and its soluble forms in atherogenesis. *Curr. Opin. Lipidol.* **12**, 419–23 (2001).
  29. Kita, T. *et al.* Role of oxidized LDL in atherosclerosis. *Ann. N. Y. Acad. Sci.* **947**, 199–206 (2006).
  30. Lopez, L. R., Kobayashi, K., Matsunami, Y. & Matsuura, E. Immunogenic oxidized low-density lipoprotein/ $\beta$ 2-glycoprotein I complexes in the diagnostic management of atherosclerosis. *Clin. Rev. Allergy Immunol.* **37**, 12–19 (2009).



31. Tsimikas, S. *et al.* Oxidized phospholipids, Lp(a) lipoprotein, and coronary artery disease. *N. Engl. J. Med.* **353**, 46–57 (2005).
32. Tsimikas, S. *et al.* Oxidation-specific biomarkers, lipoprotein(a), and risk of fatal and nonfatal coronary events. *J. Am. Coll. Cardiol.* **56**, 946–955 (2010).
33. Tsimikas, S. *et al.* Oxidized phospholipids predict the presence and progression of carotid and femoral atherosclerosis and symptomatic cardiovascular disease: five-year prospective results from the Bruneck study. *J. Am. Coll. Cardiol.* **47**, 2219–2228 (2006).
34. Seimon, T. A. *et al.* Atherogenic lipids and lipoproteins trigger CD36-TLR2-dependent apoptosis in macrophages undergoing endoplasmic reticulum stress. *Cell Metab.* **12**, 467–82 (2010).
35. Igor Mochalkin, Beisong Cheng, Olga Klezovitch, Angelo M. Scanu & Alexander Tulinsky. Recombinant kringle IV-10 modules of human apolipoprotein(a): structure, ligand binding modes, and biological relevance. (1999).
36. Boerwinkle, E. *et al.* Apolipoprotein(a) gene accounts for greater than 90% of the variation in plasma lipoprotein(a) concentrations. *J. Clin. Invest.* **90**, 52–60 (1992).
37. Utermann, G. *et al.* Lp(a) glycoprotein phenotypes. Inheritance and relation to Lp(a)-lipoprotein concentrations in plasma. *J. Clin. Invest.* **80**, 458–465 (1987).
38. White, A. L. & Lanford, R. E. Biosynthesis and metabolism of lipoprotein (a). *Curr. Opin. Lipidol.* **6**, 75–80 (1995).
39. White, A. L., Guerra, B. & Lanford, R. E. Influence of allelic variation on apolipoprotein(a) folding in the endoplasmic reticulum. *J. Biol. Chem.* **272**, 5048–55 (1997).
40. White, A. L., Hixson, J. E., Rainwater, D. L. & Lanford, R. E. Molecular basis for ‘null’ lipoprotein(a) phenotypes and the influence of apolipoprotein(a) size on plasma lipoprotein(a) level in the baboon. *J. Biol. Chem.* **269**, 9060–6 (1994).
41. Rader, D. J. *et al.* The inverse association of plasma lipoprotein(a) concentrations with apolipoprotein(a) isoform size is not due to differences in Lp(a) catabolism but to differences in production rate. *J. Clin. Invest.* **93**, 2758–63 (1994).
42. Müller, N. *et al.* IL-6 blockade by monoclonal antibodies inhibits apolipoprotein (a) expression and lipoprotein (a) synthesis in humans. *J. Lipid Res.* **56**, 1034–1042 (2015).
43. Chennamsetty, I. *et al.* Farnesoid X receptor represses hepatic human APOA gene expression. *J. Clin. Invest.* **121**, 3724–3734 (2011).
44. Chennamsetty, I., Claudel, T., Kostner, K. M., Trauner, M. & Kostner, G. M. FGF19 Signaling Cascade Suppresses APOA Gene Expression. *Arterioscler. Thromb. Vasc. Biol.* **32**, 1220–1227 (2012).
45. Chennamsetty, I. *et al.* Nicotinic acid inhibits hepatic APOA gene expression: studies in humans and in transgenic mice. *J. Lipid Res.* **53**, 2405–12 (2012).
46. Henriksson, P., Angelin, B. & Berglund, L. Hormonal regulation of serum Lp(a) levels. Opposite effects after estrogen treatment and orchidectomy in males with

- prostatic carcinoma. *J. Clin. Invest.* **89**, 1166–1171 (1992).
47. Kim, C. J., Jang, H. C., Cho, D. H. & Min, Y. K. Effects of hormone replacement therapy on lipoprotein(a) and lipids in postmenopausal women. *Arterioscler. Thromb. a J. Vasc. Biol.* **14**, 275–81 (1994).
  48. Martoglio, B. & Dobberstein, B. Signal sequences: more than just greasy peptides. *Trends Cell Biol.* **8**, 410–5 (1998).
  49. Osborne, A. R., Rapoport, T. A. & van den Berg, B. Protein translocation by the Sec61/SecY Channel. *Annu. Rev. Cell Dev. Biol.* **21**, 529–550 (2005).
  50. Keenan, R. J., Freymann, D. M., Stroud, R. M. & Walter, P. The signal recognition particle. *Annu. Rev. Biochem.* **70**, 755–775 (2001).
  51. Zlotorynski, E. Slowly (translate) but surely (translocate). *Nat. Rev. Mol. Cell Biol.* **16**, 2–3 (2015).
  52. Auclair, S. M., Bhanu, M. K. & Kendall, D. A. Signal peptidase I: cleaving the way to mature proteins. *Protein Sci.* **21**, 13–25 (2012).
  53. Mellquist, J. L., Kasturi, L., Spitalnik, S. L. & Shakin-Eshleman, S. H. The amino acid following an Asn-X-Ser/Thr sequon is an important determinant of N-linked core glycosylation efficiency. *Biochemistry* **37**, 6833–6837 (1998).
  54. Aebi, M. N-linked protein glycosylation in the ER. *Biochim. Biophys. Acta - Mol. Cell Res.* **1833**, 2430–2437 (2013).
  55. Daniels, R., Kurowski, B., Johnson, A. E. & Hebert, D. N. N-linked glycans direct the cotranslational folding pathway of influenza hemagglutinin. *Mol. Cell* **11**, 79–90 (2003).
  56. Harter, C. & Wieland, F. The secretory pathway: mechanisms of protein sorting and transport. *Biochim. Biophys. Acta - Rev. Biomembr.* **1286**, 75–93 (1996).
  57. Antonny, B. & Schekman, R. ER export: public transportation by the COPII coach. *Curr. Opin. Cell Biol.* **13**, 438–43 (2001).
  58. Plemper, R. K. & Wolf, D. H. Retrograde protein translocation: ERADication of secretory proteins in health and disease. *Trends Biochem. Sci.* **24**, 266–70 (1999).
  59. McCracken, A. A. & Brodsky, J. L. Assembly of ER-associated protein degradation in vitro: dependence on cytosol, calnexin, and ATP. *J. Cell Biol.* **132**, 291–298 (1996).
  60. Tsai, B., Ye, Y. & Rapoport, T. A. Retro-translocation of proteins from the endoplasmic reticulum into the cytosol. *Nat. Rev. Mol. Cell Biol.* **3**, 246–255 (2002).
  61. White, A. L., Rainwater, D. L. & Lanford, R. E. Intracellular maturation of apolipoprotein[a] and assembly of lipoprotein[a] in primary baboon hepatocytes. *J. Lipid Res.* **34**, 509–17 (1993).
  62. Koschinsky, M. L. *et al.* Apolipoprotein(a): expression and characterization of a recombinant form of the protein in mammalian cells. *Biochemistry* **30**, 5044–51 (1991).
  63. Frischmann, M. E. *et al.* In vivo stable-isotope kinetic study suggests intracellular assembly of lipoprotein(a). *Atherosclerosis* **225**, 322–327 (2012).

64. Becker, L., Nesheim, M. E. & Koschinsky, M. L. Catalysis of covalent Lp(a) assembly: evidence for an extracellular enzyme activity that enhances disulfide bond formation. *Biochemistry* **45**, 9919–9928 (2006).
65. Santos, R. D. *et al.* Mipomersen, an antisense oligonucleotide to apolipoprotein B-100, reduces lipoprotein(a) in various populations with hypercholesterolemia: results of 4 phase III trials. *Arterioscler. Thromb. Vasc. Biol.* **35**, 689–699 (2015).
66. Thomas, G. S. *et al.* Mipomersen, an apolipoprotein B synthesis inhibitor, reduces atherogenic lipoproteins in patients with severe hypercholesterolemia at high cardiovascular risk: a randomized, double-blind, placebo-controlled trial. *J. Am. Coll. Cardiol.* **62**, 2178–2184 (2013).
67. Samaha, F. F., McKenney, J., Bloedon, L. T., Sasiela, W. J. & Rader, D. J. Inhibition of microsomal triglyceride transfer protein alone or with ezetimibe in patients with moderate hypercholesterolemia. *Nat. Clin. Pract. Cardiovasc. Med.* **5**, 497–505 (2008).
68. Cannon, C. P. *et al.* Safety of anacetrapib in patients with or at high risk for coronary heart disease. *N. Engl. J. Med.* **363**, 2406–2415 (2010).
69. Gaudet, D. *et al.* Effect of alirocumab on lipoprotein(a) over  $\geq 1.5$  years (from the phase 3 ODYSSEY program). *Am. J. Cardiol.* **119**, 40–46 (2017).
70. Sabatine, M. S. *et al.* Evolocumab and clinical outcomes in patients with cardiovascular disease. *N. Engl. J. Med.* **376**, 1713–1722 (2017).
71. Ogorelkova, M., Gruber, A. & Utermann, G. Molecular basis of congenital lp(a) deficiency: a frequent apo(a) ‘null’ mutation in caucasians. *Hum. Mol. Genet.* **8**, 2087–2096 (1999).
72. Gries, A., Nimpf, J., Nimpf, M., Wurm, H. & Kostner, G. M. Free and Apo B-associated Lpa-specific protein in human serum. *Clin. Chim. Acta* **164**, 93–100 (1987).
73. Tam, S. P., Zhang, X. & Koschinsky, M. L. Interaction of a recombinant form of apolipoprotein[a] with human fibroblasts and with the human hepatoma cell line HepG2. *J. Lipid Res.* **37**, 518–33 (1996).
74. Hofmann, S. L. *et al.* Overexpression of human low density lipoprotein receptors leads to accelerated catabolism of Lp(a) lipoprotein in transgenic mice. *J. Clin. Invest.* **85**, 1542–7 (1990).
75. Argraves, K. M., Kozarsky, K. F., Fallon, J. T., Harpel, P. C. & Strickland, D. K. The atherogenic lipoprotein Lp(a) is internalized and degraded in a process mediated by the VLDL receptor. *J. Clin. Invest.* **100**, 2170–2181 (1997).
76. März, W. *et al.* Heterogeneous lipoprotein (a) size isoforms differ by their interaction with the low density lipoprotein receptor and the low density lipoprotein receptor-related protein/alpha 2-macroglobulin receptor. *FEBS Lett.* **325**, 271–5 (1993).
77. Niemeier, A. *et al.* Identification of megalin/gp330 as a receptor for lipoprotein(a) in vitro. *Arterioscler. Thromb. Vasc. Biol.* **19**, 552–61 (1999).
78. Sharma, M., Redpath, G. M., Williams, M. J. A. & McCormick, S. P. A. Recycling of apolipoprotein(a) after PlgRKT-mediated endocytosis of lipoprotein(a) novelty and

- significance. *Circ. Res.* **120**, 1091–1102 (2017).
79. Yang, X.-P. *et al.* Scavenger receptor-BI is a receptor for lipoprotein(a). *J. Lipid Res.* **54**, 2450–2457 (2013).
  80. Albers, J. J., Koschinsky, M. L. & Marcovina, S. M. Evidence mounts for a role of the kidney in lipoprotein(a) catabolism. *Kidney Int.* **71**, 961–2 (2007).
  81. Rubin, J. *et al.* Apolipoprotein [a] genotype influences isoform dominance pattern differently in African Americans and Caucasians. *J. Lipid Res.* **43**, 234–44 (2002).
  82. Berglund, L. & Ramakrishnan, R. Lipoprotein(a): an elusive cardiovascular risk factor. *Arterioscler. Thromb. Vasc. Biol.* **24**, 2219–2226 (2004).
  83. Clarke, R. *et al.* Genetic variants associated with Lp(a) lipoprotein level and coronary disease. *N. Engl. J. Med.* **361**, 2518–2528 (2009).
  84. Frohlich, J., Dobiášová, M., Adler, L. & Francis, M. Gender differences in plasma levels of lipoprotein (a) in patients with angiographically proven coronary artery disease. *Physiol. Res.* **53**, 481–6 (2004).
  85. Ushioda, M., Makita, K., Takamatsu, K., Horiguchi, F. & Aoki, D. Serum lipoprotein(a) dynamics before/after menopause and long-term effects of hormone replacement therapy on lipoprotein(a) levels in middle-aged and older Japanese women. *Horm. Metab. Res.* **38**, 581–586 (2006).
  86. Parra, H.-J., Luyéyé, I., Bouramoué, C., Demarquilly, C. & Fruchart, J.-C. Black-white differences in serum Lp(a) lipoprotein levels. *Clin. Chim. Acta* **168**, 27–31 (1987).
  87. Guyton, J. R., Dahlen, G. H., Patsch, W., Kautz, J. A. & Gotto, A. M. Relationship of plasma lipoprotein Lp(a) levels to race and to apolipoprotein B. *Arterioscler. An Off. J. Am. Hear. Assoc. Inc.* **5**, 265–272 (1985).
  88. Kyriakou, T. *et al.* A common null allele associates with lower lipoprotein(a) Levels and coronary artery disease risk. *Arterioscler. Thromb. Vasc. Biol.* **34**, 2095–2099 (2014).
  89. Coassin, S. *et al.* A novel but frequent variant in LPA KIV-2 is associated with a pronounced Lp(a) and cardiovascular risk reduction. *Eur. Heart J.* **38**, 1823–1831 (2017).
  90. Parson, W. *et al.* A common nonsense mutation in the repetitive kringle IV-2 domain of human apolipoprotein(a) results in a truncated protein and low plasma Lp(a). *Hum. Mutat.* **24**, 474–480 (2004).
  91. Timmis, A. *et al.* European society of cardiology: cardiovascular disease statistics 2017. *Eur. Heart J.* **39**, 508–579 (2018).
  92. Frostegård, J. Immunity, atherosclerosis and cardiovascular disease. *BMC Med.* **11**, 117 (2013).
  93. Hadi, H. A. R., Carr, C. S. & Al Suwaidi, J. Endothelial dysfunction: cardiovascular risk factors, therapy, and outcome. *Vasc. Health Risk Manag.* **1**, 183–98 (2005).
  94. Libby, P. Inflammation and cardiovascular disease mechanisms. *Am. J. Clin. Nutr.* **83**, 456S–460S (2006).

95. Förstermann, U., Xia, N. & Li, H. Roles of vascular oxidative stress and nitric oxide in the pathogenesis of atherosclerosis. *Circ. Res.* **120**, 713–735 (2017).
96. Oeckinghaus, A. & Ghosh, S. The NF-kappaB family of transcription factors and its regulation. *Cold Spring Harb. Perspect. Biol.* **1**, a000034 (2009).
97. Pan, J. & McEver, R. P. Regulation of the human P-selectin promoter by Bcl-3 and specific homodimeric members of the NF- $\kappa$ B/Rel family. *J. Biol. Chem.* **270**, 23077–23083 (1995).
98. van de Stolpe, A. *et al.* 12-O-tetradecanoylphorbol-13-acetate- and tumor necrosis factor alpha-mediated induction of intercellular adhesion molecule-1 is inhibited by dexamethasone. Functional analysis of the human intercellular adhesion molecular-1 promoter. *J. Biol. Chem.* **269**, 6185–92 (1994).
99. Iademarco, M. F., McQuillan, J. J., Rosen, G. D. & Dean, D. C. Characterization of the promoter for vascular cell adhesion molecule-1 (VCAM-1). *J. Biol. Chem.* **267**, 16323–9 (1992).
100. Schindler, U. & Baichwal, V. R. Three NF-kappa B binding sites in the human E-selectin gene required for maximal tumor necrosis factor alpha-induced expression. *Mol. Cell. Biol.* **14**, 5820–31 (1994).
101. Mori, N. & Prager, D. Transactivation of the interleukin-1alpha promoter by human T-cell leukemia virus type I and type II Tax proteins. *Blood* **87**, 3410–7 (1996).
102. Hiscott, J. *et al.* Characterization of a functional NF-kappa B site in the human interleukin 1 beta promoter: evidence for a positive autoregulatory loop. *Mol. Cell. Biol.* **13**, 6231–6240 (1993).
103. Kunsch, C. & Rosen, C. A. NF-kappa B subunit-specific regulation of the interleukin-8 promoter. *Mol. Cell. Biol.* **13**, 6137–46 (1993).
104. Ueda, A. *et al.* NF-kappa B and Sp1 regulate transcription of the human monocyte chemoattractant protein-1 gene. *J. Immunol.* **153**, 2052–63 (1994).
105. Shakhov, A. N., Collart, M. A., Vassalli, P., Nedospasov, S. A. & Jongeneel, C. V. Kappa B-type enhancers are involved in lipopolysaccharide-mediated transcriptional activation of the tumor necrosis factor alpha gene in primary macrophages. *J. Exp. Med.* **171**, 35–47 (1990).
106. Sica, A. *et al.* Interaction of NF- $\kappa$ B and NFAT with the interferon- $\gamma$  promoter. *J. Biol. Chem.* **272**, 30412–30420 (1997).
107. Witztum, J. L. & Steinberg, D. The oxidative modification hypothesis of atherosclerosis: does it hold for humans? *Trends Cardiovasc. Med.* **11**, 93–102
108. Zhao, S. P. & Xu, D. Y. Oxidized lipoprotein(a) enhanced the expression of P-selectin in cultured human umbilical vein endothelial cells. *Thromb. Res.* **100**, 501–10 (2000).
109. Zhao, S. P. & Xu, D. Y. Oxidized lipoprotein(a) increases the expression of platelet-derived growth factor-B in human umbilical vein endothelial cells. *Clin. Chim. Acta.* **296**, 121–33 (2000).
110. Cho, T., Romagnuolo, R., Scipione, C., Boffa, M. B. & Koschinsky, M. L. Apolipoprotein(a) stimulates nuclear translocation of  $\beta$ -catenin: a novel pathogenic

- mechanism for lipoprotein(a). *Mol. Biol. Cell* **24**, 210–21 (2013).
111. Libby, P., Aikawa, M. & Jain, M. K. Vascular endothelium and atherosclerosis. *Handb. Exp. Pharmacol.* 285–306 (2006).
  112. Hansson, G. K. Inflammation, atherosclerosis, and coronary artery disease. *N. Engl. J. Med.* **352**, 1685–1695 (2005).
  113. Fleetwood, A. J., Lawrence, T., Hamilton, J. A. & Cook, A. D. Granulocyte-macrophage colony-stimulating factor (CSF) and macrophage CSF-dependent macrophage phenotypes display differences in cytokine profiles and transcription factor activities: implications for CSF blockade in inflammation. *J. Immunol.* **178**, 5245–5252 (2007).
  114. Stojakovic, M., Krzesz, R., Wagner, A. H. & Hecker, M. CD154-stimulated GM-CSF release by vascular smooth muscle cells elicits monocyte activation-role in atherogenesis. *J. Mol. Med. (Berl)*. **85**, 1229–1238 (2007).
  115. Filonzi, E. L., Zoellner, H., Stanton, H. & Hamilton, J. A. Cytokine regulation of granulocyte-macrophage colony stimulating factor and macrophage colony-stimulating factor production in human arterial smooth muscle cells. *Atherosclerosis* **99**, 241–52 (1993).
  116. Hamilton, J. A. Colony-stimulating factors in inflammation and autoimmunity. *Nat. Rev. Immunol.* **8**, 533–544 (2008).
  117. Liao, F. *et al.* Minimally modified low density lipoprotein is biologically active in vivo in mice. *J. Clin. Invest.* **87**, 2253–7 (1991).
  118. Janeway, C. A. & Medzhitov, R. Innate immune recognition. *Annu. Rev. Immunol.* **20**, 197–216 (2002).
  119. Peiser, L., Mukhopadhyay, S. & Gordon, S. Scavenger receptors in innate immunity. *Curr. Opin. Immunol.* **14**, 123–8 (2002).
  120. Greig, F. H., Kennedy, S. & Spickett, C. M. Physiological effects of oxidized phospholipids and their cellular signaling mechanisms in inflammation. *Free Radic. Biol. Med.* **52**, 266–280 (2012).
  121. Miller, Y. I. *et al.* Oxidation-specific epitopes are danger-associated molecular patterns recognized by pattern recognition receptors of innate immunity. *Circ. Res.* **108**, 235–248 (2011).
  122. Hörkkö, S. *et al.* Monoclonal autoantibodies specific for oxidized phospholipids or oxidized phospholipid–protein adducts inhibit macrophage uptake of oxidized low-density lipoproteins. *J. Clin. Invest.* **103**, 117–128 (1999).
  123. Lusis, A. J. Atherosclerosis. *Nature* **407**, 233–241 (2000).
  124. Lumadue, J. A., Lanzkron, S. M., Kennedy, S. D., Kuhl, D. T. & Kickler, T. S. Cytokine induction of platelet activation. *Am. J. Clin. Pathol.* **106**, 795–798 (1996).
  125. Riches, K. *et al.* Apolipoprotein(a) acts as a chemorepellent to human vascular smooth muscle cells via integrin  $\alpha V\beta 3$  and RhoA/ROCK-mediated mechanisms. *Int. J. Biochem. Cell Biol.* **45**, 1776–1783 (2013).
  126. Liu, L. *et al.* Apolipoprotein(a) stimulates vascular endothelial cell growth and

- migration and signals through integrin  $\alpha V\beta 3$ . *Biochem. J.* **418**, 325–336 (2009).
127. Faggiotto, A., Ross, R. & Harker, L. Studies of hypercholesterolemia in the nonhuman primate. I. Changes that lead to fatty streak formation. *Arteriosclerosis* **4**, 323–40 (1984).
  128. Kubota, K., Okazaki, J., Louie, O., Kent, K. C. & Liu, B. TGF-beta stimulates collagen (I) in vascular smooth muscle cells via a short element in the proximal collagen promoter. *J. Surg. Res.* **109**, 43–50 (2003).
  129. Davidson, J. M., Zoia, O. & Liu, J.-M. Modulation of transforming growth factor-beta 1 stimulated elastin and collagen production and proliferation in porcine vascular smooth muscle cells and skin fibroblasts by basic fibroblast growth factor, transforming growth factor-b, and insulin-like gro. *J. Cell. Physiol.* **155**, 149–156 (1993).
  130. Sadler, J. E. Biochemistry and genetics of von Willebrand factor. *Annu. Rev. Biochem.* **67**, 395–424 (1998).
  131. Libby, P. Inflammation in atherosclerosis. *Nature* **420**, 868–874 (2002).
  132. Ferrari, R. *et al.* A ‘diamond’ approach to personalized treatment of angina. *Nat. Rev. Cardiol.* **15**, 120–132 (2018).
  133. Eberhardt, W. *et al.* Nitric oxide modulates expression of matrix metalloproteinase-9 in rat mesangial cells. *Kidney Int.* **57**, 59–69 (2000).
  134. Uemura, S. *et al.* Diabetes mellitus enhances vascular matrix metalloproteinase activity: role of oxidative stress. *Circ. Res.* **88**, 1291–8 (2001).
  135. Yeang, C., Cotter, B. & Tsimikas, S. Experimental animal models evaluating the causal role of lipoprotein(a) in atherosclerosis and aortic stenosis. *Cardiovasc. Drugs Ther.* **30**, 75–85 (2016).
  136. Edelstein, C. *et al.* Lysine-phosphatidylcholine adducts in kringle V impart unique immunological and potential pro-inflammatory properties to human apolipoprotein(a). *J. Biol. Chem.* **278**, 52841–52847 (2003).
  137. Kadl, A. *et al.* Oxidized phospholipid-induced inflammation is mediated by Toll-like receptor 2. *Free Radic. Biol. Med.* **51**, 1903–1909 (2011).
  138. Silva, A. R. *et al.* Monocyte chemoattractant protein-1 and 5-lipoxygenase products recruit leukocytes in response to platelet-activating factor-like lipids in oxidized low-density lipoprotein. *J. Immunol.* **168**, 4112–4120 (2002).
  139. Lee, H. *et al.* Role for peroxisome proliferator-activated receptor alpha in oxidized phospholipid-induced synthesis of monocyte chemotactic protein-1 and interleukin-8 by endothelial cells. *Circ. Res.* **87**, 516–21 (2000).
  140. Que, X. *et al.* Oxidized phospholipids are proinflammatory and proatherogenic in hypercholesterolaemic mice. *Nature* (2018).
  141. Cho, T., Jung, Y. & Koschinsky, M. L. Apolipoprotein(a), through Its strong lysine-binding site in KIV 10, mediates increased endothelial cell contraction and permeability via a Rho/Rho kinase/MYPT1-dependent pathway. *J. Biol. Chem.* **283**, 30503–30512 (2008).

142. O'Neil, C. H., Boffa, M. B., Hancock, M. A., Pickering, J. G. & Koschinsky, M. L. Stimulation of vascular smooth muscle cell proliferation and migration by apolipoprotein(a) is dependent on inhibition of transforming growth factor-beta activation and on the presence of kringle IV type 9. *J. Biol. Chem.* **279**, 55187–95 (2004).
143. Feric, N. T., Boffa, M. B., Johnston, S. M. & Koschinsky, M. L. Apolipoprotein(a) inhibits the conversion of Glu-plasminogen to Lys-plasminogen: a novel mechanism for lipoprotein(a)-mediated inhibition of plasminogen activation. *J. Thromb. Haemost.* **6**, 2113–20 (2008).
144. Romagnuolo, R., DeMarco, K., Scipione, C. A., Boffa, M. B. & Koschinsky, M. L. Apolipoprotein(a) inhibits the conversion of Glu-plasminogen to Lys-plasminogen on the surface of vascular endothelial and smooth muscle cells. *Thromb. Res.* **169**, 1–7 (2018).
145. Rahman, M. N. *et al.* Comparative analyses of the lysine binding site properties of apolipoprotein(a) kringle IV types 7 and 10. *Biochemistry* **41**, 1149–1155 (2002).
146. Feric, N. T., Boffa, M. B., Johnston, S. M. & Koschinsky, M. L. Apolipoprotein(a) inhibits the conversion of Glu-plasminogen to Lys-plasminogen: a novel mechanism for lipoprotein(a)-mediated inhibition of plasminogen activation. *J. Thromb. Haemost.* **6**, 2113–2120 (2008).
147. Palabrica, T. M. *et al.* Antifibrinolytic activity of apolipoprotein(a) in vivo: human apolipoprotein(a) transgenic mice are resistant to tissue plasminogen activator-mediated thrombolysis. *Nat. Med.* **1**, 256–9 (1995).
148. Biemond, B. J. *et al.* Apolipoprotein(a) attenuates endogenous fibrinolysis in the rabbit jugular vein thrombosis model in vivo. *Circulation* **96**, 1612–1615 (1997).
149. Etingin, O. R., Hajjar, D. P., Hajjar, K. A., Harpel, P. C. & Nachman, R. L. Lipoprotein (a) regulates plasminogen activator inhibitor-1 expression in endothelial cells. A potential mechanism in thrombogenesis. *J. Biol. Chem.* **266**, 2459–65 (1991).
150. Buechler, C. *et al.* Lipoprotein (a) up-regulates the expression of the plasminogen activator inhibitor 2 in human blood monocytes. *Blood* **97**, 981–6 (2001).
151. Caplice, N. M. *et al.* Lipoprotein (a) binds and inactivates tissue factor pathway inhibitor: a novel link between lipoproteins and thrombosis. *Blood* **98**, 2980–7 (2001).
152. Boffa, M. B. & Koschinsky, M. L. Lipoprotein (a): truly a direct prothrombotic factor in cardiovascular disease? *J. Lipid Res.* **57**, 745–757 (2016).
153. Erqou, S. *et al.* Apolipoprotein(a) isoforms and the risk of vascular disease. *J. Am. Coll. Cardiol.* **55**, 2160–2167 (2010).
154. Kamstrup, P. R., Tybjaerg-Hansen, A., Steffensen, R. & Nordestgaard, B. G. Genetically elevated lipoprotein(a) and increased risk of myocardial infarction. *JAMA* **301**, 2331 (2009).
155. López, S. *et al.* Genome-wide linkage analysis for identifying quantitative trait loci involved in the regulation of lipoprotein a (Lpa) levels. *Eur. J. Hum. Genet.* **16**, 1372–1379 (2008).



156. Zabaneh, D. *et al.* Meta analysis of candidate gene variants outside the LPA locus with Lp(a) plasma levels in 14,500 participants of six white European cohorts. *Atherosclerosis* **217**, 447–451 (2011).
157. Nordestgaard, B. G. *et al.* Lipoprotein(a) as a cardiovascular risk factor: current status. *Eur. Heart J.* **31**, 2844–2853 (2010).
158. Helgadottir, A. *et al.* Apolipoprotein(a) genetic sequence variants associated with systemic atherosclerosis and coronary atherosclerotic burden but not with venous thromboembolism. *J. Am. Coll. Cardiol.* **60**, 722–729 (2012).
159. Thanassoulis, G. *et al.* Genetic associations with valvular calcification and aortic stenosis. *N. Engl. J. Med.* **368**, 503–512 (2013).
160. Emdin, C. A. *et al.* Phenotypic characterization of genetically lowered human lipoprotein(a) levels. *J. Am. Coll. Cardiol.* **68**, 2761–2772 (2016).
161. Emerging Risk Factors Collaboration *et al.* Lipoprotein(a) concentration and the risk of coronary heart disease, stroke, and nonvascular mortality. *JAMA* **302**, 412 (2009).
162. Waters, D. D. *et al.* Treating to new targets (TNT) study: does lowering low-density lipoprotein cholesterol levels below currently recommended guidelines yield incremental clinical benefit? *Am. J. Cardiol.* **93**, 154–8 (2004).
163. Khera, A. V. *et al.* Lipoprotein(a) concentrations, rosuvastatin therapy, and residual vascular risk. *Circulation* **129**, 635–642 (2014).
164. Tsimikas, S. A test in context: lipoprotein(a). *J. Am. Coll. Cardiol.* **69**, 692–711 (2017).
165. Raal, F. J. *et al.* PCSK9 inhibition-mediated reduction in Lp(a) with evolocumab: an analysis of 10 clinical trials and the LDL receptor's role. *J. Lipid Res.* **57**, 1086–1096 (2016).
166. McInnes, I. B. *et al.* Effect of interleukin-6 receptor blockade on surrogates of vascular risk in rheumatoid arthritis: MEASURE, a randomised, placebo-controlled study. *Ann. Rheum. Dis.* **74**, 694–702 (2015).
167. García-Gómez, C. *et al.* Lipoprotein(a) concentrations in rheumatoid arthritis on biologic therapy: Results from the CARdiovascular in rheuMATology study project. *J. Clin. Lipidol.* **11**, 749-756.e3 (2017).
168. Leren, T. P. Sorting an LDL receptor with bound PCSK9 to intracellular degradation. *Atherosclerosis* **237**, 76–81 (2014).
169. Romagnuolo, R. *et al.* Lipoprotein(a) catabolism is regulated by proprotein convertase subtilisin/kexin type 9 through the low density lipoprotein receptor. *J. Biol. Chem.* **290**, 11649–62 (2015).
170. Raal, F. J. *et al.* Reduction in lipoprotein(a) with PCSK9 monoclonal antibody evolocumab (AMG 145). *J. Am. Coll. Cardiol.* **63**, 1278–1288 (2014).
171. Watts, G. F. *et al.* Controlled study of the effect of proprotein convertase subtilisin-kexin type 9 inhibition with evolocumab on lipoprotein(a) particle kinetics. *Eur. Heart J.* **39**, 2577–2585 (2018).
172. Villard, E. F. *et al.* PCSK9 modulates the secretion but not the cellular uptake of

- lipoprotein(a) ex vivo. *JACC Basic to Transl. Sci.* **1**, 419–427 (2016).
173. Viney, N. J. *et al.* Antisense oligonucleotides targeting apolipoprotein(a) in people with raised lipoprotein(a): two randomised, double-blind, placebo-controlled, dose-ranging trials. *Lancet* **388**, 2239–2253 (2016).
  174. Melquist, S. Targeting apolipoprotein(a) with a novel RNAi delivery platform as a prophylactic treatment to reduce risk of cardiovascular events in individuals with elevated lipoprotein(a). (2018).
  175. Ray, K. K. *et al.* Inclisiran in patients at high cardiovascular risk with elevated LDL cholesterol. *N. Engl. J. Med.* **376**, 1430–1440 (2017).
  176. Ray, K. K. *et al.* Effect of an siRNA therapeutic targeting PCSK9 on atherogenic lipoproteins. *Circulation* **138**, 1304–1316 (2018).
  177. Gurakar, A., Hoeg, J. M., Kostner, G., Papadopoulos, N. M. & Brewer, H. B. Levels of lipoprotein Lp(a) decline with neomycin and niacin treatment. *Atherosclerosis* **57**, 293–301 (1985).
  178. Millar, J. S. *et al.* Anacetrapib lowers LDL by increasing ApoB clearance in mildly hypercholesterolemic subjects. *J. Clin. Invest.* **125**, 2510–2522 (2015).
  179. Thomas, T. *et al.* CETP (Cholesteryl Ester Transfer Protein) inhibition with anacetrapib decreases production of lipoprotein(a) in mildly hypercholesterolemic subjects. *Arterioscler. Thromb. Vasc. Biol.* **37**, 1770–1775 (2017).
  180. Davidson, M. H. *et al.* Clinical utility of inflammatory markers and advanced lipoprotein testing: Advice from an expert panel of lipid specialists. *J. Clin. Lipidol.* **5**, 338–367 (2011).
  181. Albers, J. J. *et al.* Relationship of apolipoproteins A-1 and B, and lipoprotein(a) to cardiovascular outcomes. *J. Am. Coll. Cardiol.* **62**, 1575–1579 (2013).
  182. AIM-HIGH Investigators *et al.* Niacin in patients with low HDL cholesterol levels receiving intensive statin therapy. *N. Engl. J. Med.* **365**, 2255–2267 (2011).
  183. Landray, M. J. *et al.* Effects of extended-release niacin with laropiprant in high-risk patients. *N. Engl. J. Med.* **371**, 203–215 (2014).
  184. Waldmann, E. & Parhofer, K. G. Lipoprotein apheresis to treat elevated lipoprotein (a). *J. Lipid Res.* **57**, 1751–1757 (2016).
  185. Rosada, A. *et al.* Does regular lipid apheresis in patients with isolated elevated lipoprotein(a) levels reduce the incidence of cardiovascular events? *Artif. Organs* **38**, 135–141 (2014).
  186. Roeseler, E. *et al.* Lipoprotein apheresis for lipoprotein(a)-associated cardiovascular disease highlights. *Arterioscler. Thromb. Vasc. Biol.* **36**, 2019–2027 (2016).
  187. Jaeger, B. R. *et al.* Longitudinal cohort study on the effectiveness of lipid apheresis treatment to reduce high lipoprotein(a) levels and prevent major adverse coronary events. *Nat. Rev. Cardiol.* **6**, 229–239 (2009).
  188. Borrelli, M. J., Youssef, A., Boffa, M. B. & Koschinsky, M. L. New frontiers in Lp(a)-targeted therapies. *Trends Pharmacol. Sci.* **40**, 212–225 (2019).

189. van der Valk, F. M. *et al.* Oxidized phospholipids on lipoprotein(a) elicit arterial wall inflammation and an inflammatory monocyte response in humans. *Circulation* **134**, 611–24 (2016).
190. Scipione, C. Oxidative modifications of apolipoprotein(a): implications for proinflammatory and prothrombotic roles of lipoprotein(a) in the vasculature. *Electron. Theses Diss.* (2016).
191. Russell, W. C., Graham, F. L., Smiley, J. & Nairn, R. Characteristics of a human cell line transformed by DNA from human adenovirus type 5. *J. Gen. Virol.* **36**, 59–72 (1977).
192. Bonen, D. K., Hausman, A. M. L., Hadjiagapiou, C., Skarosi, S. F. & Davidson, N. O. Expression of a recombinant apolipoprotein(a) in HepG2 cells. Evidence for intracellular assembly of lipoprotein(a). *J. Biol. Chem.* **272**, 5659–5667 (1997).
193. Robinson, P. J. Differential stimulation of Protein Kinase C activity by phorbol ester or calcium/phosphatidylserine in vitro and in intact synaptosomes. *J. Biol. Chem.* **267**, 21637–21644 (1992).
194. Chiesa, G. *et al.* Reconstitution of lipoprotein(a) by infusion of human low density lipoprotein into transgenic mice expressing human apolipoprotein(a). *J. Biol. Chem.* **267**, 24369–74 (1992).
195. White, A. L. & Lanford, R. E. Cell surface assembly of lipoprotein(a) in primary cultures of baboon hepatocytes. *J. Biol. Chem.* **269**, 28716–23 (1994).
196. Kronenberg, F. & Utermann, G. Lipoprotein(a): resurrected by genetics. *J. Intern. Med.* **273**, 6–30 (2013).
197. Trpkovic, A. *et al.* Oxidized low-density lipoprotein as a biomarker of cardiovascular diseases. *Crit. Rev. Clin. Lab. Sci.* **52**, 70–85 (2015).
198. Tybjaerg-Hansen, A. Using human genetics to predict the effects and side effects of lipoprotein(a) lowering drugs. *Curr. Opin. Lipidol.* **27**, 105–111 (2016).
199. Bernales, S., Papa, F. R. & Walter, P. Intracellular signaling by the unfolded protein response. *Annu. Rev. Cell Dev. Biol.* **22**, 487–508 (2006).
200. Kozutsumi, Y., Segal, M., Normington, K., Gething, M.-J. & Sambrook, J. The presence of malfolded proteins in the endoplasmic reticulum signals the induction of glucose-regulated proteins. *Nature* **332**, 462–464 (1988).
201. Dara, L., Ji, C. & Kaplowitz, N. The contribution of endoplasmic reticulum stress to liver diseases. *Hepatology* **53**, 1752–63 (2011).
202. Basseri, S. & Austin, R. C. ER stress and lipogenesis: a slippery slope toward hepatic steatosis. *Dev. Cell* **15**, 795–6 (2008).
203. Colgan, S. M., Tang, D., Werstuck, G. H. & Austin, R. C. Endoplasmic reticulum stress causes the activation of sterol regulatory element binding protein-2. *Int. J. Biochem. Cell Biol.* **39**, 1843–1851 (2007).
204. Lee, J. N. & Ye, J. Proteolytic activation of sterol regulatory element-binding protein induced by cellular stress through depletion of Insig-1. *J. Biol. Chem.* **279**, 45257–45265 (2004).

205. Horton, J. D. Sterol regulatory element-binding proteins: transcriptional activators of lipid synthesis. *Biochem. Soc. Trans.* **30**, 1091–1095 (2002).
206. Bertolotti, A., Zhang, Y., Hendershot, L. M., Harding, H. P. & Ron, D. Dynamic interaction of BiP and ER stress transducers in the unfolded-protein response. *Nat. Cell Biol.* **2**, 326–332 (2000).
207. Olofsson, L. E. *et al.* CCAAT/enhancer binding protein  $\alpha$  (C/EBP $\alpha$ ) in adipose tissue regulates genes in lipid and glucose metabolism and a genetic variation in C/EBP $\alpha$  is associated with serum levels of triglycerides. *J. Clin. Endocrinol. Metab.* **93**, 4880–4886 (2008).
208. Krohn, S., Garin, A., Gabay, C. & Proudfoot, A. E. I. The activity of CCL18 is principally mediated through interaction with glycosaminoglycans. *Front. Immunol.* **4**, 193 (2013).
209. Chenivesse, C. *et al.* Pulmonary CCL18 recruits human regulatory T cells. *J. Immunol.* **189**, 128–37 (2012).
210. Adema, G. J. *et al.* A dendritic-cell-derived C–C chemokine that preferentially attracts naive T cells. *Nature* **387**, 713–717 (1997).
211. Schutyser, E., Richmond, A. & Damme, J. Van. Involvement of CC chemokine ligand 18 (CCL18) in normal and pathological processes. *J. Leukoc. Biol.* **78**, 14–26 (2005).
212. Schraufstatter, I. U., Zhao, M., Khaldoyanidi, S. K. & DiScipio, R. G. The chemokine CCL18 causes maturation of cultured monocytes to macrophages in the M2 spectrum. *Immunology* **135**, 287–298 (2012).
213. Reape, T. J. *et al.* Expression and cellular localization of the CC chemokines PARC and ELC in human atherosclerotic plaques. *Am. J. Pathol.* **154**, 365–74 (1999).
214. Zhu, M., Janssen, E., Leung, K. & Zhang, W. Molecular Cloning of a Novel Gene Encoding a Membrane-associated Adaptor Protein (LAX) in Lymphocyte Signaling. *J. Biol. Chem.* **277**, 46151–46158 (2002).
215. Tedgui, A. & Mallat, Z. Cytokines in atherosclerosis: pathogenic and regulatory pathways. *Physiol. Rev.* **86**, 515–581 (2006).
216. Galkina, E. & Ley, K. Immune and inflammatory mechanisms of atherosclerosis. *Annu. Rev. Immunol.* **27**, 165–97 (2009).
217. Thair, S. A. *et al.* TNFAIP2 inhibits early TNF $\alpha$ -induced NF- $\kappa$ B signaling and decreases survival in septic shock patients. *J. Innate Immun.* **8**, 57–66 (2016).
218. Watanabe, R. *et al.* Emerging roles of tumor necrosis factor-stimulated gene-6 in the pathophysiology and treatment of atherosclerosis. *Int. J. Mol. Sci.* **19**, 465 (2018).
219. Wang, E. C. Y. On death receptor 3 and its ligands.... *Immunology* **137**, 114–116 (2012).
220. Li, X.-Y., Hou, H.-T., Chen, H.-X., Wang, Z.-Q. & He, G.-W. Increased circulating levels of tumor necrosis factor-like cytokine 1A and decoy receptor 3 correlate with SYNTAX score in patients undergoing coronary surgery. *J. Int. Med. Res.* **46**, 5167–5175 (2018).
221. Kato, M., Khan, S., d’Aniello, E., McDonald, K. J. & Hart, D. N. J. The novel

- endocytic and phagocytic C-type lectin receptor DCL-1/CD302 on macrophages is colocalized with F-actin, suggesting a role in cell adhesion and migration. *J. Immunol.* **179**, 6052–6063 (2007).
222. Guo, Y.-L. *et al.* Role of junctional adhesion molecule-like protein in mediating monocyte transendothelial migration. *Arterioscler. Thromb. Vasc. Biol.* **29**, 75–83 (2009).
223. Allen, S. *et al.* Expression of adhesion molecules by lp(a): a potential novel mechanism for its atherogenicity. *FASEB J.* **12**, 1765–76 (1998).
224. Papakonstantinou, E. *et al.* The differential distribution of hyaluronic acid in the layers of human atheromatic aortas is associated with vascular smooth muscle cell proliferation and migration. *Atherosclerosis* **138**, 79–89 (1998).
225. Levesque, H. *et al.* Localization and solubilization of hyaluronan and of the hyaluronan-binding protein hyaluronectin in human normal and arteriosclerotic arterial walls. *Atherosclerosis* **105**, 51–62 (1994).
226. Nandi, A., Estess, P. & Siegelman, M. H. Hyaluronan anchoring and regulation on the surface of vascular endothelial cells is mediated through the functionally active form of CD44. *J. Biol. Chem.* **275**, 14939–14948 (2000).
227. DeGrendele, H. C., Estess, P., Picker, L. J. & Siegelman, M. H. CD44 and its ligand hyaluronate mediate rolling under physiologic flow: a novel lymphocyte-endothelial cell primary adhesion pathway. *J. Exp. Med.* **183**, 1119–1130 (1996).
228. Bot, P. T., Hofer, I. E., Piek, J. J. & Pasterkamp, G. Hyaluronic acid: targeting immune modulatory components of the extracellular matrix in atherosclerosis. *Curr. Med. Chem.* **15**, 786–91 (2008).
229. Viola, M. *et al.* Extracellular matrix in atherosclerosis: hyaluronan and proteoglycans insights. *Curr. Med. Chem.* **23**, 2958–2971 (2016).
230. Cipollone, F. *et al.* Overexpression of functionally coupled cyclooxygenase-2 and prostaglandin E synthase in symptomatic atherosclerotic plaques as a basis of prostaglandin E2-dependent plaque instability. *Circulation* **104**, 921–927 (2001).
231. Schönbeck, U., Sukhova, G. K., Graber, P., Coulter, S. & Libby, P. Augmented expression of cyclooxygenase-2 in human atherosclerotic lesions. *Am. J. Pathol.* **155**, 1281–91 (1999).
232. Sussmann, M. *et al.* Induction of hyaluronic acid synthase 2 (HAS2) in human vascular smooth muscle cells by vasodilatory prostaglandins. *Circ. Res.* **94**, 592–600 (2004).

## Curriculum Vitae

<b>Name</b>	Matthew Borrelli
<b>Post-secondary education and degrees</b>	Western University London, Ontario, Canada 2012-2017 BMSc  Western University London, Ontario, Canada 2017-2019 MSc
<b>Honours and Awards</b>	Karen Pooley Scholarship in Ovarian Cancer Research (2019)  Dean's Undergraduate Research Opportunities Program (DUROP) (2017)
<b>Related work experience</b>	Teaching Assistant – Physiology 2130 Western University 2018-2019  Teaching Assistant – Physiology 1021 Western University 2017-2018
<b>Published works</b>	<u>Borrelli M.J.</u> , Youssef A.Y., Boffa M.B., Koschinsky, M.L. (2019) New frontiers in Lp(a)-targeted therapies. <i>Trends in Pharmacological Sciences</i> 40 (3), 212-225.
<b>Publications in submission</b>	Schnitzler J.G., Hoogeveen R.M., Ali L., Prange K.H.M., van Weeghel M., Bachmann J.C., Versloot M., <u>Borrelli M.J.</u> , Yeang C., Houtkooper R., Koschinsky M.L., de Winther M.P.J., Groen A.K., Witztum J.L., Tsimikas S., Stroes E.S.G., Kroon J. Targeting lipoprotein(a)-induced endothelial cell metabolic reprogramming reverses inflammation and leukocyte migration. Submitted to <i>Cell Metabolism</i> .
<b>Presentations</b>	<u>Borrelli M.J.</u> , Koschinsky M.L. Characterizing missense mutations of human origin in apolipoprotein(a) kringle IV <sub>10</sub> . Accepted for feature platform presentation at London Health Research Day, London ON, April 2019.